AD-A043 432 TOLEDO UNIV OH DEPT OF ELECTRICAL ENGINEERING F/G 9/5
UTILIZATION OF SOURCE IMPEDANCE TO DECREASE THE WEIGHT OF D.C. --ETC(U)
JUL 77 T A STUART AF-AFOSR-2997-76
UNCLASSIFIED AFOSR-TR-77-0985 NL

1 OF 2
AD
A043432

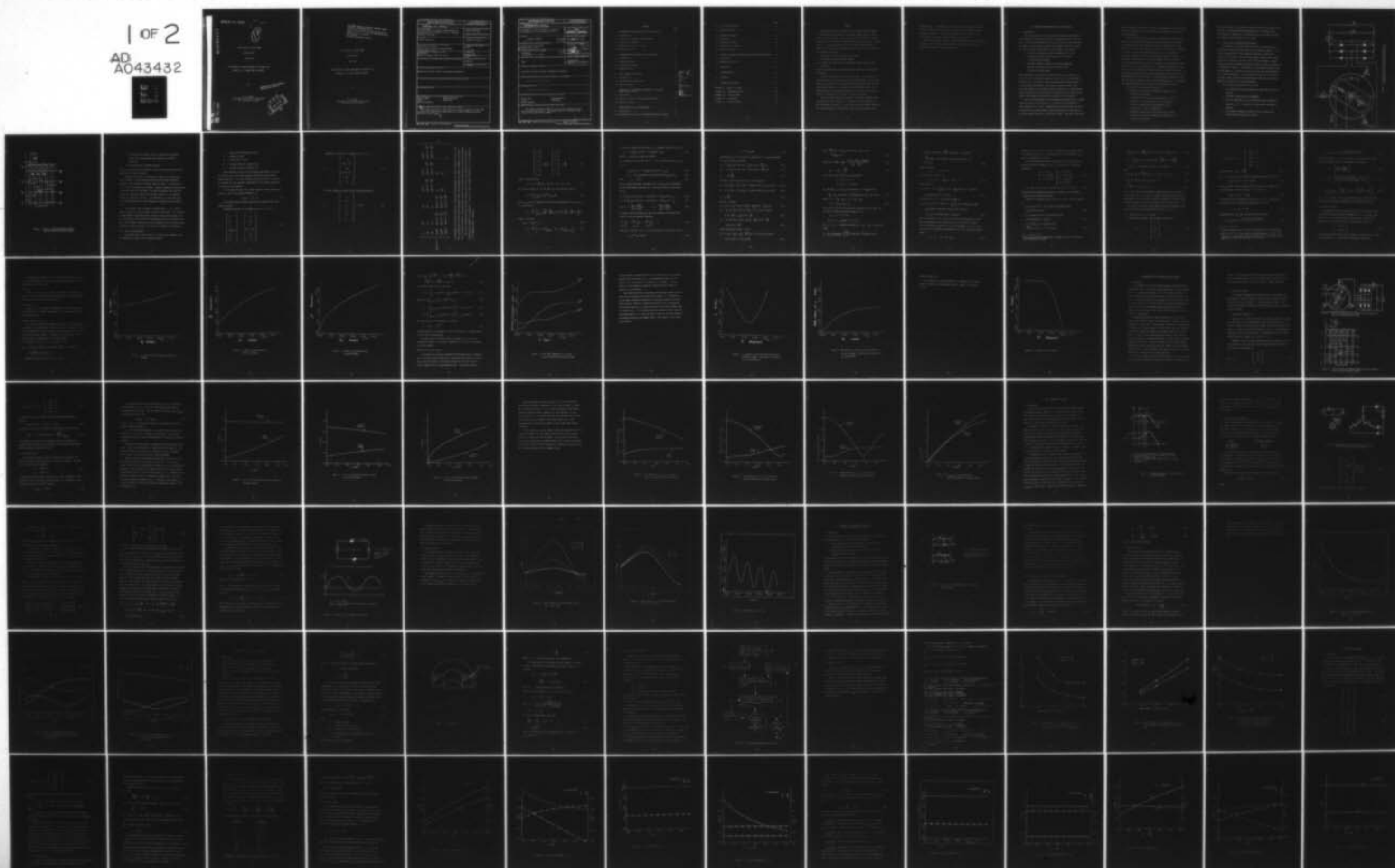

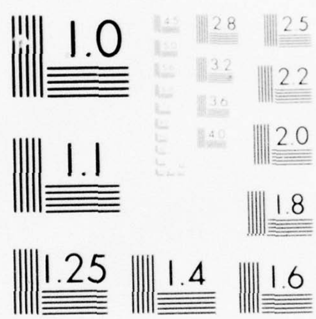
1.0
1.1
1.25
1.4
1.6
1.8
2.0
2.2
2.5
2.8
3.2
3.6
4.0

AFOSR-TR- 77-0985

ADA043432

12

Final Report on AFOSR GRANT

AFOSR-76-2997

July 1977

"UTILIZATION OF SOURCE IMPEDANCE TO DECREASE THE WEIGHT OF D.C. POWER SUPPLY FILTERS"

by

T. A. Stuart
Department of Electrical Engineering
The University of Toledo

Final Report on AFOSR GRANT

AFOSR-76-2997

July 1977

"UTILIZATION OF SOURCE IMPEDANCE TO DECREASE THE WEIGHT OF D.C. POWER SUPPLY FILTERS"

by

T. A. Stuart
Department of Electrical Engineering
The University of Toledo

UNCLASSIFIED

SECURITY CLASSIFICATION OF THIS PAGE (When Data Entered)

REPORT DOCUMENTATION PAGE		READ INSTRUCTIONS BEFORE COMPLETING FORM
1. REPORT NUMBER AFOSR-TR- 77-0985	2. GOVT ACCESSION NO.	3. RECIPIENT'S CATALOG NUMBER
4. TITLE (and Subtitle) UTILIZATION OF SOURCE IMPEDANCE TO DECREASE THE WEIGHT OF D.C. POWER SUPPLY FILTERS		5. TYPE OF REPORT & PERIOD COVERED FINAL REPORT 6. PERFORMING ORG. REPORT NUMBER
7. AUTHOR(s) Stuart, Thomas A.		8. CONTRACT OR GRANT NUMBER(s) AFOSR-76-2997
9. PERFORMING ORGANIZATION NAME AND ADDRESS University of Toledo Department of Electrical Engineering Toledo, Ohio 43606		10. PROGRAM ELEMENT, PROJECT, TASK AREA & WORK UNIT NUMBERS 61102F 2305 D9
11. CONTROLLING OFFICE NAME AND ADDRESS AFOSR/NE Bldg 410, Bolling AFB, DC 20332		12. REPORT DATE 18 July 1977 13. NUMBER OF PAGES 153
14. MONITORING AGENCY NAME & ADDRESS (if different from Controlling Office)		15. SECURITY CLASS. (of this report) UNCLAS 15a. DECLASSIFICATION/DOWNGRADING SCHEDULE

16. DISTRIBUTION STATEMENT (of this Report)

Approved for public release; distribution unlimited.

17. DISTRIBUTION STATEMENT (of the abstract entered in Block 20, if different from Report)

18. SUPPLEMENTARY NOTES

19. KEY WORDS (Continue on reverse side if necessary and identify by block number)

Power Supply
Filter
Source Impedance
Superconducting
Alternator

20. ABSTRACT (Continue on reverse side if necessary and identify by block number)

This report presents a study of how the source impedance can be used to reduce the weight of the output filter of a rectified superconducting alternator power supply.

DD FORM 1 JAN 73 1473 EDITION OF 1 NOV 65 IS OBSOLETE

UNCLASSIFIED

SECURITY CLASSIFICATION OF THIS PAGE (When Data Entered)

SECURITY CLASSIFICATION OF THIS PAGE (When Data Entered)

REPORT DOCUMENTATION PAGE

READ INSTRUCTIONS BEFORE COMPLETING FORM

1. REPORT NUMBER (11) (19) **AFOSR-TR-77-0985** / 2. GOVT ACCESSION NO. ------	3. RECIPIENT'S CATALOG NUMBER -------
4. TITLE (and Subtitle) (6) Utilization of Source Impedance to Decrease the Weight of D.C. Power Supply Filters,	5. TYPE OF REPORT & PERIOD COVERED (9) Final Report. Jun[redacted] 1976—Jun[redacted] 1977,
	6. PERFORMING ORG. REPORT NUMBER ----------
7. AUTHOR(s) (10) Thomas A. Stuart	8. CONTRACT OR GRANT NUMBER(s) (15) AF-AFOSR-76-2997-76,
9. PERFORMING ORGANIZATION NAME AND ADDRESS (1) The University of Toledo (2) Toledo, Ohio 43606 (3) Dept of Elec. Engrg	10. PROGRAM ELEMENT, PROJECT, TASK AREA & WORK UNIT NUMBERS 9768-03 (16) 2305 (17) 03, D9
11. CONTROLLING OFFICE NAME AND ADDRESS AFOSR(PMD) Bolling AFB, D.C. 20332 (11) 18	12. REPORT DATE Jul[redacted] 1977
	13. NUMBER OF PAGES 153 (12) 161p.
14. MONITORING AGENCY NAME & ADDRESS (if different from Controlling Office) Same	15. SECURITY CLASS. (of this report) Unclassified
	15a. DECLASSIFICATION/DOWNGRADING SCHEDULE -------------

16. DISTRIBUTION STATEMENT (of this Report)

Approved for public release; distribution unlimited.

17. DISTRIBUTION STATEMENT (of the abstract entered in Block 20, if different from Report)

----

18. SUPPLEMENTARY NOTES

----

19. KEY WORDS (Continue on reverse side if necessary and identify by block number)

Power Supply
Filter
Source Impedance
Superconducting
Alternator

20. ABSTRACT (Continue on reverse side if necessary and identify by block number)

This report presents a study of how the source impedance can be used to reduce the weight of the output filter of a rectified superconducting alternator power supply.

DD FORM 1 JAN 73 1473 EDITION OF 1 NOV 65 IS OBSOLETE New 410 351

SECURITY CLASSIFICATION OF THIS PAGE (When Data Entered)

CONTENTS

SUMMARY

This report presents an analysis of a DC power supply consisting of a superconducting alternator, a rectifier bridge, and an LC output filter. The main purpose of this research was to determine if changes in the size of the alternator inductances would allow the use of a smaller filter. To perform this study it was necessary to examine the behavior of the filter and to determine how its operation was affected by the alternator parameters.

Basically, the filter performs two functions:

1. It attenuates the output ripple voltage.
2. It limits the initial fault current when a short circuit occurs at the load.

Both of these functions also depend upon the values of the alternator inductances.

Since the first function refers to the steady state behavior, it was necessary to develop a model for this operating mode. This was done first for a system with an uncontrolled rectifier bridge and then these results were extended to a controlled rectifier bridge system. The second function is a transient phenomenon, so it was also necessary to develop a second model to describe the transient behavior.

Once the system models were complete, a study was performed where the unfiltered ripple voltage was calculated for various values of the alternator inductances. It was found that under certain conditions the ripple voltage can be decreased by increasing the armature self

inductance (L_a). A program was then written which calculated the weight of the LC filter that was required for a given set of specifications and alternator parameters. This program indicated that an increase in L_a could decrease the required filter weight by as much as 22%.

Other investigations included a sensitivity analysis of the alternator inductances and the design and testing of a phase controlled voltage regulator with current overload protection.

1. ALTERNATOR WITH UNCONTROLLED RECTIFIER BRIDGE

1.1 Introduction

Recent advancements in superconducting alternators have created a strong interest in using these machines for airborne electric power supplies. The predominant advantage of this power source is its relatively low weight for applications requiring multi-megawatt outputs at several kV. This low weight characteristic occurs because of two factors:

1. Even with the required cryogenic equipment, the superconducting alternator system weighs much less than a conventional alternator.

2. The higher armature voltages of the superconducting machine may eliminate the need for heavy output inverters and transformers.

These attributes are discussed in further detail in such references as [1] - [12], and a very recent example of such a machine is described by McCabria, et al. in [13,14]. This particular machine develops 10MVA at 5 kV and weighs approximately 1,000 pounds (alternator weight only). This same reference also includes projected estimates for a 25MVA machine weighing between 1882 and 2160 pounds, depending on rated output voltage (again, these figures only include the weight of the alternator).

The potential advantages of superconducting alternators have prompted extensive research in this area, most of which has concentrated on ac loads (again see [1] - [14]). Applications for these machines also exist in high power dc systems however, where the alternator is connected to a rectifier bridge followed by a large filter choke. This mode of operation has been studied in detail for conventional alternators, (see [15] through [21]), but until now no such analysis has been presented for the superconducting machine.

One of the more rigorous analyses of conventional rectified alternators is that presented by Franklin [17,18] for salient pole machines. By assuming constant flux linkages for the rotor windings, this study derives a set of nonlinear equations in terms of the electrical variables of interest. Certain approximations then lead to a linearization involving a constant K factor, and an explicit solution is obtained. The advantages of this approach are readily apparent since it provides a closed form expression for each of the variables, once the proper K factor has been found. The determination of K is somewhat distracting however, since it is load dependent and requires the use of numerical methods. In the following section it will be shown that this K factor can actually be eliminated from the final solution if a Newton-Raphson algorithm is used. This new approach appears to have certain advantages since it is somewhat less complicated and does not depend on any linearization factors.

The essence of the work presented here is:

1. Franklin's basic analysis methods are extended to the superconducting machine.
2. The dependence on the previously mentioned K factor is eliminated. As stated above, this is accomplished by using a Newton-Raphson algorithm where a K=1 is used only to find a starting point.
3. A numerical example predicting the rectified characteristics of the machine described by McCabria, et al. in [13,14] is included.

The overall intent is to provide an analytical model of the steady state behavior of the superconducting alternator with a rectified output. This analysis is regarded as a preliminary step to the eventual design and testing of these machines for D.C. loads.

1.2 Steady State Alternator-Rectifier Model

The armature of the superconducting machine is assumed to be Y connected as indicated for the basic two pole machine in Figure 1. The d and q windings shown in this figure are equivalent windings that account for the effect of the cylindrical damper shield located between the rotor and the stator (see [5], [13] or [14] for example). Output voltage and current waveforms are shown in Figure 2, where the indicated θ corresponds to Figure 1. Formulation of this problem proceeds in much the same manner as in [17,18], but there are some important differences in the machine parameters. It also should be noted that the method of solution is quite different from these earlier references, and certain equations are employed in a different manner.

The following approximations are utilized:

1. All winding and diode resistances are quite small and can be ignored.
2. All diode voltage drops are negligible.
3. The load inductance, L_o, is sufficiently large to maintain a constant I_L, i.e., the effect of load current variations is ignored.
4. Each armature winding is assumed to have a perfect sinusoidal distribution about the stator.

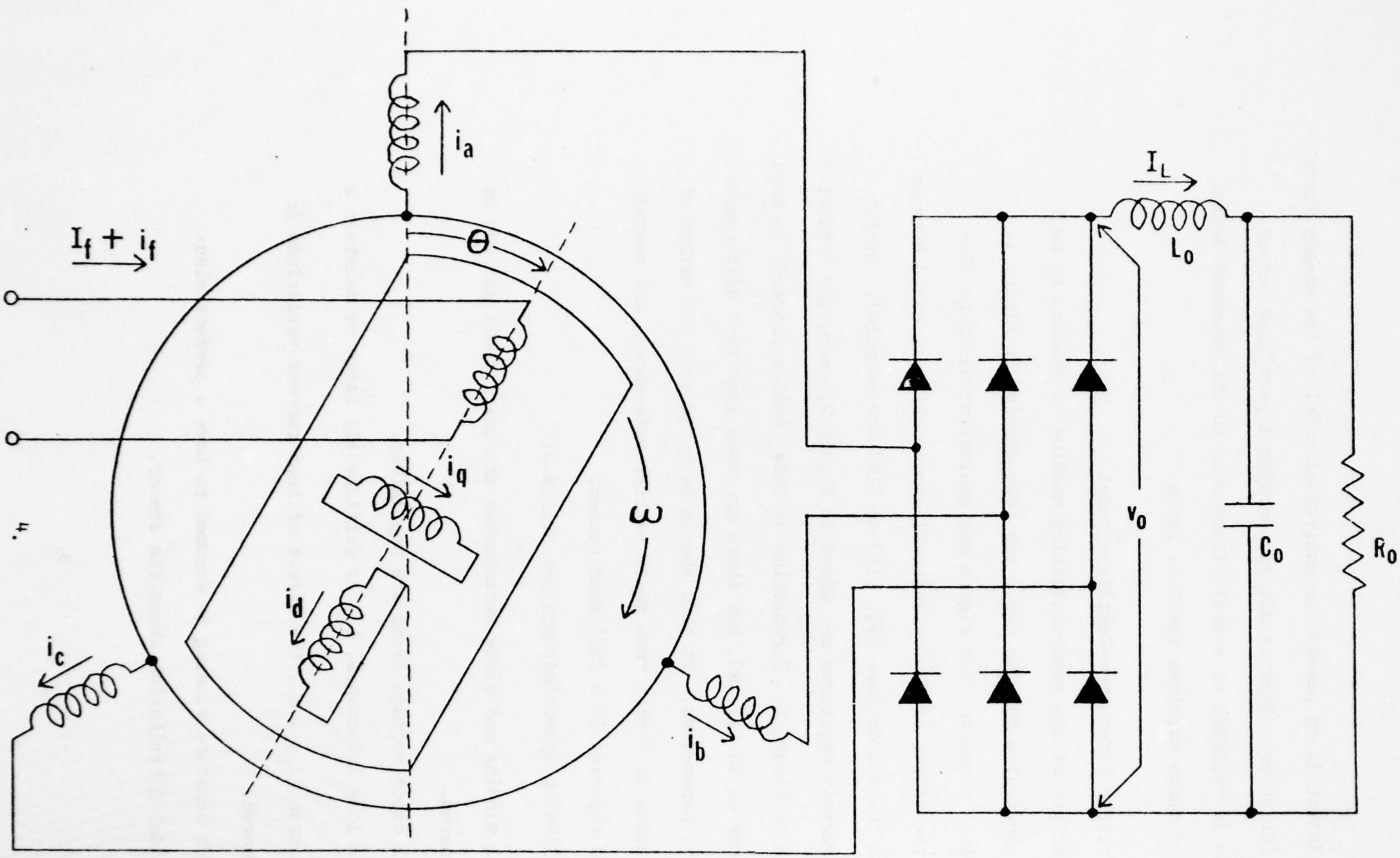

Figure 1. Equivalent Circuit for the Superconducting Alternator with Uncontrolled Rectifier Bridge.

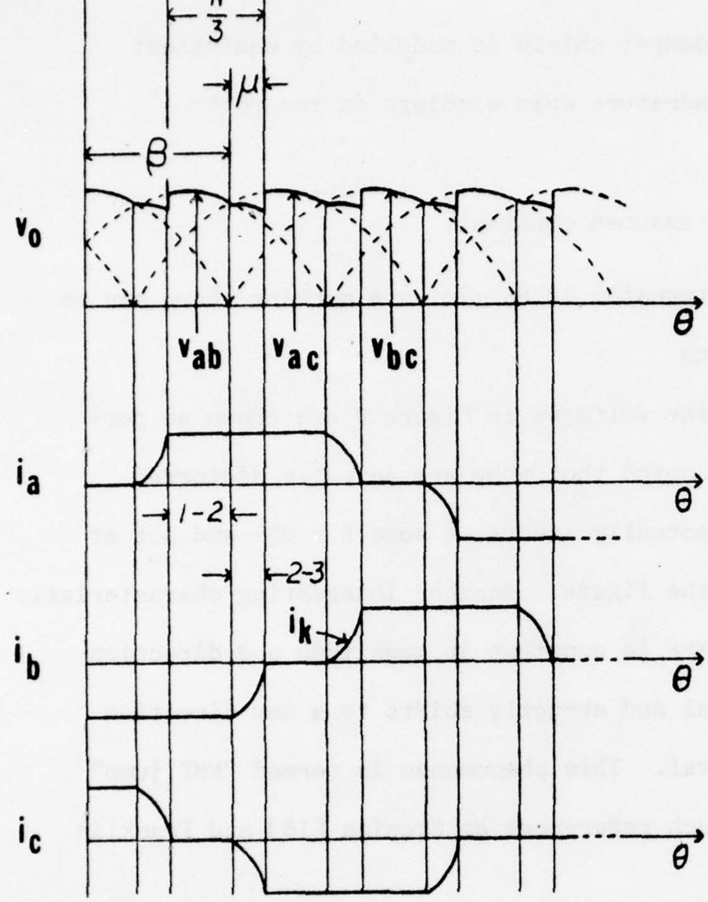

Figure 2. Output Voltage and Armature Currents with Uncontrolled Rectifier Bridge.

5. The effect of the damper shield is modelled by equivalent direct axis and quadrature axis windings on the rotor (d and q).

6. The rotor speed is assumed constant.

Since the superconducting alternator is an air core machine there are no saturation or saliency effects.

Although the line to line voltages in Figure 2 are shown as perfact sinusoids, it should be noted that they are actually distorted somewhat. Thus commutation actually starts at some $\beta > 90°$ and not at $\theta = \beta = 90°$ as indicated in the figure. Another interesting characteristic is the fact that the stator MMF is constant in magnitude and direction during the conduction interval and abruptly shifts to a new direction during the commutation interval. This phenomenon is termed "MMF jump" as is described further in such references as Stepina [16] and Franklin [17].

The waveforms shown in Figure 2 indicate that $\mu < \pi/3$. Franklin points out that it is also possible to reach a mode where $\mu = \frac{\pi}{3}$. Although a large number of simulations were conducted in this present study, the $\mu = \pi/3$ mode was never reached for the machine used in the numerical example. The conclusion drawn was that this appeared to be an unlikely operating mode for this application, so it was not included in the analysis.

1.3 Steady State Equations

The primary goal of this section is to derive five equations that are expressed in terms of the following variables:

β = angle at which commutation starts

μ = commutation angle

I_f = average field current

W = variable defined by equation (20.)

V = variable defined by equation (21.)

These equations turn out to be nonlinear with respect to β and μ, but they can be solved by some numerical method such as the Newton-Raphson algorithm. Once these variables have been found it is possible to determine the time dependent expressions for the output voltage and the current in each winding.

It is assumed that the field current consists of the constant component, I_f, and a time varying component, i_f,

$$i_{f(tot)} = I_f + i_f \tag{1.}$$

The winding currents during conduction and commutation are indicated as follows,

Conduction (Interval 1-2 in Figure 2), $\beta + \mu - \pi/3 \leq \theta < \beta$

$$\underline{i} = \begin{bmatrix} i_a \\ i_b \\ i_c \\ i_{f(tot)} \\ i_d \\ i_q \end{bmatrix} = \begin{bmatrix} I_L \\ -I_L \\ 0 \\ (I_f + i_f) \\ i_d \\ i_q \end{bmatrix} \tag{2.}$$

Commutation (Interval 2-3 in Figure 2), $\beta \leq \theta < \beta + \mu$

$$\underline{i} = \begin{bmatrix} I_L \\ (-I_L + i_k) \\ -i_k \\ (I_f + i_f) \\ i_d \\ i_q \end{bmatrix} \tag{3.}$$

The flux linkages are given by the following expression,

$$\underline{\lambda} = \begin{bmatrix} \lambda_a \\ \lambda_b \\ \lambda_c \\ \lambda_f \\ \lambda_d \\ \lambda_q \end{bmatrix} = [L]\,\underline{i} \tag{4.}$$

$$
\text{where, } [L] = \begin{bmatrix}
L_a & -M_a & -M_a & M_f\cos\theta & M_d\cos\theta & -M_d\sin\theta \\
-M_a & L_a & -M_a & M_f\cos(\theta - \frac{2\pi}{3}) & M_d\cos(\theta - \frac{2\pi}{3}) & -M_d\sin(\theta - \frac{2\pi}{3}) \\
-M_a & -M_a & L_a & M_f\cos(\theta - \frac{4\pi}{3}) & M_d\cos(\theta - \frac{4\pi}{3}) & -M_d\sin(\theta - \frac{4\pi}{3}) \\
M_f\cos\theta & M_f\cos(\theta - \frac{2\pi}{3}) & M_f\cos(\theta - \frac{4\pi}{3}) & L_f & M_{fd} & 0 \\
M_d\cos\theta & M_d\cos(\theta - \frac{2\pi}{3}) & M_d\cos(\theta - \frac{4\pi}{3}) & M_{fd} & L_d & 0 \\
-M_d\sin\theta & -M_d\sin(\theta - \frac{2\pi}{3}) & -M_d\sin(\theta - \frac{4\pi}{3}) & 0 & 0 & L_d
\end{bmatrix} \quad (5.
$$

[L] represents the inductance matrix for a superconducting alternator, as given by Kirtley in [5,6]. Note that L_d and M_d are the same for the equivalent direct and quadrature axis damper "windings" (as pointed out in the above references, these equivalents account for the damper shield and are not actual windings).

The d and q windings are short circuited, implying that λd and λq are constant since the winding resistances are assumed to be negligible. Likewise, λf may be assumed constant if $I_f + i_f$ is supplied by a low impedance source. Therefore,

$$\underline{v} = \begin{bmatrix} v_a \\ v_b \\ v_c \\ v_f \\ v_d \\ v_q \end{bmatrix} = -\frac{d}{dt}\underline{\lambda} = \begin{bmatrix} v_a \\ v_b \\ v_c \\ 0 \\ 0 \\ 0 \end{bmatrix} = -\omega \frac{d\lambda}{d\theta} \qquad (6.)$$

Figure 2 indicates that,

$$v_o = v_{ab} = -\omega \frac{d}{d\theta}[\lambda_a - \lambda_b], \ \beta+\mu - \pi/3 < \omega t < \beta+\mu \qquad (7.)$$

The average voltage, V_L, at the output of the rectifier bridge is,

$$V_L = \frac{3}{\pi}\left[\int_{\beta+\mu-\pi/3}^{\beta} v_{012}\, d\theta + \int_{\beta}^{\beta+\mu} v_{023}\, d\theta\right] \qquad (8.)$$

where v_{012} and v_{023} represent the output voltage functions over 1-2 and 2-3 respectively.

$$V_L = -\frac{3\omega}{\pi}\left[\int_{\beta+\mu-\pi/3}^{\beta} \left[\frac{d\lambda_a}{d\theta} - \frac{d\lambda_b}{d\theta}\right]_{12} d\theta + \int_{\beta}^{\beta+\mu} \left[\frac{d\lambda_a}{d\theta} - \frac{d\lambda_b}{d\theta}\right]_{23} d\theta\right] \qquad (9.)$$

Figure 2 indicates

$$v_{012} = v_{023} \ @ \ \theta = \beta \qquad (10.)$$

$$V_L = -\frac{3\omega}{\pi}\left[(\lambda_a - \lambda_b)_{23}\Big|_{(\beta+\mu)} - (\lambda_a - \lambda_b)_{12}\Big|_{(\beta+\mu-\pi/3)}\right] \qquad (11.)$$

(2.) and (3.) become the same when $i_k = 0$, therefore using (3.) and (5.),

$$\lambda_q = -\sqrt{3}\, I_L M_d \sin(\theta+\pi/6) + \sqrt{3}\, i_k M_d \cos\theta + i_q L_d \tag{12.}$$

where $i_k = 0$ over the conduction interval.

λ_q is assumed to be constant over 1-3. At $\theta = \beta+\mu-\pi/3$ we have $i_q = i_{qo}$, $i_k = 0$.

$$\lambda_q\,(\beta+\mu-\pi/3) = -\sqrt{3}\, I_L M_d \sin(\beta+\mu-\pi/6) + i_{qo}\, L_d \tag{13.}$$

$$i_q = -\sqrt{3}\, I_L K_q [\sin(\beta+\mu-\pi/6) - \sin(\theta+\pi/6)] - \sqrt{3}\, i_k K_q \cos\theta + i_{qo} \tag{14.}$$

where $$K_q = M_d/L_d \tag{15.}$$

Using a similar procedure, expressions for λ_f and λ_d may be determined. The two simultaneous equations for λ_f and λ_d may then be solved for i_f and i_d,

$$i_d = \sqrt{3}\, I_L K_d\, [\cos(\beta+\mu-\pi/6) - \cos(\theta+\pi/6)] - \sqrt{3}\, i_k K_d \sin\theta + i_{do} \tag{16.}$$

$$i_f = \sqrt{3}\, I_L K_f\, [\cos(\beta+\mu-\pi/6) - \cos(\theta+\pi/6)] - \sqrt{3}\, i_k K_f \sin\theta + i_{fo} \tag{17.}$$

$$\text{where } K_f = \frac{M_f L_d - M_d M_{fd}}{L_f L_d - (M_{fd})^2}, \qquad K_d = \frac{M_d L_f - M_f M_{fd}}{L_f L_d - (M_{fd})^2} \tag{18.}$$

As pointed out by Shilling [15], the rotor currents are periodic with respect to the 6th harmonic; therefore,

$$\int_{\beta+\mu-\pi/3}^{\beta+\mu} i_f\, d\theta = \int_{\beta+\mu-\pi/3}^{\beta+\mu} i_d\, d\theta = \int_{\beta+\mu-\pi/3}^{\beta+\mu} i_q\, d\theta = 0 \tag{19.}$$

Since $i_k = 0$ for $\beta+\mu - \frac{\pi}{3} < \theta \le \beta$, we may define the following constants

$$W \equiv \int_{\beta}^{\beta+\mu} i_k \sin\theta\, d\theta \tag{20.}$$

$$V \equiv \int_{\beta}^{\beta+\mu} i_k \cos\theta d\theta \qquad (21.)$$

Integrating (14.), (16.) and (17.) over $\beta+\mu-\frac{\pi}{3} \leq \theta \leq \beta+\mu$ and solving for i_{qo}, i_{do} and i_{fo} produces,

$$i_{qo} = \sqrt{3}\, I_L K_q \,[\sin(\beta+\mu-\pi/6) - \frac{3}{\pi}\sin(\beta+\mu)] + \frac{3\sqrt{3}}{\pi} K_q V \qquad (22.)$$

$$i_{do} = -\sqrt{3}\, I_L K_d \,[\cos(\beta+\mu-\pi/6) - \frac{3}{\pi}\cos(\beta+\mu)] + \frac{3\sqrt{3}}{\pi} K_d W \qquad (23.)$$

$$i_{fo} = i_{do}\,(\frac{K_f}{K_d}) \qquad (24.)$$

Therefore, substituting into (14.), (16.) and (17.),

$$i_q = \sqrt{3}\, K_q \,\{\frac{3}{\pi}[V - I_L \sin(\beta+\mu)] + [I_L \sin(\theta+\pi/6) - i_k \cos(\theta)]\} \qquad (25.)$$

$$i_d = \sqrt{3}\, K_d \,\{\frac{3}{\pi}[W + I_L \cos(\beta+\mu)] - [I_L \cos(\theta+\pi/6) + i_k \sin(\theta)]\} \qquad (26.)$$

$$i_f = i_d\,(\frac{K_f}{K_d}) \qquad (27.)$$

Drom (4.), we have,

$$\lambda_a = I_L (L_a + M_a) + [(I_f + i_f) M_f + i_d M_d] \cos\theta - i_q M_d \sin\theta \qquad (28.)$$

$$\lambda_b = - I_L (L_a + M_a) + i_k (L_a + M_a) + [(I_f + i_f) M_f + i_d M_d] \cos(\theta - \frac{2\pi}{3}) - i_q M_d \sin(\theta - \frac{2\pi}{3}) \qquad (29.)$$

$$\lambda_c = - i_k (L_a + M_a) + [(I_f + i_f) M_f + i_d M_d] \cos(\theta - \frac{4\pi}{3}) - i_q M_d \sin(\theta - \frac{4\pi}{3}) \qquad (30.)$$

Using the results of (25.) - (27.),

$$(I_f + i_f) M_f + i_d M_d = I_f M_f + \frac{3\sqrt{3}}{\pi} M_o W - \sqrt{3}\, I_L M_o [\cos(\theta+\pi/6) - \frac{3}{\pi}\cos(\beta+\mu)] - \sqrt{3}\, i_k M_o \sin\theta \qquad (31.)$$

$$i_q M_d = \frac{3\sqrt{3}}{\pi} M_{oo} V + \sqrt{3}\, I_L M_{oo} \, [\sin(\theta+\pi/6) - \frac{3}{\pi}\sin(\beta+\mu)]$$

$$- \sqrt{3}\, i_k M_{oo} \cos\theta \qquad (32.)$$

$$\text{where, } M_o = (K_f M_f + K_d M_d) = \frac{M_f^{\,2} L_d + M_d^{\,2} L_f - 2 M_d M_f M_{fd}}{L_d L_f - (M_{fd})^2} \qquad (33.)$$

$$M_{oo} = K_q M_d = \frac{M_d^{\,2}}{L_d} \qquad (34.)$$

(11.) can be used to find V_L, by noting that

$$i_k = I_L \text{ @ } \theta = \beta + \mu$$

$$i_k = 0 \text{ @ } \theta = \beta + \mu - \pi/3,$$

$$V_L = \frac{3\omega}{\pi} \{\frac{3}{4} I_L \Delta_o + \frac{3}{2} I_L \Lambda_d \cos(2\beta+2\mu+\pi/3) + \sqrt{3}\, I_f M_f \sin(\beta+\mu)$$

$$+ \frac{9}{2\pi} I_L \Lambda_d \sin(2\beta+2\mu) + \frac{9}{\pi}[M_o W \sin(\beta+\mu) + M_{oo} V\cos(\beta+\mu)]\} \qquad (35.)$$

$$\text{where, } \Lambda_f = (M_o + M_{oo}), \quad \Lambda_d = (M_o - M_{oo})$$

$$\Delta_o = \frac{4}{3}(L_a + M_a) - \Lambda_f \qquad (36.)$$

The current i_k exists only during the commutation period where the "b" and "c" phases are shorted together, i.e.,

$$v_{bc} = 0, \ \beta \le \theta \le \beta+\mu$$

$$\therefore \quad (\lambda_b - \lambda_c) = \text{constant}, \ \beta \le \theta \le \beta+\mu$$

For $\theta = \beta$, $i_k = 0$, therefore setting $(\lambda_b - \lambda_c)_\theta = (\lambda_b - \lambda_c)_\beta$ one obtains,

$$i_k = \frac{1}{[\Delta_o + \Lambda_d \cos(2\theta)]} \left[\frac{2MfI_f}{\sqrt{3}} (\sin\beta - \sin\theta) + \frac{6}{\pi} M_o W(\sin\beta - \sin\theta) \right.$$

$$+ \frac{6}{\pi} M_{oo} V (\cos\beta - \cos\theta) + \frac{3I_L \Lambda_d}{\pi} [\sin(2\beta+\mu) - \sin(\beta+\mu+\theta)]$$

$$- \frac{3I_L \Lambda_f}{\pi} [\sin\mu + \sin(\theta-\beta-\mu)] - I_L \Lambda_d [\cos(2\beta-\pi/3) - \cos$$

$$(2\theta-\pi/3)] \Bigg] \qquad (37.)$$

Again utilizing,

$$v_{bc} = 0, \quad \beta \leq \theta \leq \beta + \mu$$

we have for $i_k = 0$ @ $\theta = \beta$,

$$(v_b - v_c)_\beta = -\omega \frac{d}{d\theta} (\lambda_b - \lambda_c)_\beta = 0 \qquad (38.)$$

which leads to,

$$-\Lambda_d \sin(2\beta - \pi/3) = \frac{1}{\sqrt{3}} \frac{I_f}{I_L} M_f \cos\beta + \frac{3}{\pi I_L} (M_o W \cos\beta - M_{oo} V \sin\beta)$$

$$+ \frac{3}{2\pi} [\Lambda_d \cos(2\beta+\mu) + \Lambda_f \cos\mu] \qquad (39.)$$

Utilizing $i_k = I_L$ @ $\theta = \beta+\mu$ in (37.) leads to,

$$\Delta_o + 2\Lambda_d \cos(2\beta+\mu) \cos(\mu+\pi/3) = -\frac{4}{\sqrt{3}} \frac{I_f}{I_L} M_f [\cos(\beta+\frac{\mu}{2}) \sin(\frac{\mu}{2})]$$

$$+ \frac{6}{\pi I_L} [M_o W(\sin\beta - \sin(\beta+\mu)) + M_{oo} V (\cos\beta - \cos(\beta+\mu))]$$

$$- \frac{3}{\pi} [2\Lambda_d \cos(2\beta+\frac{3\mu}{2}) \sin(\frac{\mu}{2}) + \Lambda_f \sin(\mu)] \qquad (40.)$$

One could substitute (37.) into (20.) and (21.) and integrate to find two more equations, which along with (35.), (39.) and (40.) would yield five nonlinear equations for the five unknowns, I_f, β, μ, V and W. This process is simplified considerably by use of the following approximation,

$$\Lambda_d \simeq 0, \quad (\text{i.e., } M_o \simeq M_{oo}) \qquad (41.)$$

Equations (35.), (37.), (39.) and (40.) indicate that Λ_d always appears in conjunction with Λ_f or Δ_o. Therefore, (41.) is acceptable if Λ_d is small in comparison to Λ_f and Δ_o.

The superconducting alternator considered in this study (the same machine described by McCabria, et al., in [13,14] has the following parameters[1]:

$$
\begin{aligned}
L_f &= 1.2 \text{ H.} & M_f &= 7.9 \times 10^{-3}\text{H.} \\
L_d &= 8.2 \times 10^{-8}\text{H.} & M_{fd} &= 1.9 \times 10^{-4}\text{H.} \\
L_a &= 3.0 \times 10^{-4}\text{H.} & M_d &= 3.8 \times 10^{-6}\text{H.} \\
& & M_a &= 1.5 \times 10^{-4}\text{H.}
\end{aligned} \tag{42.}
$$

$$\Lambda_d = 0.01 \times 10^{-4} \text{ H.}, \ \Lambda_f = 3.5 \times 10^{-4} \text{ H.}, \ \Delta_o = 2.5 \times 10^{-4} \text{ H.} \tag{43.}$$

Therefore the approximation given by (41.) appears to be acceptable, at least for this particular example.

Using (41.), equations (20.), (21.), (35.), (39.) and (40.) reduce to,

$$
\begin{aligned}
0 = \Delta_o W &+ A\,(\cos\,(\beta+\mu) - \cos\,\beta) + \frac{B}{4}\,(2\mu-\sin(2\beta+2\mu)+\sin 2\beta) \\
&+ \frac{C}{2}\,(\sin^2(\beta+\mu)-\sin^2\beta)
\end{aligned} \tag{44.}
$$

$$
\begin{aligned}
0 = \Delta_o V &+ A(\sin\beta-\sin(\beta+\mu)) + \frac{B}{2}\,(\sin^2(\beta+\mu)-\sin^2\beta) \\
&+ \frac{C}{4}\,(2\mu+\sin(2\beta+2\mu) - \sin(2\beta))
\end{aligned} \tag{45.}
$$

$$
\begin{aligned}
0 = -V_L &+ \frac{3\omega}{\pi}\Big[\frac{3}{4}\, I_L \Delta_o + \sqrt{3}\, I_f M_f \sin\,(\beta+\mu) \\
&+ \frac{9M_{oo}}{\pi}\,(W \sin\,(\beta+\mu) + V \cos\,(\beta+\mu))\Big]
\end{aligned} \tag{46.}
$$

---

[1] These parameters were supplied by H. Southall of the U.S. Air Force Aero Propulsion Laboratory.

$$0 = \frac{I_f}{\sqrt{3}\, I_L} M_f \cos\beta + \frac{3M_{oo}}{\pi I_L} (W \cos\beta - V \sin\beta) + \frac{3}{\pi} M_{oo} \cos\mu \quad (47.)$$

$$0 = -\Delta_o - \frac{4\, I_f}{\sqrt{3}\, I_L} M_f \cos(\beta + \frac{\mu}{2}) \sin(\frac{\mu}{2}) - \frac{6\, M_{oo}}{\pi} \sin\mu + \frac{6\, M_{oo}}{\pi I_L}.$$

$$[W (\sin\beta - \sin(\beta+\mu)) + V (\cos\beta - \cos(\beta+\mu))] \quad (48.)$$

where

$$A = \frac{2}{\sqrt{3}} I_f M_f \sin\beta + \frac{6\, M_{oo}}{\pi} (W \sin\beta + V \cos\beta - I_L \sin\mu) \quad (49.)$$

$$B = \frac{2}{\sqrt{3}} I_f M_f + \frac{6}{\pi} M_{oo} (W + I_L \cos(\beta + \mu)) \quad (50.)$$

$$C = \frac{6\, M_{oo}}{\pi} (V - I_L \sin(\beta + \mu)) \quad (51.)$$

(44.) - (48.) provide five nonlinear equations which are functions of the variables I_f, β, μ, V and W. Actually, these equations are linear with respect to I_f, V and W so it would be possible to eliminate these variables and have a set of two equations which are functions of β and μ. The equations involved in this reduction are quite cumbersome however, so one might as well work directly with (44.) - (48.).

1.4 Solution for I_f, β, μ, V and W

Rewriting the variables and equations in matrix form,

$$\underline{x} \equiv \begin{bmatrix} \beta \\ \mu \\ I_f \\ V \\ W \end{bmatrix} \quad (52.)$$

$$\underline{f}\,(\underline{x}) \equiv \text{R.H.S. of} \begin{bmatrix} (44.) \\ (45.) \\ (46.) \\ (47.) \\ (48.) \end{bmatrix} \tag{53.}$$

$$\text{Jacobian matrix} \equiv F\,(\underline{x}) \equiv \frac{\partial \underline{f}(\underline{x})}{\partial \underline{x}} \tag{54.}$$

(52.) - (54.) can be used to form the standard Newton-Raphson equation,

$$F\,(\underline{x}_o)\,(\underline{x} - \underline{x}_o) = \underline{f}\,(\underline{x}) - \underline{f}\,(\underline{x}_o) \tag{55.}$$

where $\underline{x}_o$ is some initial starting point which must be reasonably close to the desired $\underline{x}$. In this case $\underline{f}\,(\underline{x}) = \underline{0}$, so we have,

$$F\,(\underline{x}_o)\,(\underline{x} - \underline{x}_o) = -\,\underline{f}\,(\underline{x}_o) \tag{56.}$$

It remains to find a satisfactory value for $\underline{x}_o$. This is accomplished by making use of the linearization suggested by Franklin[1],

$$i_k \simeq (\theta - \beta)\,\frac{I_L}{\mu} \tag{57.}$$

Substituting (57.) into (20.) and (21.) gives the result,

$$W = -I_L \cos(\beta+\mu) + \frac{2\,I_L \sin(\mu/2)\cos(\beta+\mu/2)}{\mu} \tag{58.}$$

---

[1] Actually, Franklin uses a "K factor" as mentioned in the Introduction, where $0.5 \leq K \leq 0.9$. This produces the approximation, $i_k \simeq K(\theta-\beta)\,\frac{I_L}{\mu}$. Since (57.) is only used to find a starting point for the Newton-Raphson algorithm, K is not critical, and K = 1.0 is used.

$$V = I_L \sin(\beta+\mu) - \frac{2\, I_L \sin(\mu/2) \cos(\beta+\mu/2)}{\mu} \tag{59.}$$

After substituting (57.) - (59.) into (35.), (39.) and (40.) and performing some rather laborious calculations, one obtains,

$$\mu = \cos^{-1} \left[\frac{4\pi V_L - 9\omega I_L \Delta_o}{4\pi V_L + 9\omega I_L \Delta_o} \right] \tag{60.}$$

$$\beta = \tan^{-1} \left[\frac{\pi\Delta_o \mu + 12\, M_{oo} (\sin \frac{\mu}{2})^2 (1 - \cos\mu)}{12\, M_{oo} \sin(\mu/2) \cos(\frac{\mu}{2}) (1 - \cos\mu)} \right] \tag{61.}$$

$$I_f = \frac{1}{\sqrt{3}\, M_f \sin(\beta+\mu)} \left[\frac{\pi V_L}{3\omega} - \frac{3}{4}\, I_L \Delta_o - \frac{18\, I_L M_{oo}}{\pi\mu} (\sin \frac{\mu}{2})^2 \right] \tag{62.}$$

(58.) - (62.) provide a value of $\underline{x}_o$ which produces convergence within three or four iterations, depending on the convergence tolerance.

1.5 Numerical Results

This example is based on the same 4 pole, 400 Hz, 10 MVA/5kV superconducting alternator described by McCabria, et al. in [13,14]. When operating into a bridge rectifier at full load with a large filter inductance, this system will have the output values (see [24]),

$$V_L = 6760 \text{ V. dc}$$
$$I_L = 1420 \text{ A. dc} \tag{64.}$$

The following results assume that the system is operating with a closed loop controller, i.e., I_f is varied to maintain a constant V_L.

The inductance parameters for this machine are indicated in (42.). All data is presented in terms of the actual magnitudes, but a per unit system would serve just as well.

I_f vs. I_L:

Figure 3. shows I_f vs. I_L, where I_f is varied to maintain a constant V_L. As seen from the curve, the variation in I_f is approximately linear up to 200% of the full load value of I_L.

β and μ vs. I_L:

Figures 4. and 5. indicate the variation in β and μ respectively with respect to I_L. Figure 5. indicates that μ remains less than 60° as mentioned earlier.

Harmonic Content of v_o vs. I_L:

One of the more important problems in this type of power system is the weight of the output filter (L_o and C_o as shown in Figure 1.). In order to minimize the combined weight of these components it is necessary to know the harmonic content of v_o under all load conditions. The output voltage is obtained from (7.) by substitution:

Conduction period ($i_k = 0$), $\beta + \mu - \pi/3 < \theta \leq \beta$,

$$v_{012} = \omega\,(\sqrt{3}\; I_f\, M_f + \frac{9}{\pi} M_{oo}\, W)\sin(\theta+\pi/6) + \frac{9\omega}{\pi} M_{oo}\, V\cos(\theta+\pi/6)$$

$$+ \frac{9\omega\, I_L\, M_{oo}}{\pi}\sin(\theta+\pi/6-\beta-\mu) \qquad (65.)$$

Commutation period ($i_k \neq 0$), $\beta < \theta \leq \beta + \mu$,

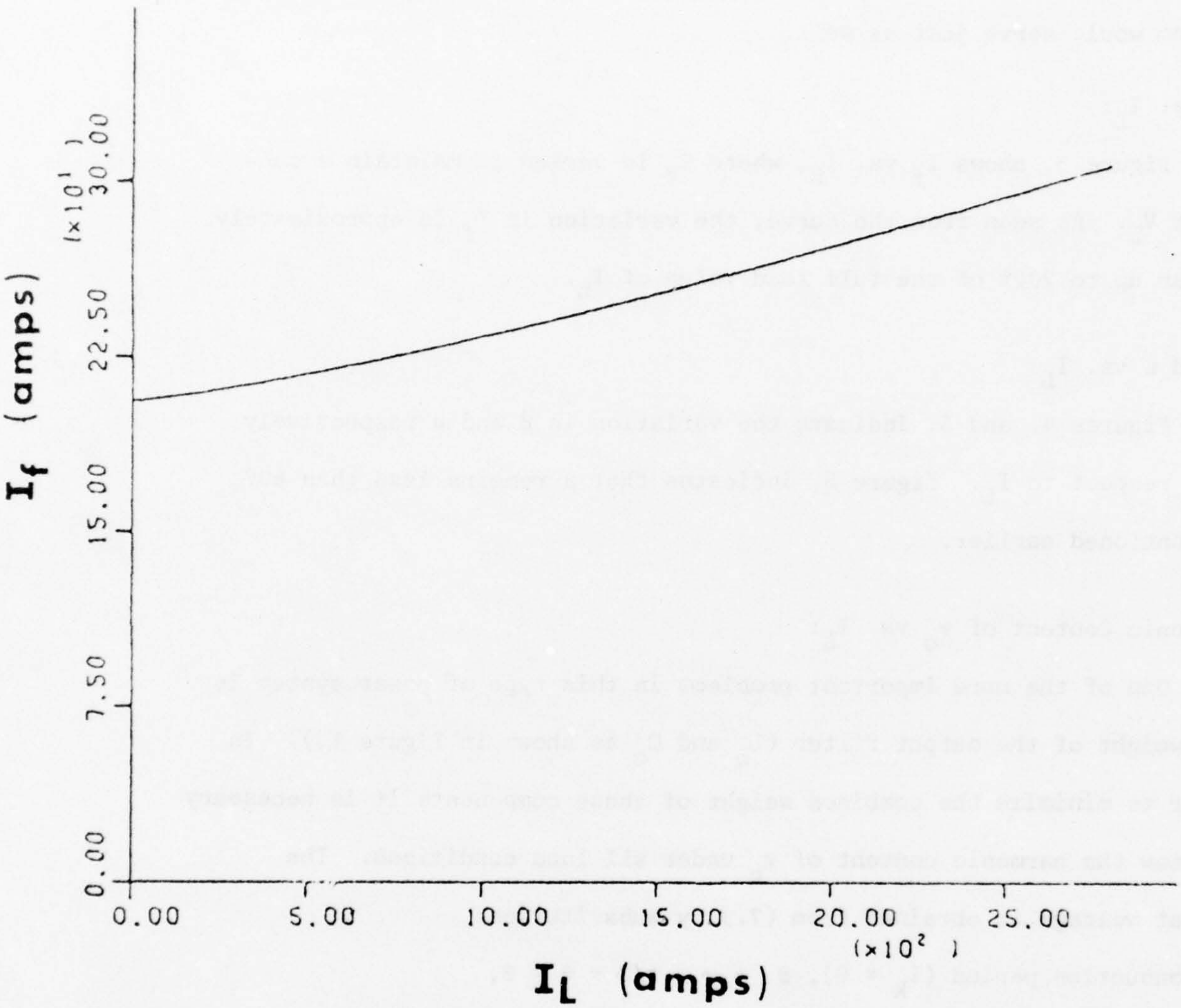

Figure 3. I_f versus I_L with Uncontrolled Rectifier Bridge.

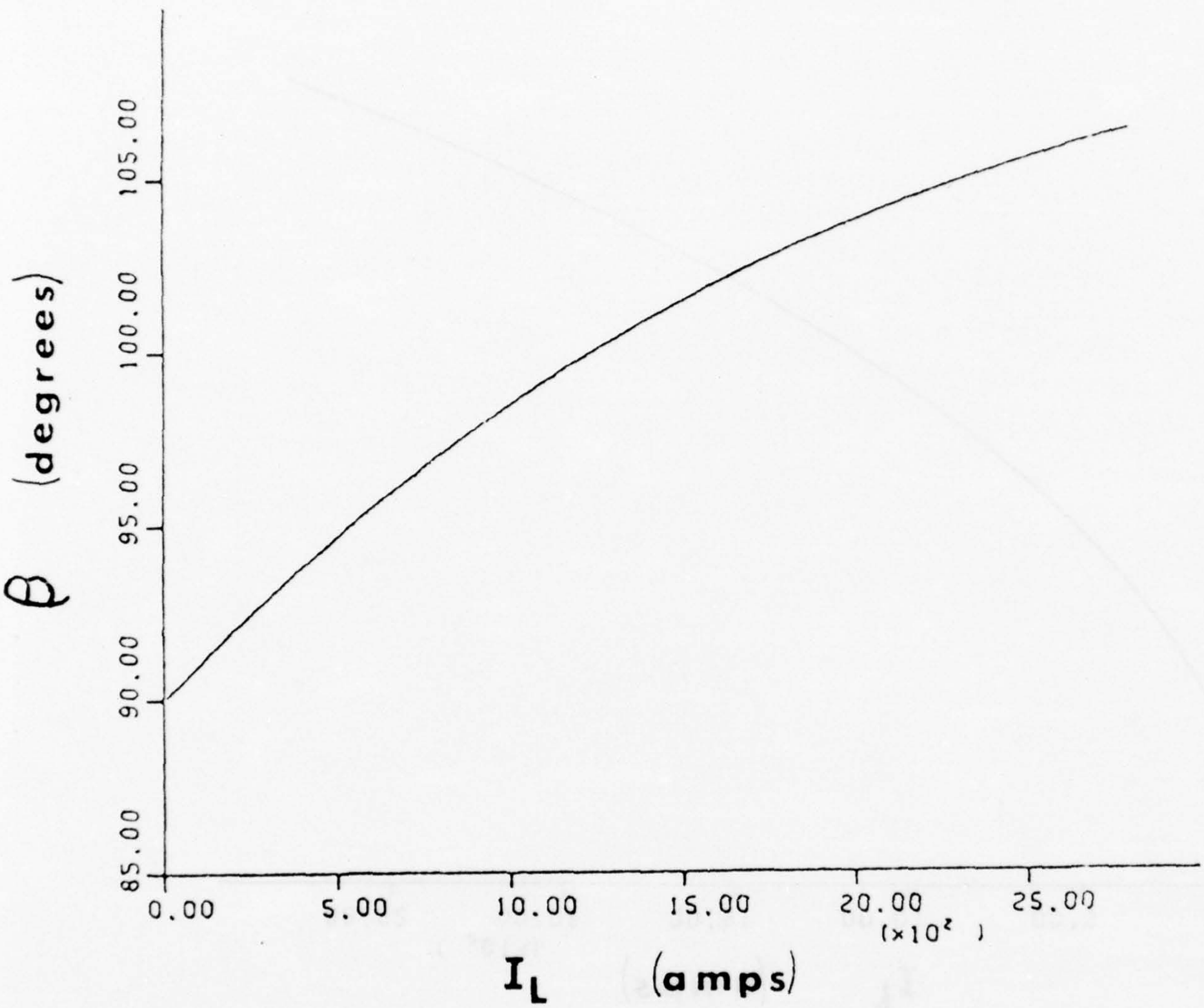

Figure 4. β versus I_L with Uncontrolled Rectifier Bridge.

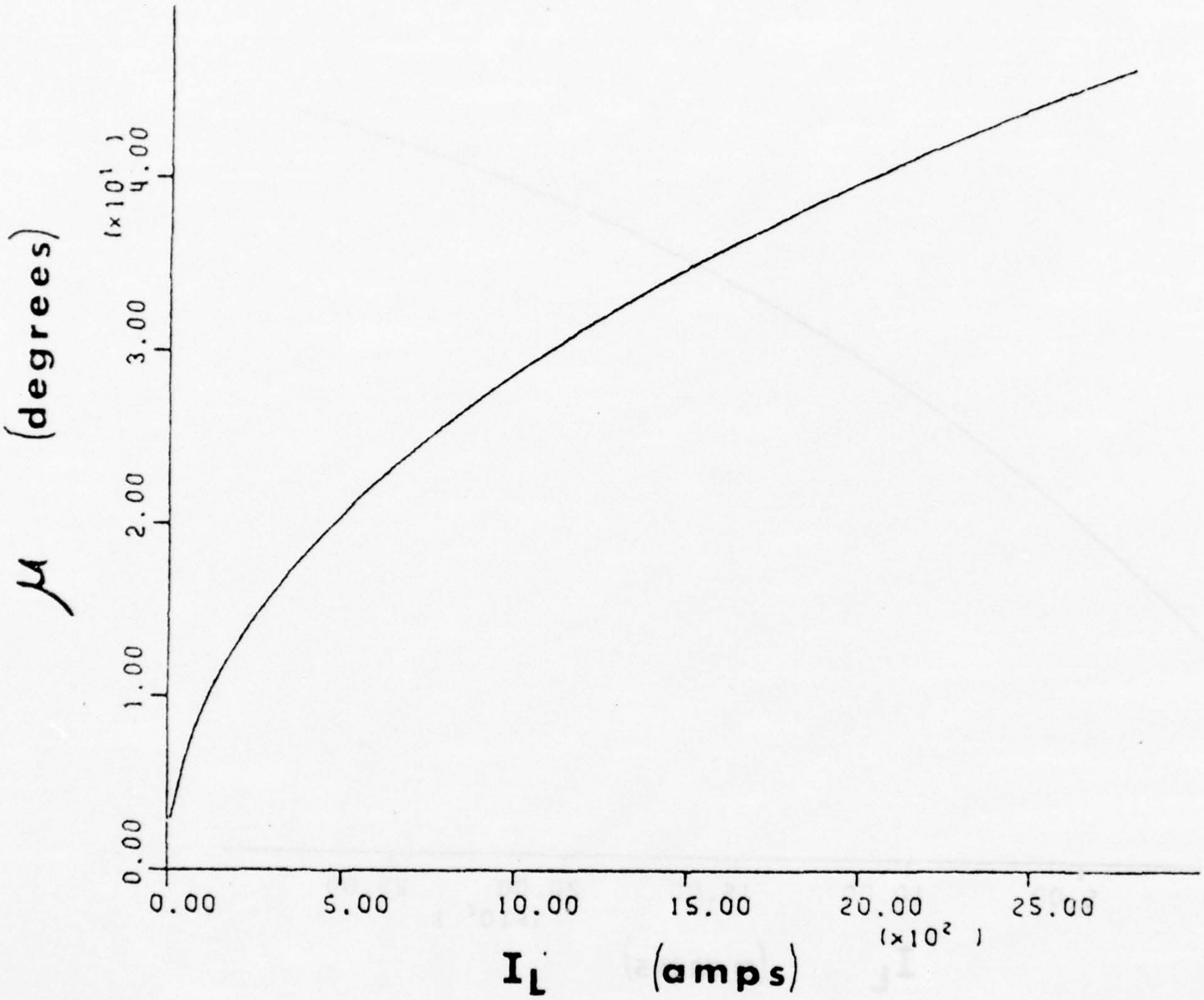

Figure 5. μ versus I_L with Uncontrolled Rectifier Bridge.

$$v_{o23} = v_{012} + \frac{\omega}{\Delta_o}\left(\frac{3M_{oo}}{2} - L_a - M_a\right)\left[\left(\frac{2M_f I_f}{\sqrt{3}} + \frac{6M_{oo}W}{\pi}\right)\cos\theta\right.$$

$$\left. - \frac{6M_{oo}V}{\pi}\sin\theta + \frac{6I_L M_{oo}}{\pi}\cos(\theta-\beta-\mu)\right] \qquad (66.)$$

The Fourier series for v_o *is given by,*

$$v_o = V_L + \sum_{n=6}^{\infty} a_n \cos(n\omega t) + \sum_{n=6}^{\infty} b_n \sin(n\omega t) \quad n = 6,12,18,\ldots \qquad (67.)$$

where $V_L = \frac{6}{\pi}\int_{\beta+\mu-\pi/3}^{\beta} v_{012}\, d\theta + \frac{6}{\pi}\int_{\beta}^{\beta+\mu} v_{023}\, d\theta$ (68.)

$$a_n = \frac{6}{\pi}\int_{\beta+\mu-\pi/3}^{\beta} v_{012}\cos(n\theta)\, d\theta + \frac{6}{\pi}\int_{\beta}^{\beta+\mu} v_{023}\cos(n\theta)\, d\theta \qquad (69.)$$

$$b_n = \frac{6}{\pi}\int_{\beta+\mu-\pi/3}^{\beta} v_{012}\sin(n\theta)\, d\theta + \frac{6}{\pi}\int_{\beta}^{\beta+\mu} v_{023}\sin(n\theta)\, d\theta \qquad (70.)$$

The peak value of the nth harmonic is given by,

$$c_n = (a_n^2 + b_n^2)^{1/2} \qquad (71.)$$

Although tedious, the evaluation of these coefficients is straightforward and will not be included here.

The peak value of the first three ac harmonics of v_o vs. I_L are indicated in Figure 6. As would be expected, the ac content is dominated by the 6th harmonic.

Variation in i_f, i_d, and i_q:

As pointed out in various references ([8] through [11], for example), one of the more critical problems in a superconducting machine is heating due to induced currents in the field winding since this may cause the field to depart from the superconducting mode. The thermal analysis

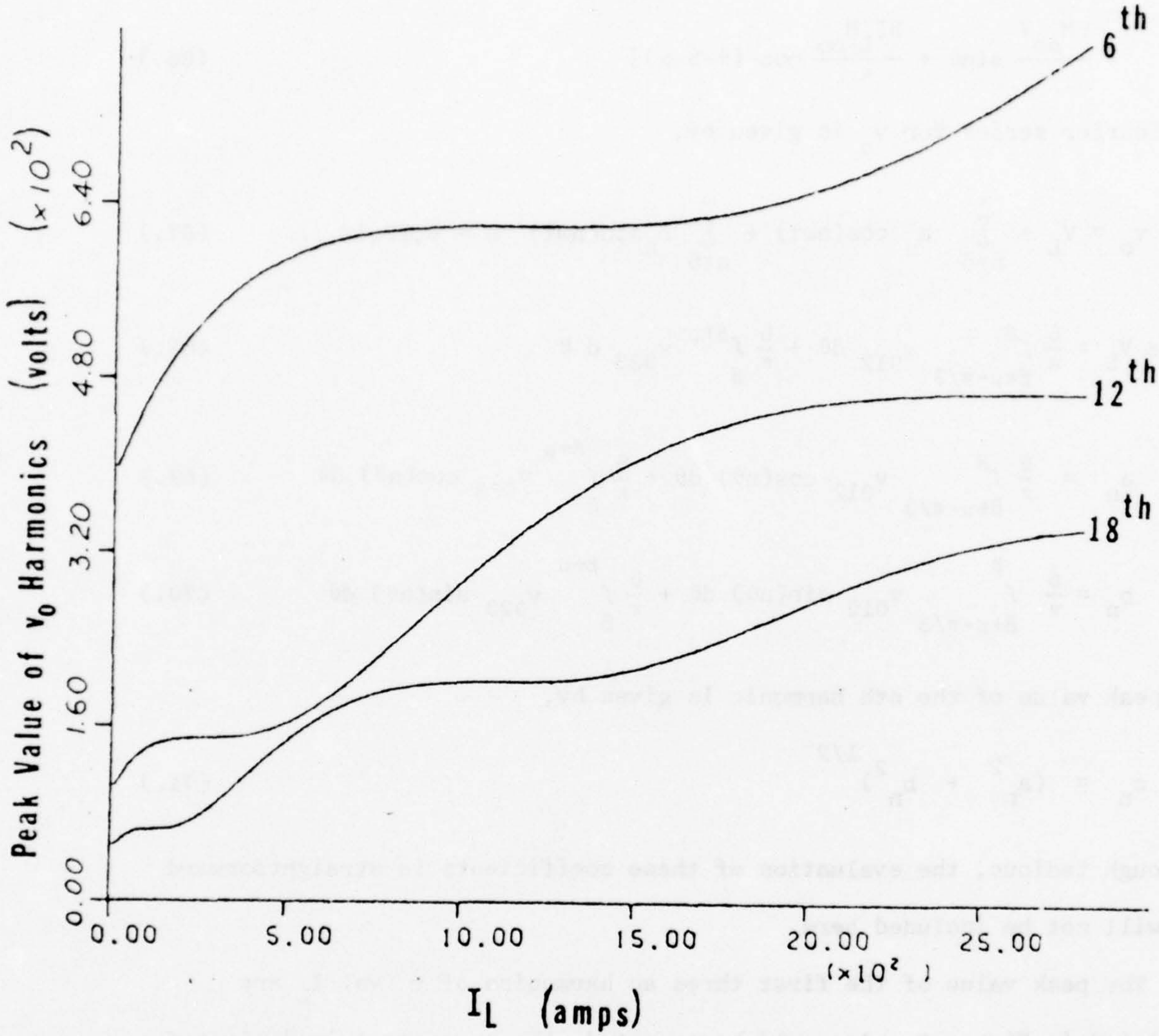

Figure 6. First Three Harmonics of v_o versus I_L with Uncontrolled Rectifier Bridge

of this windinq is bevond the scope of this report, but it is certainly related to the variations in i_f. The instantaneous value of i_f is qiven bv (27.) and plotted as a function of θ in Fiqure 7. The rms value of i_f was obtained bv numerical inteqration and is shown as a function of I_L in Fiqure 8.

Since laboratorv data on an actual rectified superconducting alternator was not available at the time of this report, it is difficult to say how these calculated variables will eventually compare with experimental results. However, an analytical review of the i_f calculations does indicate that the i_f's shown in Figures 7 and 8 may be higher than the actual values. It is believed that the reason for this is that the inductance matrix in (5.) does not fully account for the high frequency attenuation provided by the damper shield. This effect is still under investigation.

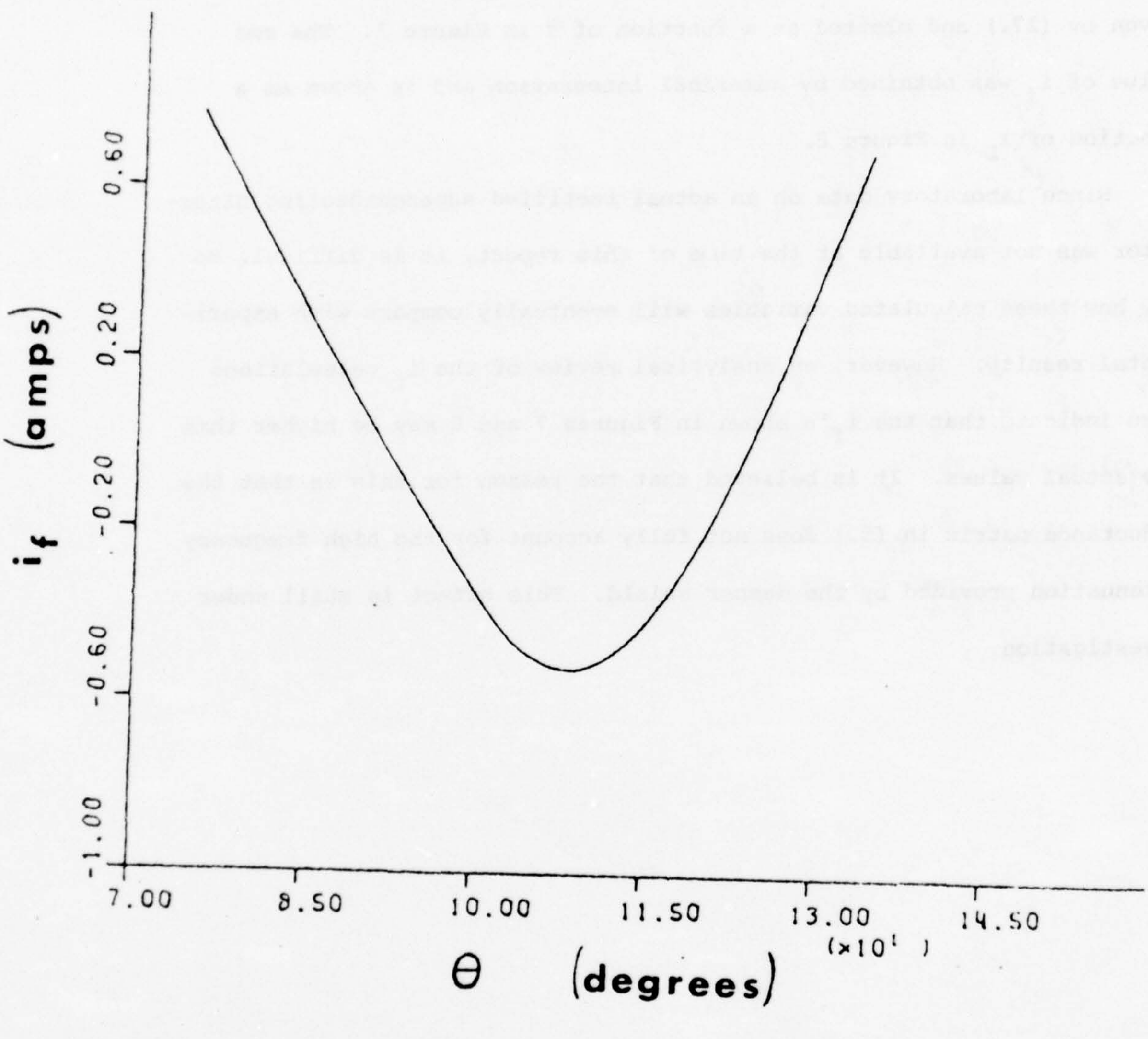

Figure 7. i_f versus θ at Full Load with Uncontrolled Rectifier Bridge. (See text for discussion of i_f calculations.)

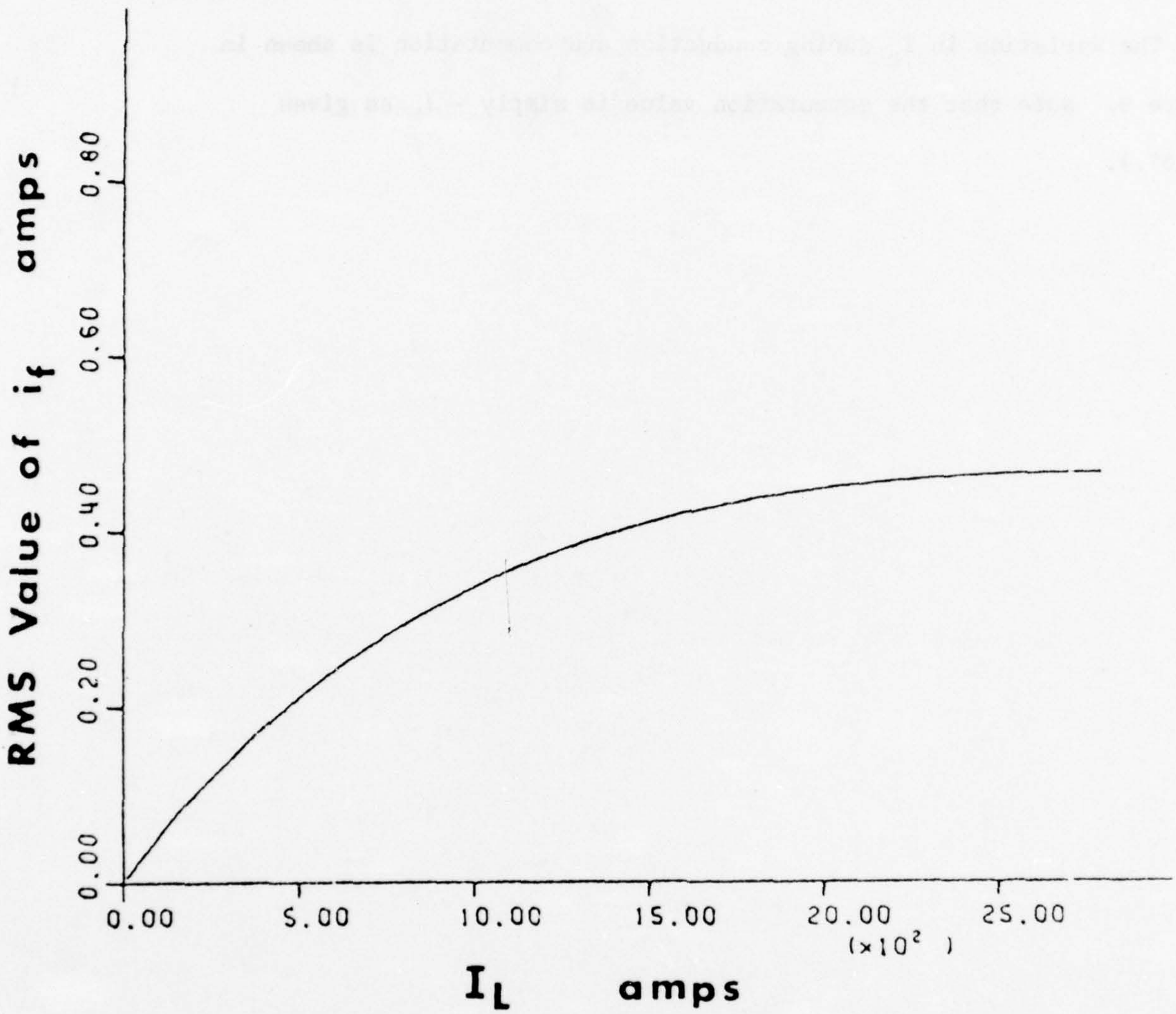

Figure 8. RMS value of i_f versus I_L with uncontrolled Rectifier Bridge. (See text for discussion of i_f calculations.)

Armature Current vs θ:

The variation in i_c during conduction and commutation is shown in Figure 9. Note that the commutation value is simply $-i_k$ as given by (37.).

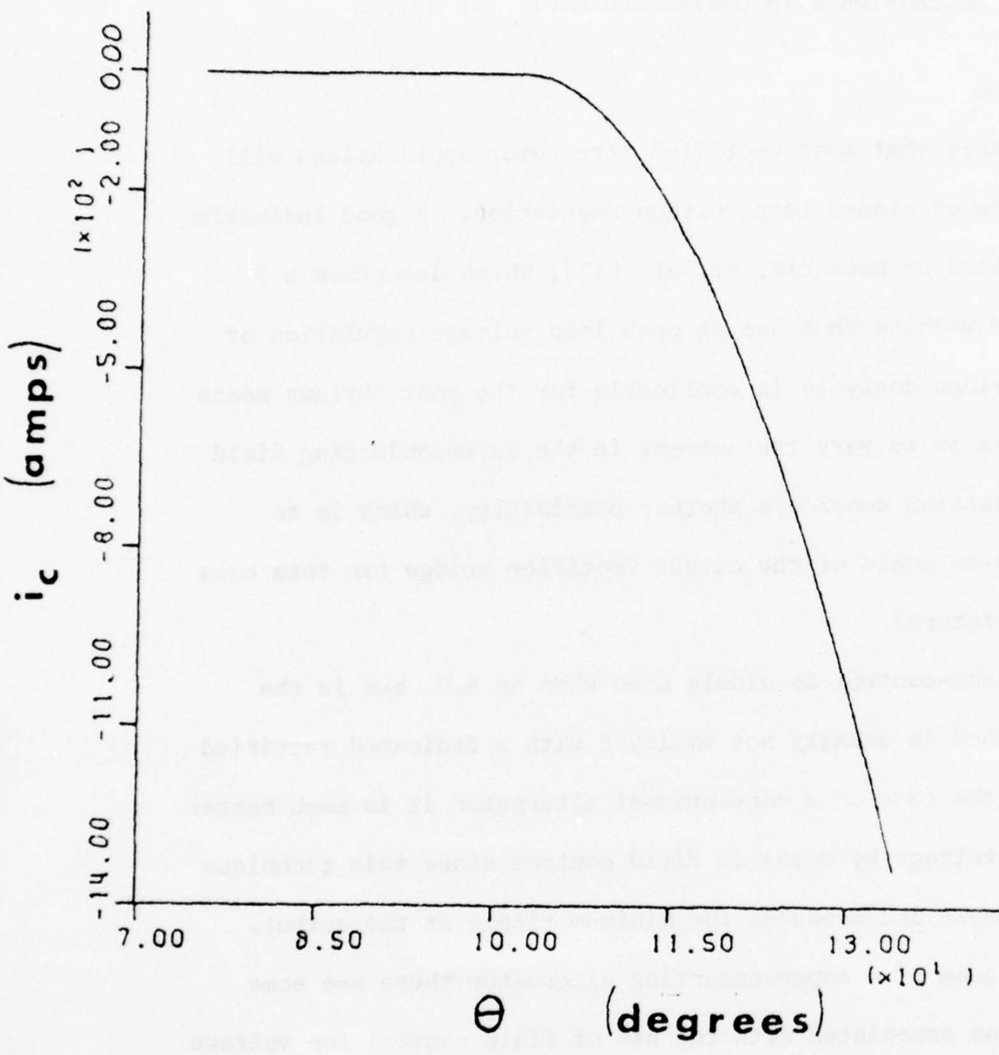

Figure 9. i_c versus θ at Full Load.

2. ALTERNATOR WITH CONTROLLED RECTIFIER BRIDGE

2.1 Introduction

It is probable that most rectified alternator applications will require some type of closed loop voltage regulation. A good indication of this is provided by McCabria, et. al. [13], which describes a 3 phase 10 MVA/5kV machine that has an open loop voltage regulation of 26.5%. The previous analysis is applicable for the most obvious means of control, which is to vary the current in the superconducting field winding. This section considers another possibility, which is to control the turn-on angle of the output rectifier bridge (in this case composed of thyristors).

Although phase-control is widely used when an A.C. bus is the source, this method is usually not employed with a dedicated rectified alternator. In the case of a conventional alternator it is much better to regulate the voltage by means of field control since this technique is relatively simple and produces the minimum ripple at the output. However, in the case of a superconducting alternator there are some potential problems associated with the use of field control for voltage regulation (see [10]). One area of concern is the fact that abrupt variations in field current may cause this winding to leave the superconducting mode. Another problem is the long time constant of the field circuit which produces a very slow step response.

The use of a phase controlled rectifier bridge on the output should provide relatively lower field current variations and a faster step response. It also should be noted that gated devices may be required for the rectifier bridge in order to provide short circuit protection. Thus these same devices can be used to provide voltage regulation.

2.2 Steady State Model

The schematic diagram for the alternator with a controlled rectifier bridge is shown in Figure 10, and the output voltage and current waveforms are shown in Figure 11. The approximations used in this section are identical to those used for the analysis of the uncontrolled rectifier bridge.

2.3 Steady State Equations

Equations (44.) - (48.) of the previous section provide five expressions which can be solved numerically to find the variables I_f, β, μ, V and W. However, with the thyristor bridge, commutation does not start when $v_c = v_b$ but at some later time when $v_c \geq v_b$, i.e., β is controlled externally to produce the desired V_L. This means that (47.) no longer applies since it is based on $v_c = v_b$ at $\theta = \beta$.

Therefore, there are only four equations to work with, (44.), (45.), (46.) and (48.), and I_f is held constant slightly above the minimum value required for maximum I_L.

$$\text{Let, } \underline{x}' \equiv \begin{bmatrix} \beta \\ \mu \\ V \\ W \end{bmatrix} \tag{72.}$$

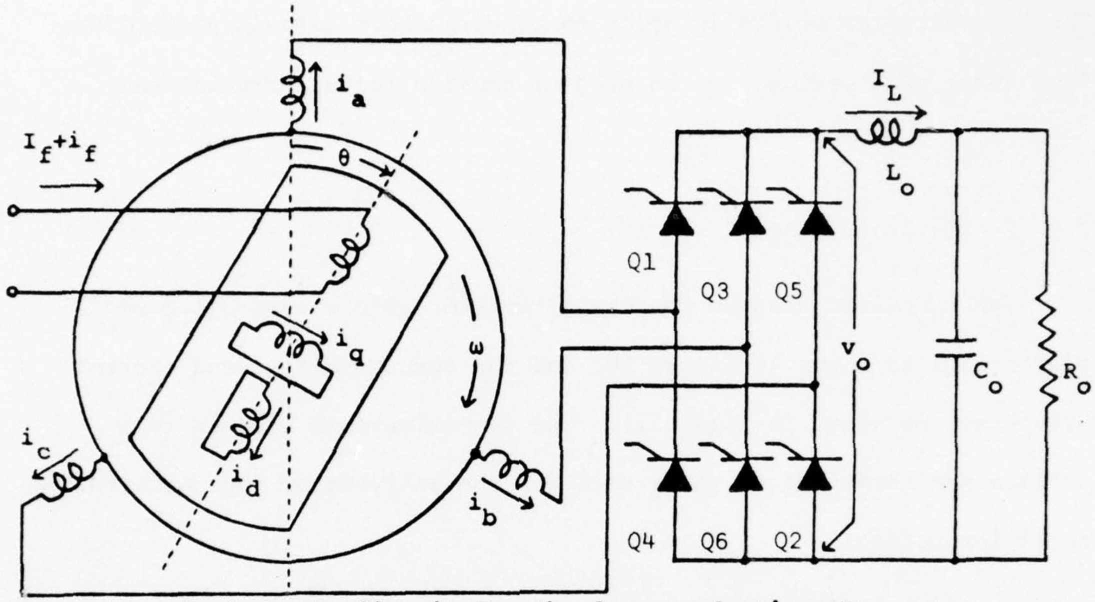

Figure 10. Equivalent Circuit for the Superconducting Alternator with Controlled Rectifier Bridge.

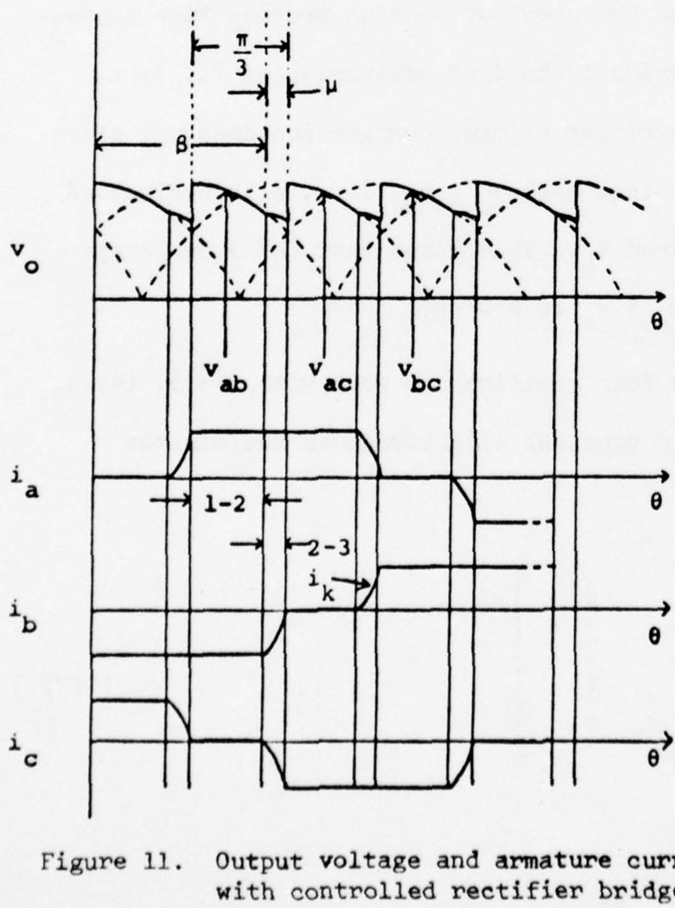

Figure 11. Output voltage and armature currents for the alternator with controlled rectifier bridge.

$$\underline{f}'(\underline{x}') \equiv \text{R.H.S. of} \begin{bmatrix} (44.) \\ (45.) \\ (46.) \\ (48.) \end{bmatrix} \tag{73.}$$

A solution for $\underline{x}'$ can be obtained from the standard Newton-Raphson equation,

$$F(\underline{x}'_o)\,(\underline{x}' - x'_o) = \underline{f}'(\underline{x}') - \underline{f}'(\underline{x}'_o) \tag{74.}$$

where $\underline{x}'_o$ is some initial starting point sufficiently close to $\underline{x}'$ and,

$$F(\underline{x}'_o) = \text{the Jacobian matrix} = \left.\frac{\partial \underline{f}'(\underline{x}')}{\partial \underline{x}'}\right|_{\underline{x}'=\underline{x}'_o} \tag{75.}$$

A satisfactory value for $\underline{x}'_o$ is obtained by using the previous diode bridge solution, $\underline{x}$, where I_f is a variable, or by using the approximate method reported by Franklin in [17,18].

2.4 Numerical Results

This numerical example is based on the same 4 pole, 400 Hz., 10 MVA/5kV superconducting machine used in the previous example. The same full load conditions are assumed,

$$\begin{aligned} V_L &= 6760 \text{ V.D.C.} \\ I_L &= 1420 \text{ A.D.C.} \end{aligned} \tag{76.}$$

The minimum value of I_f that will produce $I_L = 1420\text{A}$ corresponds to the solution for the uncontrolled rectifier bridge (i.e., minimum β). This current is found from the first section,

$$I_{f(\min.)} = 250\text{A}. \tag{77.}$$

In an actual system it will be desirable to set I_f at some value above that given by (77.). This will insure against low voltage if I_f decreases for any reason. For this example, the high value, $I_{f(max.)}$, was arbitrarily taken to be,

$$I_{f(max.)} = 1.1\, I_{f(min.)} \tag{78.}$$

A plot of I_f vs. I_L for both the controlled and uncontrolled rectifier bridge is shown in Figure 12.

β, μ, the first three harmonics of v_o, and the rms value of i_f are plotted vs. I_L in Figures 13 through 18 respectively. Note that the corresponding values for the diode bridge case are included for reference purposes.

As would be expected, Figure 13 indicates that the thyristor bridge β must exceed the diode bridge β to compensate for the higher I_f. The thyristor bridge β also drops as I_L increases in order to compensate for the higher voltage drop across the armature windings.

Figure 14 reveals an interesting characteristic in that the μ for the thyristor bridge is considerably less than the μ for the diode bridge. This is not too surprising when Figures 10 and 11 are considered. Referring to these figures, it is observed that because of the delayed β_1 commutation from b to c does not start until $v_{bc} > 0$. Therefore, more voltage is present to force the commutation process than in the diode case where commutation begins at $v_{bc} = 0$. Because of this higher v_{bc}, i_b will be driven to zero in less time, thus producing a smaller μ for the thyristor case.

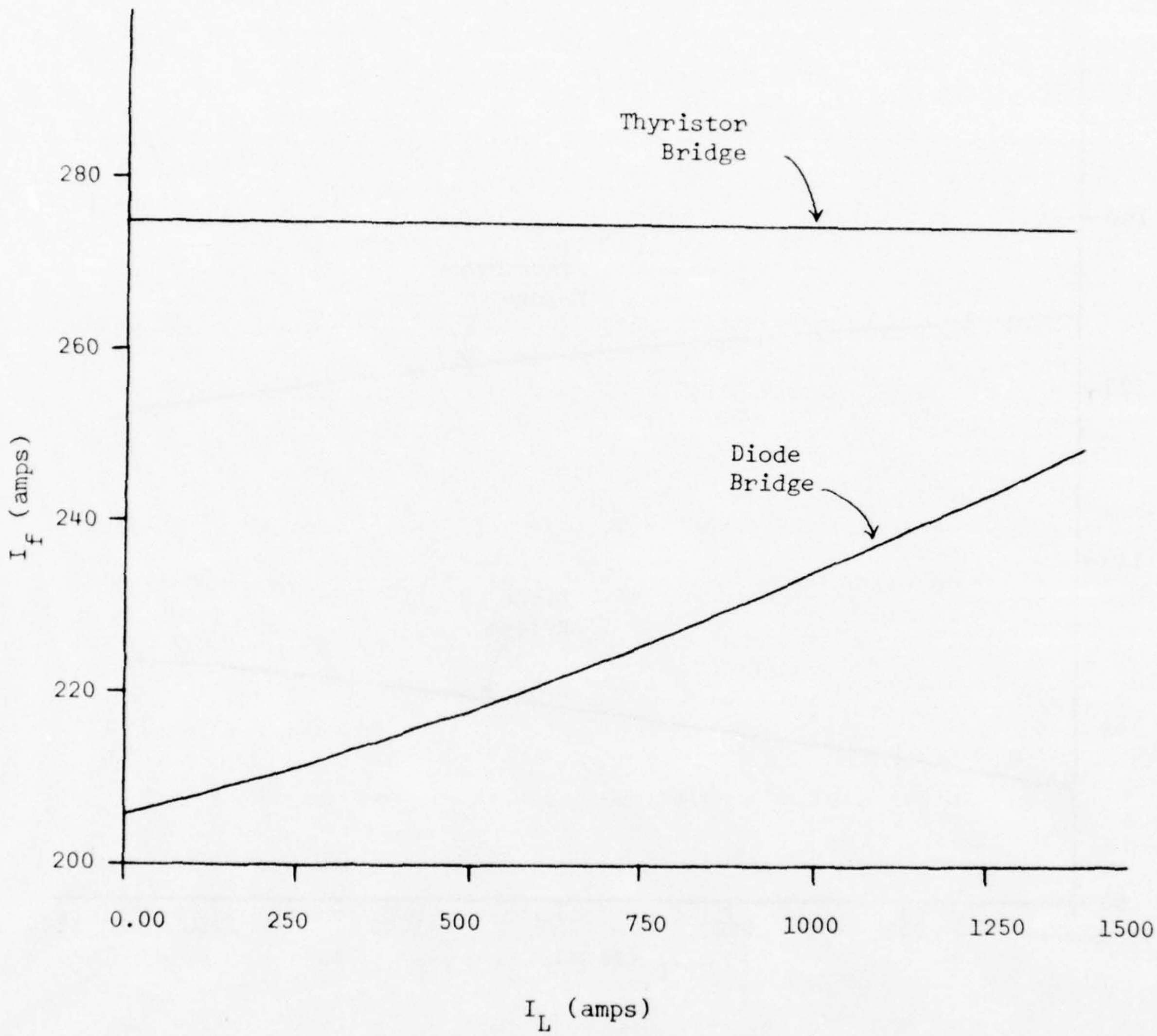

Figure 12. I_f vs. I_L for both the thyristor bridge and the diode bridge.

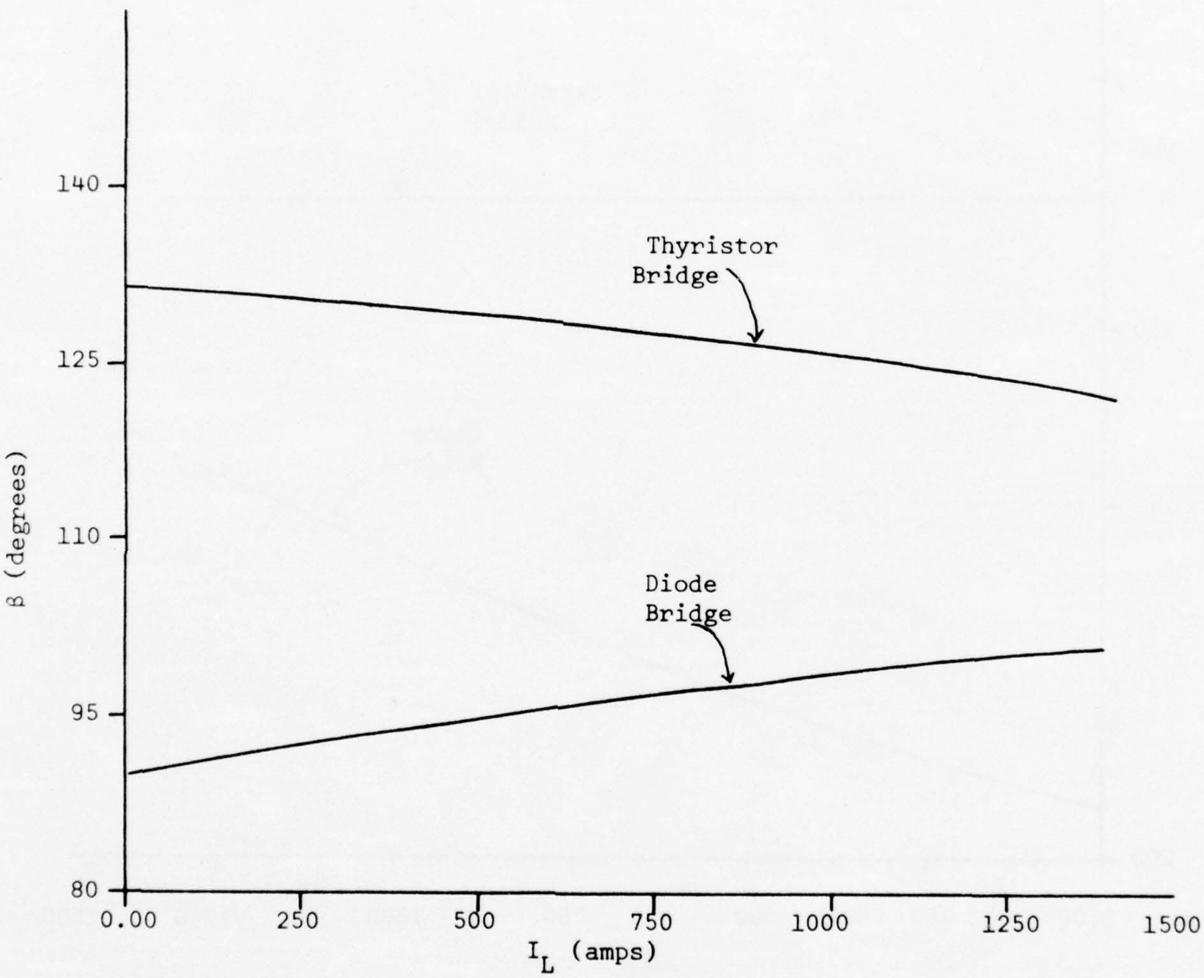

Figure 13. β vs. I_L for both the thyristor bridge and the diode bridge.

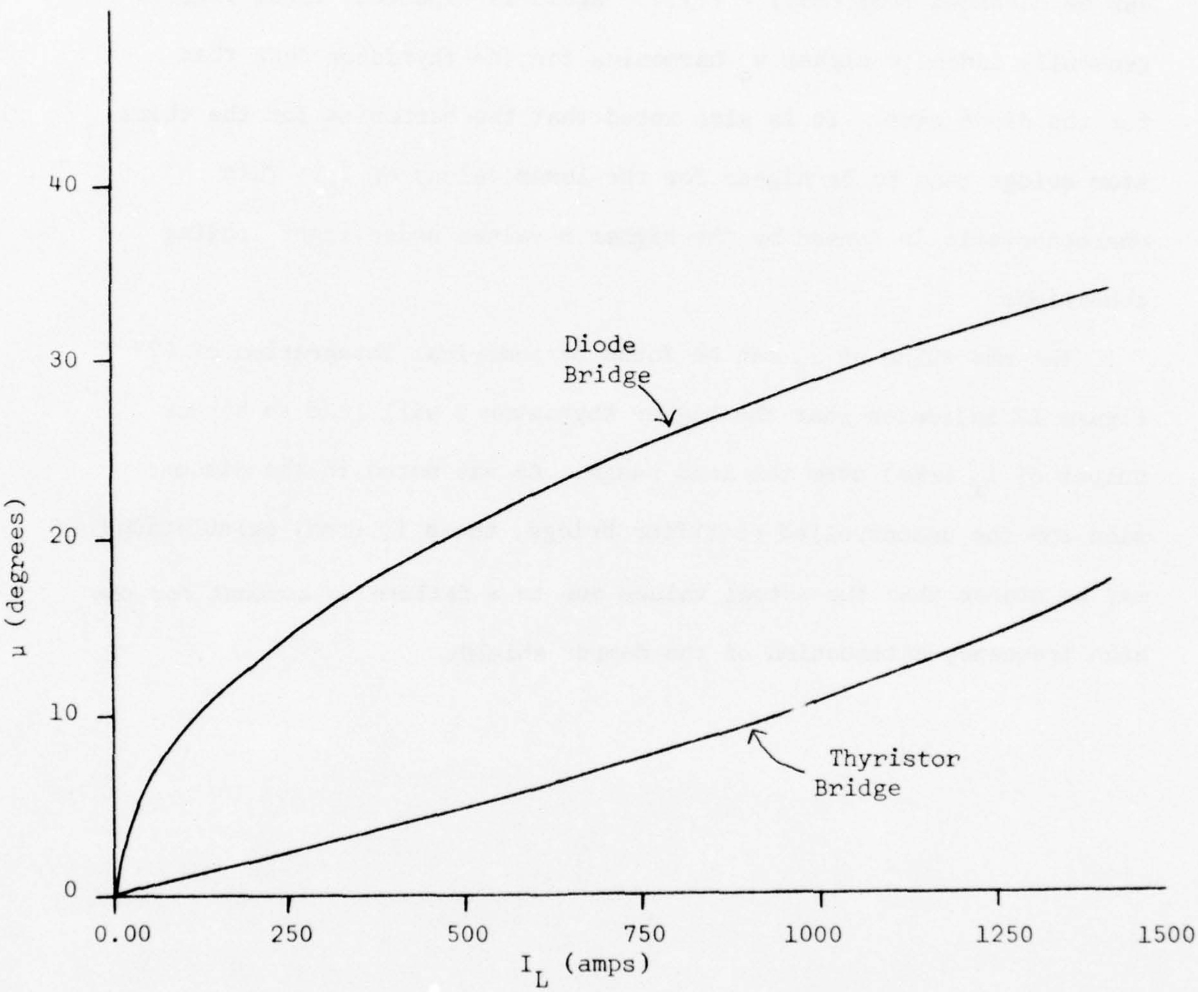

Figure 14. μ vs. I_L for both the thyristor bridge and the diode bridge.

The voltage harmonics shown in Figure 15 to 17 are obtained by calculating the Fourier coefficients of the output voltage, v_o, which can be obtained from (65.) - (71.). Again as expected, those figures generally indicate higher v_o harmonics for the thyristor case than for the diode case. It is also noted that the harmonics for the thyristor bridge tend to be higher for the lower values of I_L. This characteristic is caused by the higher β values under light loading conditions.

The rms value of i_f can be found by numerical integration of (27.). Figure 18 indicates that the higher thyristor β will lead to higher values of i_f (rms) over the load range. As was noted in the discussion for the uncontrolled rectifier bridge, these i_f (rms) calculations may be higher than the actual values due to a failure to account for the high frequency attenuation of the damper shield.

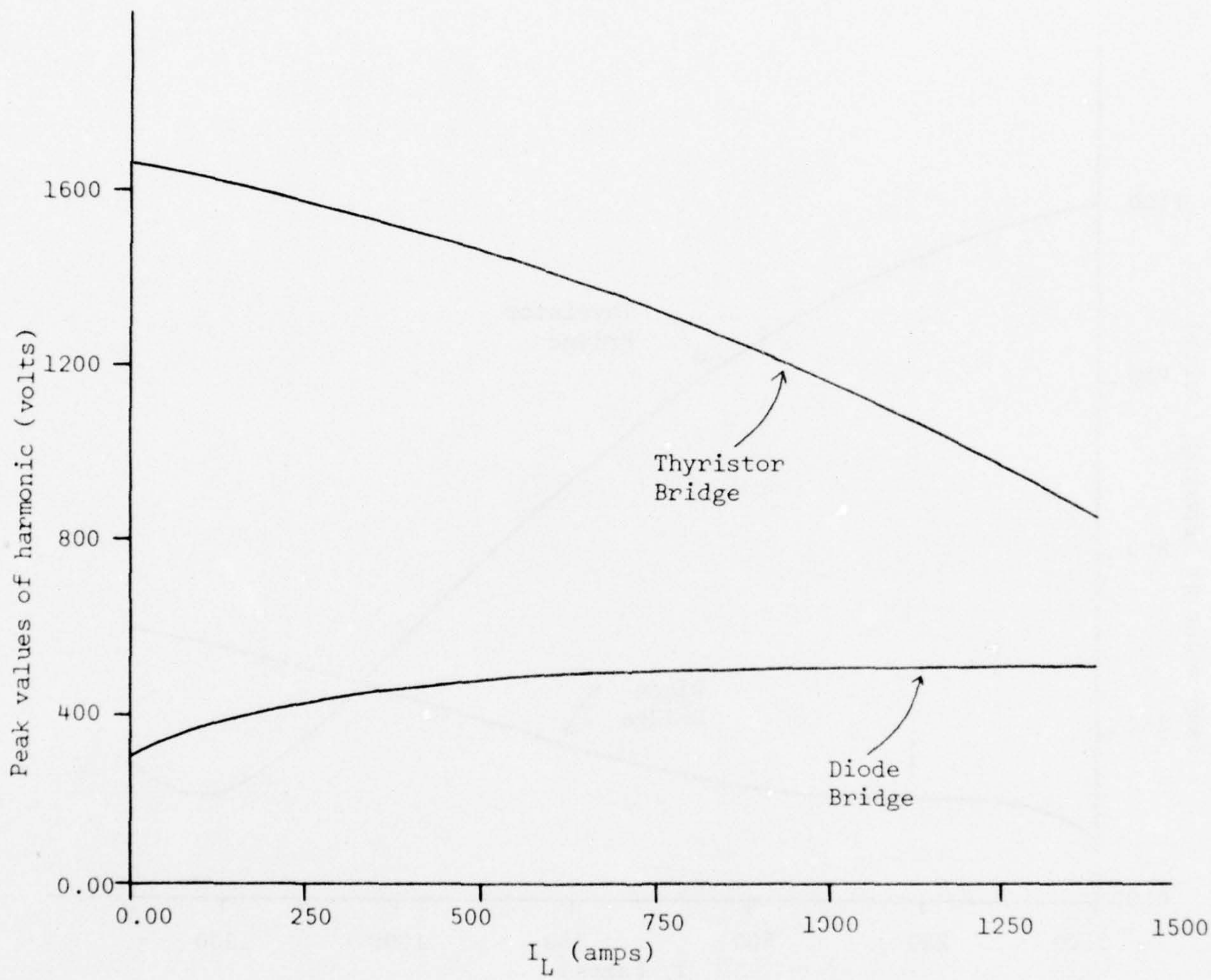

Figure 15. 6th harmonic of v_o vs. I_L for both the thyristor bridge and the diode bridge.

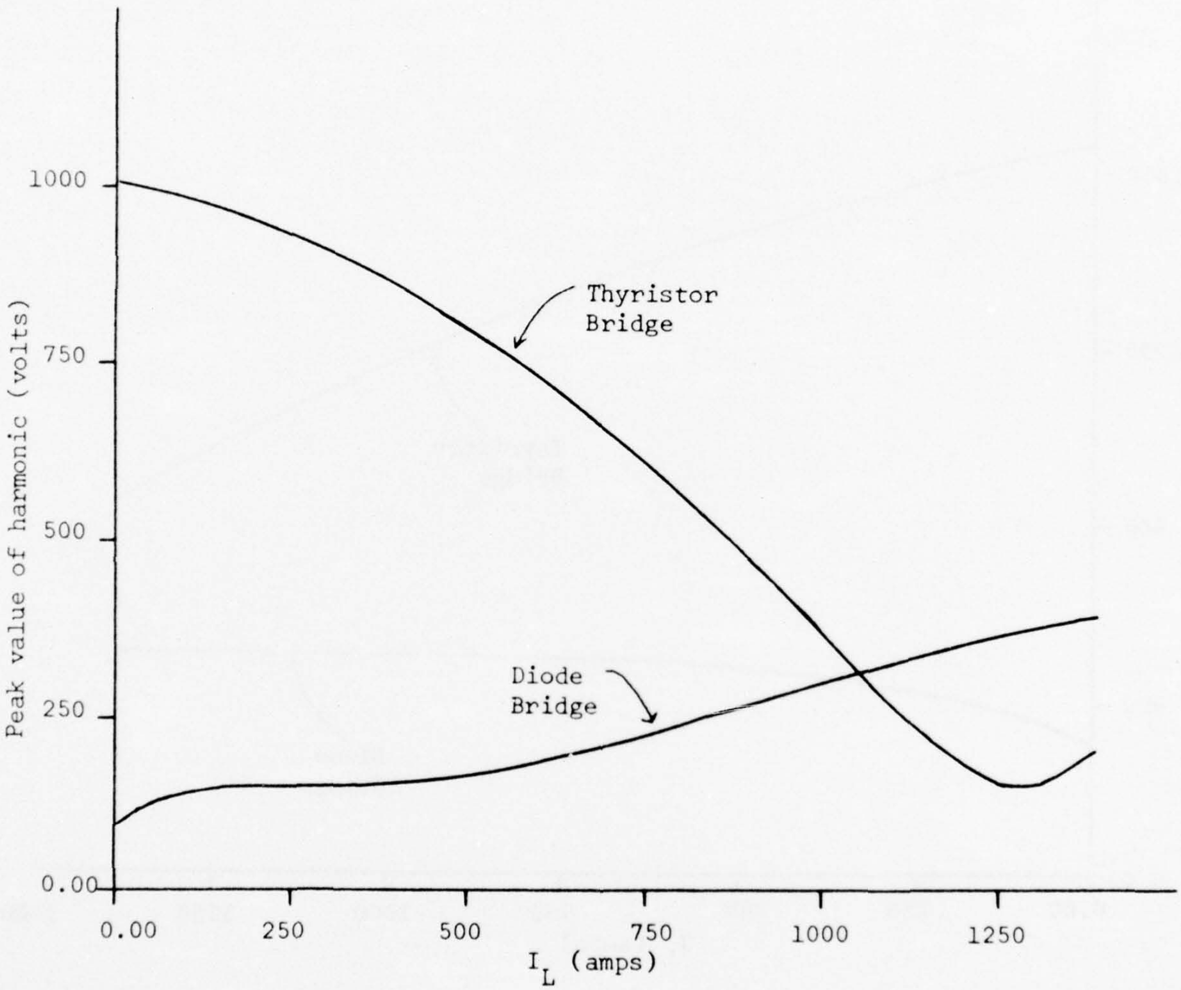

Figure 16. 12th harmonic of v_o vs. I_L for both the thyristor bridge and the diode bridge.

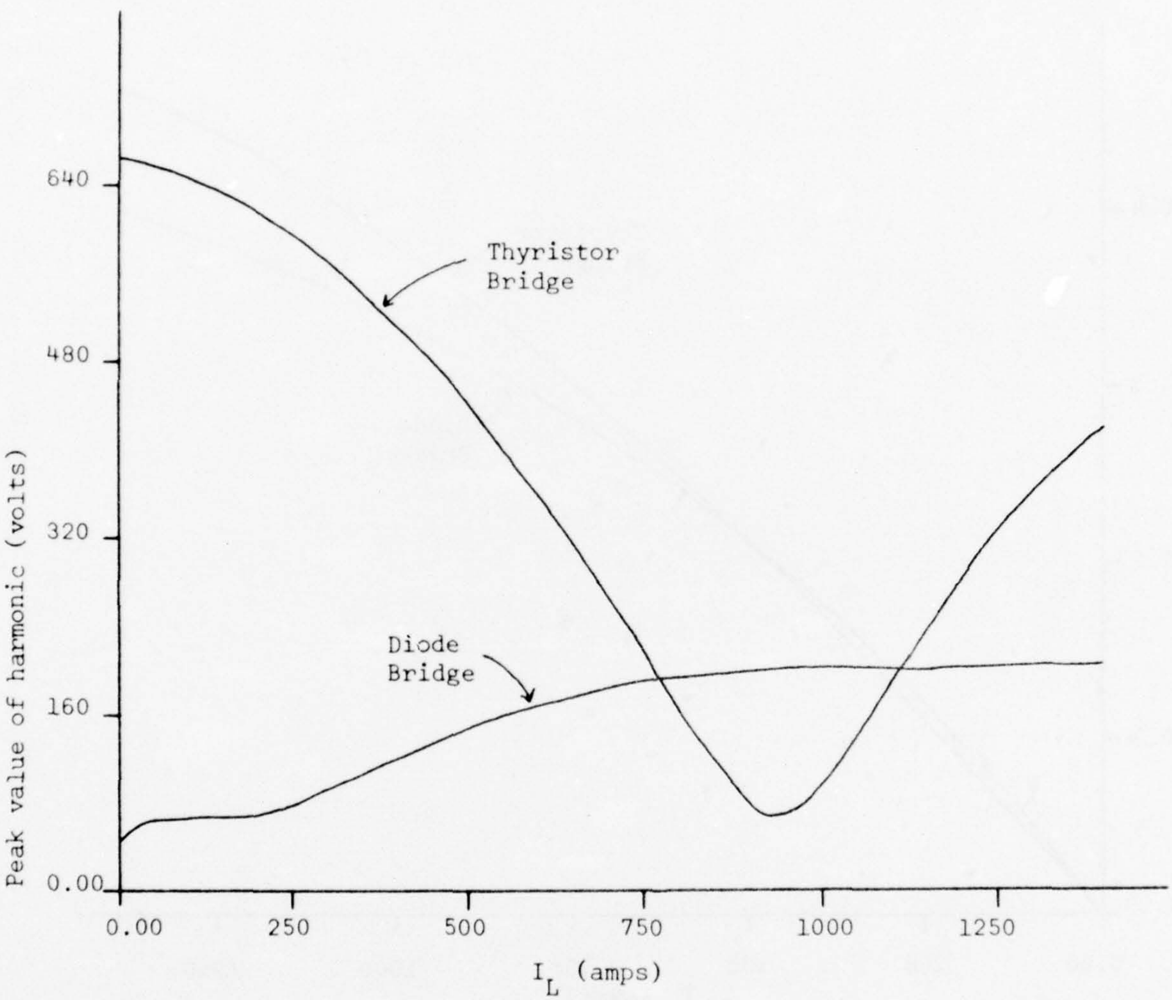

Figure 17. 18th harmonic of v_o vs. I_L for both the thyristor bridge and the diode bridge.

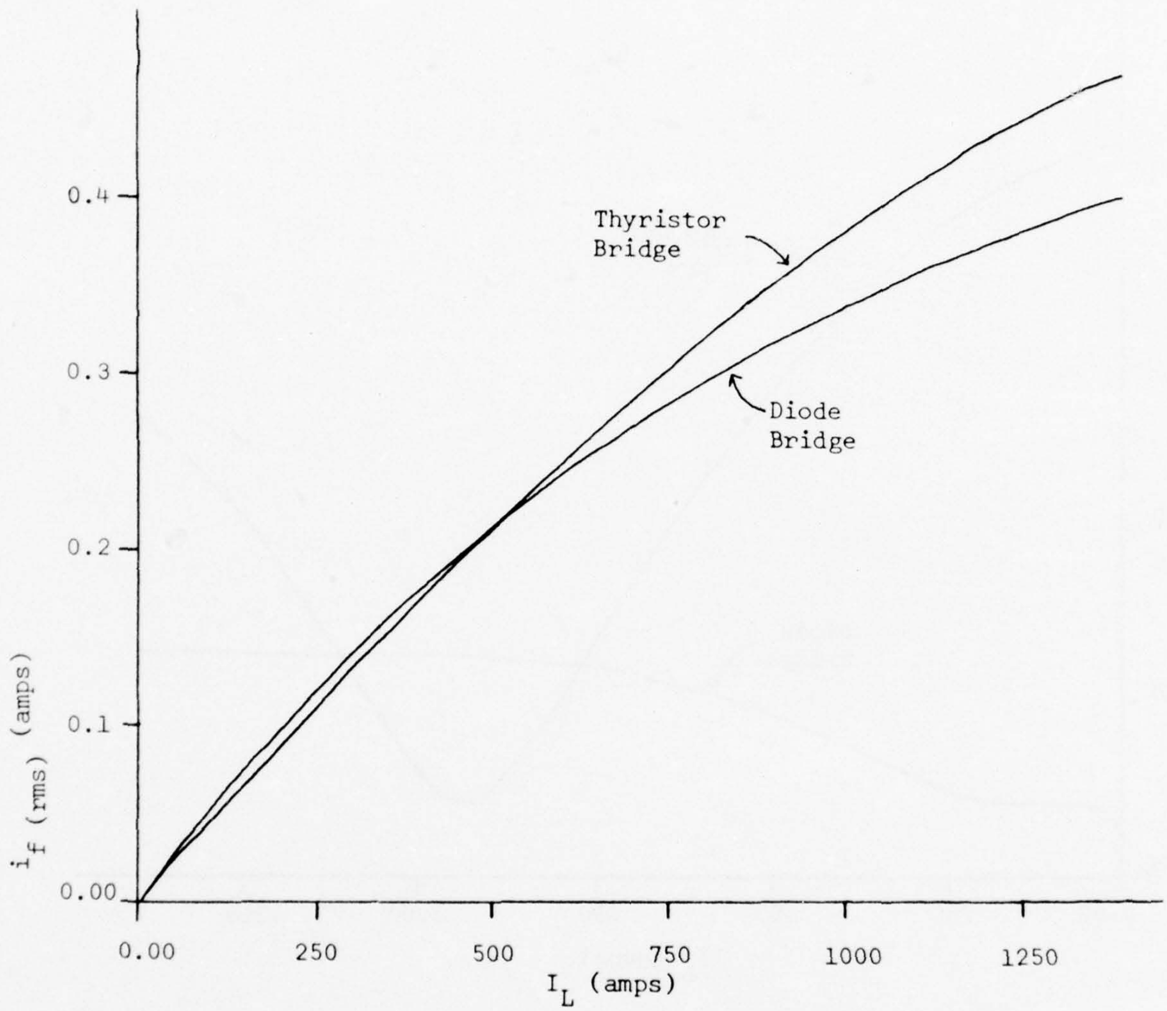

Figure 18. $i_{f\ (rms)}$ vs. I_L for both the thyristor bridge and the diode bridge.

3. FAULT CURRENT CALCULATIONS

3.1 Introduction

This discussion is based only on the controlled rectifier bridge configuration shown in Figure 10. The reason for this choice is that this circuit has the capability of fast turn off in the event of a fault. Fast turn off can be achieved by the system in Figure 1 only if some type of series switch is added to the circuit.

In addition to filtering the output voltage, the inductor, L_o, in Figure 10 must be capable of limiting I_L in the event of a short across the load. The length of time that L_o must perform this function is limited however, since the bridge can be turned off on the next cycle after the fault is detected. It is also common to select L_o to limit the C_o charging current when the system is initially turned on. This can also be accomplished by a further delay in β however, so charging current will not be used as a constraint in this analysis.

To determine if L_o is of adequate size, it will be necessary to calculate the transient load current, i_{LF}, that occurs after the fault. Since the differential equations involved have time varying coefficients, a numerical solution will be required. In this particular study it is assumed that the fault occurs at the beginning of a conduction period and that the bridge will not be turned off until this conduction period, the next commutation period, and a final conduction period are complete. This corresponds to the interval, AE, shown in Figure 19. The rationale behind this choice is that some time is required for i_{LF} to exceed $I_{L(max.)}$, at which time a current overload sensing circuit is enabled to

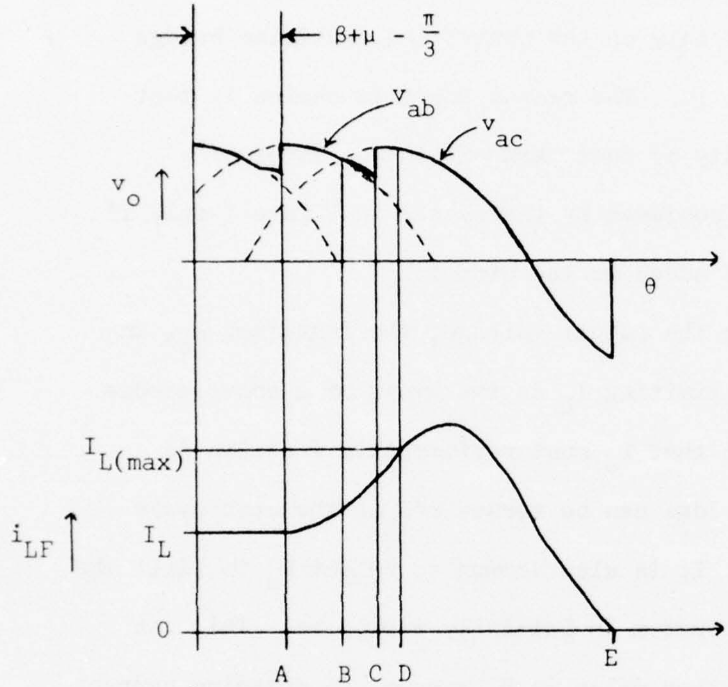

A: Fault occurs at the start of a conduction period
B: On-coming thyristors fire and commutation begins
C: Commutation interval ends
D: $I_{L(max)}$ is exceeded, next trigger signal is blanked
E: i_{LF} decays to 0

Figure 19. Transient Behavior for the Controlled Rectifier Bridge.

blank all the thyristor gate signals. Other choices are certainly possible, such as assuming that the fault occurs at the start of a commutation period and that the thyristor gates are blanked before the next firing pulse.

3.2 Circuit Model and Equations

Figure 20 represents the equivalent circuit with phase "a" conducting and a short across the load. Note that the armature resistance R_a and the parasitic resistance of the filter choke, R_p, have been included since they aid in limiting the fault current. The periods AB, BC, etc. in Figure 19 will correspond to the following thyristors being on:

Period	Thyristors Conducting
AB, conduction	Q1, Q6
BC, commutation	Q1, Q6, Q2
CE, conduction	Q1, Q2

The steady state analysis has assumed that the winding resistances are negligible. That practice will be continued here for all windings except those on the armature; as before, it implies that λf, λd and λq are approximately constant over the relatively short transient period, AE, and that the voltages across the closed f, d and q windings are approximately zero.

The equations for the commutation period, BC, are found to be,

$$[A] \frac{d\underline{i}}{dt} = [B] \underline{i} \tag{79.}$$

where

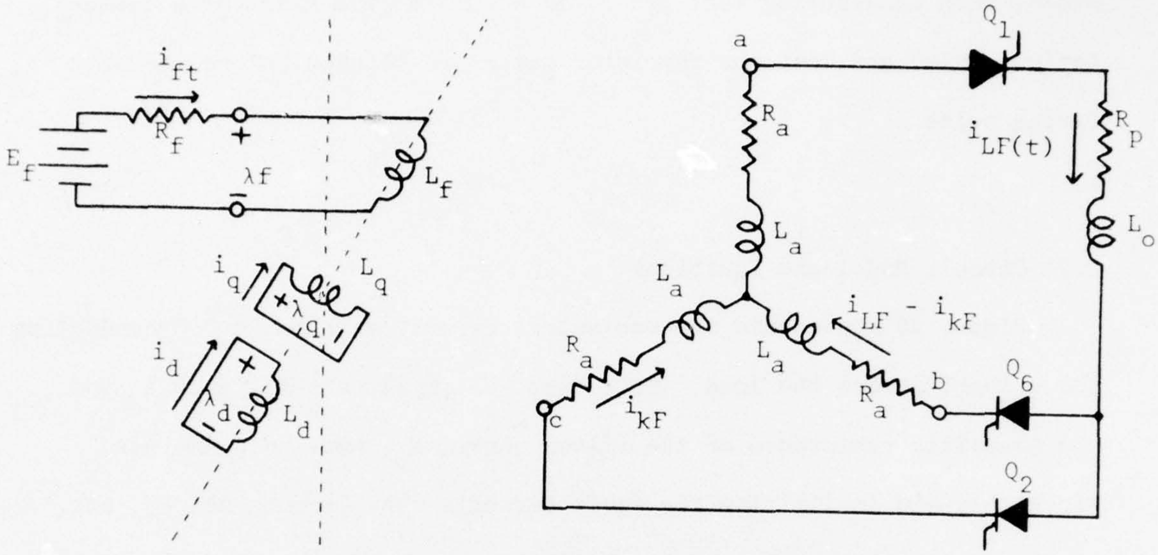

Figure 20. Equivalent circuit for conduction and commutation periods while fault is present.

$$\underline{i} \equiv \begin{bmatrix} i_{LF} \\ i_{f(tot)} \\ i_d \\ i_q \\ \hdashline i_{kF} \end{bmatrix} \equiv \begin{bmatrix} \underline{i}' \\ \hdashline i_{kF} \end{bmatrix} \qquad (80.)$$

and the [A] and [B] matrices are defined in Appendix II.

The equations for the conduction period, AB, (Q2 off) can be expressed in a similar manner,

$$[A_{11}] \frac{d\underline{i}'}{dt} = [B_{11}] \underline{i}' \tag{81.}$$

where $[A_{11}]$, $[B_{11}]$ and $\underline{i}'$ are submatrices of [A], [B] and $\underline{i}$. These submatrices are also defined in Appendix II.

Since the fault is assumed to occur at A in Figure 19, (81.) will be solved first, then (79.). It is unnecessary to formulate equations specifically for the second conduction period, CE, since this period can be analyzed by using (81.).

As predicted earlier, [A] and [B] have time dependent elements. This implies that $\underline{i}$ must be found by some numerical integration technique. The modified Euler method was chosen for this particular study, but other techniques could also be employed.

Starting with the conduction period, AB, (81.) can be solved for $\frac{d\underline{i}'}{dt}$ at each time increment, Δt, and the next value of $\underline{i}'$ can then be found by using the standard modified Euler equations (see [27.]). This process is simplified however, if the approximation of constant λf, λd, and λq is again utilized. Writing the flux linkage equations for the most general case (the commutation period, BC), one obtains,

$$\begin{bmatrix} \lambda f \\ \lambda d \\ \lambda q \end{bmatrix} = \begin{bmatrix} \sqrt{3}\, M_f \cos(\omega t+\pi/6) \\ \sqrt{3}\, M_d \cos(\omega t+\pi/6) \\ \sqrt{3}\, M_d \sin(\omega t+\pi/6) \end{bmatrix} i_{LF} + \begin{bmatrix} \sqrt{3}\, M_f \sin(\omega t) \\ \sqrt{3}\, M_d \sin(\omega t) \\ \sqrt{3}\, M_d \cos(\omega t) \end{bmatrix} i_{kF}$$

(cont.)

$$+ \begin{bmatrix} L_f & M_{fd} & 0 \\ M_{fd} & L_d & 0 \\ 0 & 0 & L_d \end{bmatrix} \begin{bmatrix} i_{f(tot)} \\ i_d \\ i_q \end{bmatrix} \tag{82.}$$

or in vector notation, $\underline{\lambda}_{fdq} = \underline{x} i_{LF} + \underline{y}\ i_{kF} + [C]\ \underline{i}_{fdq}$. (83.)

$\underline{\lambda}_{fdq}$ can be found initially by substituting the steady state values for $\underline{i}_{fdq}$, i_{LF} and i_{kF} at $\omega t = \beta+\mu-\pi/3$ (i.e., $\underline{i}_{fdq}$ is found from (25.), (26.), (27.) and $i_{LF} = I_L, i_{kF} = 0$). At each time increment i_{LF} and i_{kF} can be found from the modified Euler equations while $\underline{i}_{fdq}$ can be found from (83.) (using the constant value of $\underline{\lambda}_{fdq}$).

Figure 19 indicates that the firing angle is delayed before the fault, but not afterwards (point B). The reason for this is that once the output is shorted the voltage regulator will call for the minimum firing angle, and the oncoming thyristors will conduct as soon as possible. Since the load current is no longer constant, the steady state equations that yield β(min.) (i.e., the firing angle for an uncontrolled rectifier bridge) do not apply, and the firing angle (point B) must be found by determining the first point at which $v_{bc} \geq 0$. As v_{bc} becomes positive Q2 will start to conduct and the commutation of Q6 will commence. V_{bc} for the AB conduction state can be readily found from the bc loop,

$$\begin{aligned} v_{bc} = {} & R_a\ i_{LF} + (L_a+M_a)\frac{di_{LF}}{dt} - \sqrt{3}\sin(\omega t)\left(M_f \frac{di_{f(tot)}}{dt} + M_d \frac{di_d}{dt}\right) \\ & - \sqrt{3}\ M_d \cos(\omega t)\frac{di_q}{dt} - \sqrt{3}\ \omega\cos(\omega t)\left(M_f\ i_{f(tot)} + M_d\ i_d\right) \\ & + \sqrt{3}\ \omega\ M_d \sin(\omega t)\ i_q \end{aligned} \tag{84.}$$

v_{bc} is tested at each time increment of the AB interval; at the first point where $v_{bc} \geq 0$ the computer program branches to the equations for the BC commutation interval. It will also be necessary to perform some test to determine when the commutation period ends at point C. This is done by comparing i_{LF} and i_{kF} at each time increment of the BC interval; the commutation period ends at the first point where $i_{kF} \geq i_{LF}$.

It should be noted that it may take several machine cycles to commutate the thyristors after the firing signals have been blanked. This can be illustrated conceptually by the simplified model shown in Figure 21 (this model is of little quantitative use however, since it does not account for the winding resistances and inductances of the machine). If $e_{s(t)} = v_{ab}$ and the thyristors start to conduct at $\omega t = \pi/3$ (approximate), $i_{(t)}$ will have the form,

$$i_{(t)} = I_L + \frac{\sqrt{2}V}{\omega L_o}(1/2 - \cos(\omega t)) \qquad (85.)$$

where I_L = load current at $\omega t = \pi/3$.

At $\omega t = \frac{2\pi}{3}$ (approximate), conduction switches from phase b to phase c so the source voltage becomes $e_{s(t)} = v_{ac}$. The load current now has the form,

$$i_{(t)} = I_L + \frac{\sqrt{2}V}{\omega L_o}\left(\frac{3}{2} - \cos(\omega t - 2\pi/3)\right) \qquad (86.)$$

Even if the bridge is blanked duri~g the v_{ac} cycle (to prevent the next commutation) (86.) never goes negative, meaning that the conducting thyristors will not turn off.

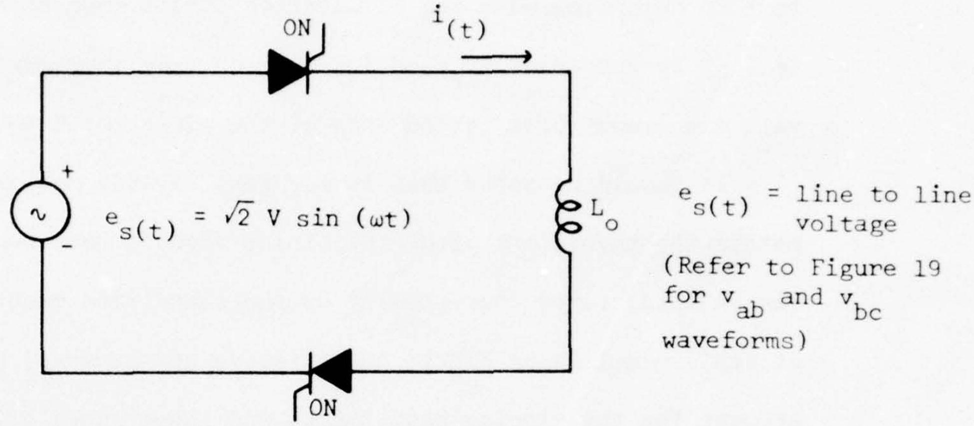

(a.) Simplified equivalent circuit during fault.

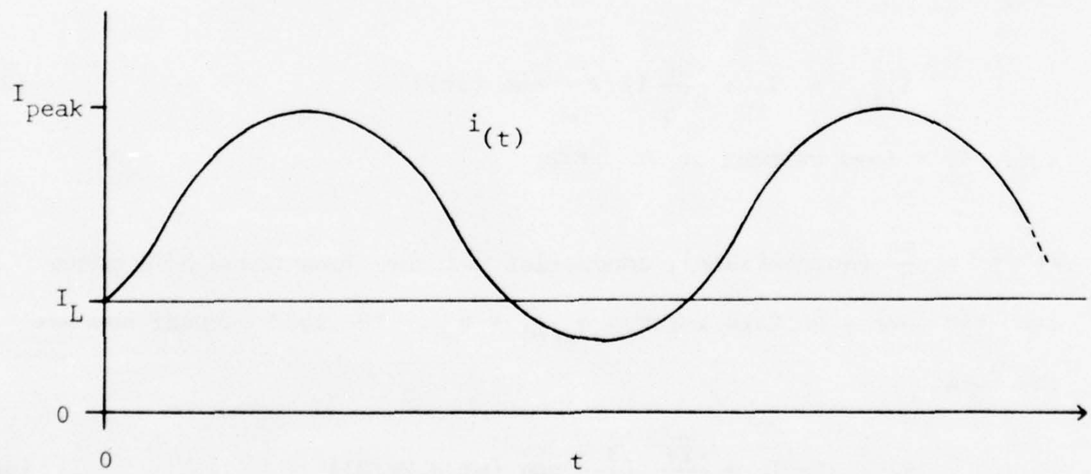

(b.) Fault current.

Note: Actual waveform will be damped due to presence of $2R_a + R_p$

Figure 21. Effect of L_o in limiting fault current.

A similar phenomenon can occur in the actual physical circuit, except that $i_{(t)}$ will eventually decay to zero due to resistive damping. This may require several cycles however, and more cycles will be required for larger values of L_o. Thus if L_o is large, several cycles may be required to complete turn off; however, if it is too small the peak fault current will be excessive.

3.3 Numerical Results

The transient analysis algorithm can be used to plot post fault current waveforms for various values of L_o and R_p. Two parametric studies of i_{LF} for variations in L_o and R_p are shown in Figures 22 and 23 respectively. Figure 24 shows a plot of i_{LF} that requires three cycles for i_{LF} to reach zero. Presumably commutation would occur on the fourth cycle where i_{LF} would attempt to go negative.

This algorithm could also be used to plot $i_{f(tot)}$, i_d and i_q during a fault condition. However, as stated earlier for the steady state calculations, the $i_{f(tot)}$ values may be too high since the model does not include the high frequency attenuation of the damper shield.

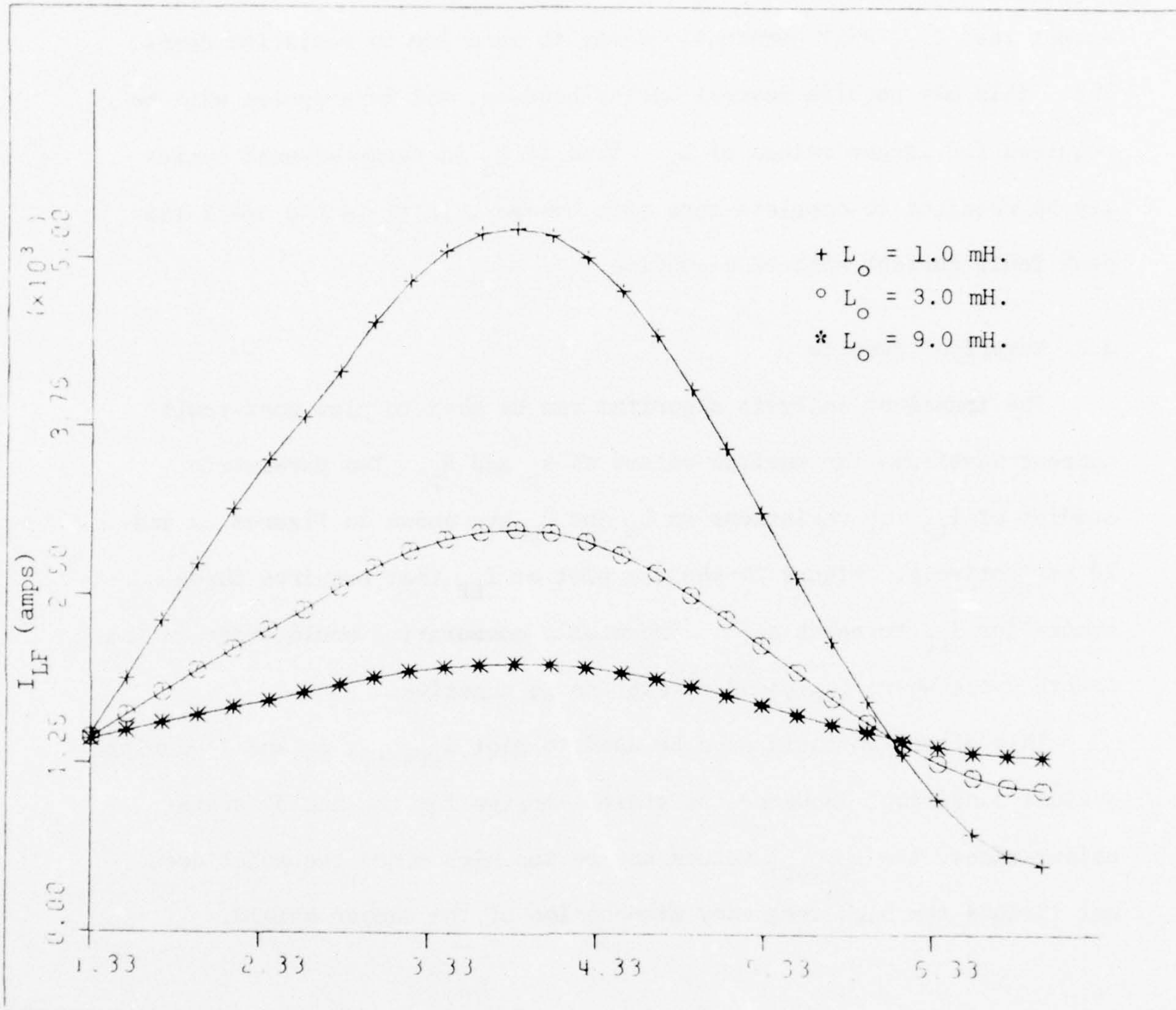

θ (radians)

Figure 22. Fault current vs. θ for different values of L_o. $R_p = 0.05\Omega$

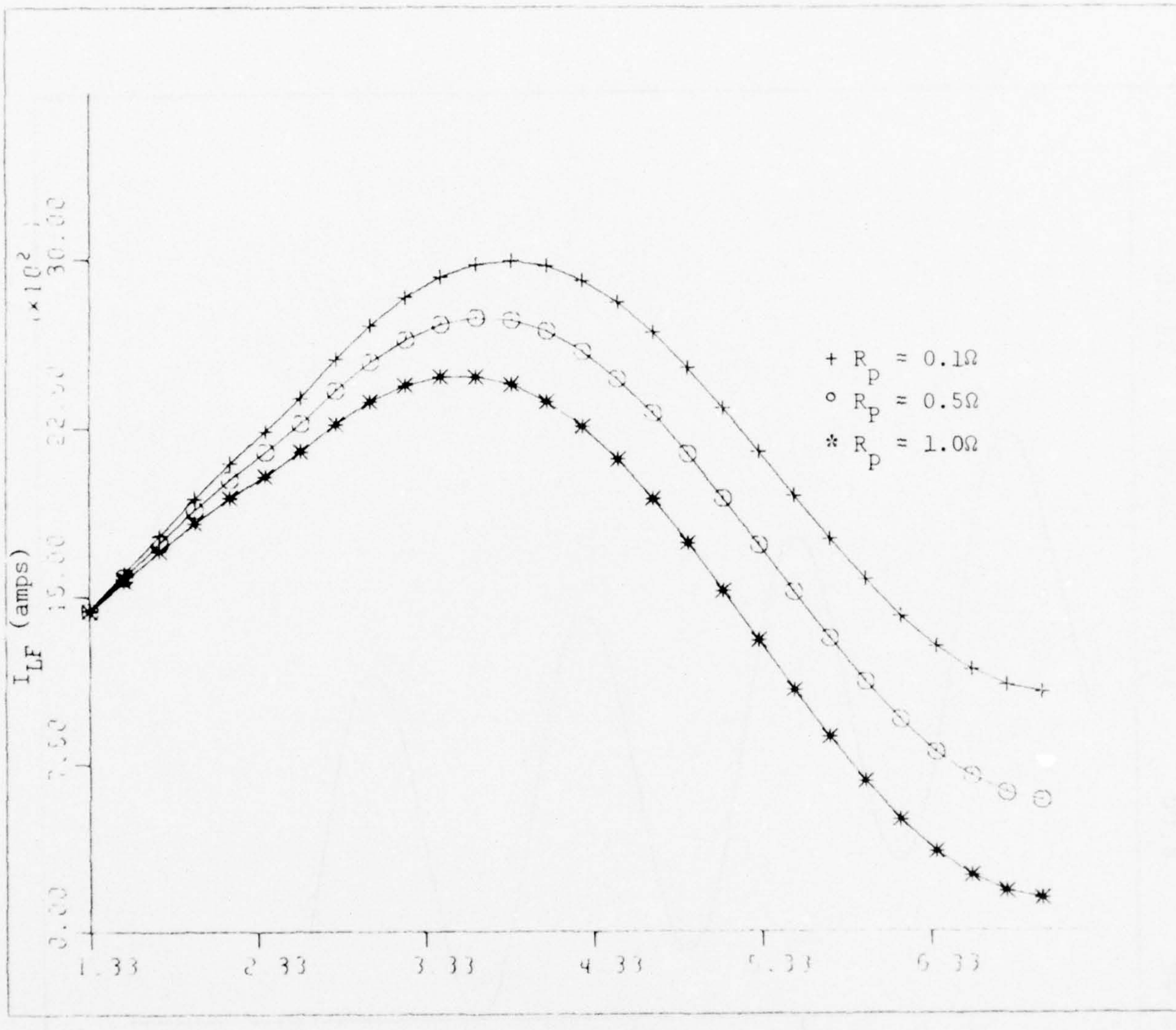

θ (radians)

Figure 23. Fault current vs. θ for different values of R_p. L_o = 3.0 mH.

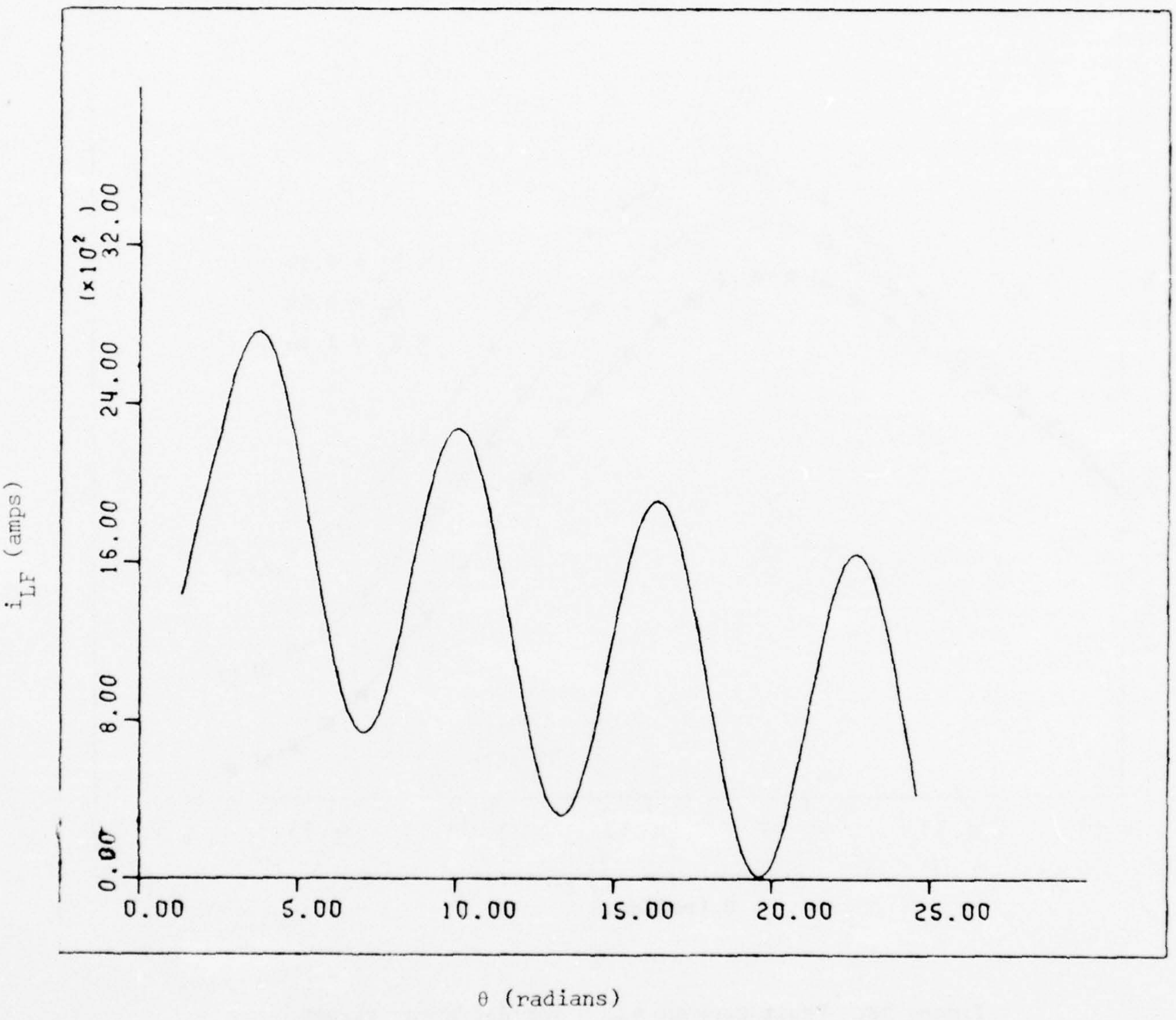

Figure 24. Exponential decay of i_{LF}

4. VARIATION OF THE ALTERNATOR PARAMETERS TO DECREASE OUTPUT RIPPLE VOLTAGE

4.1 Introduction

As noted previously, there are two basic methods for regulating the dc output voltage, V_L, of the rectified alternator:

1. Use an uncontrolled rectifier bridge, and regulate V_L by controlling the average field current, I_f.
2. Hold I_f constant, and regulate the voltage by means of a controlled rectifier bridge.

The first method provides the minimum ripple voltage, but it tends to have a slow response time due to the long time constant of the field winding. Therefore the analysis of this section is based on the controlled rectifier bridge.

If the alternator is modeled by an ideal ac voltage in series with an inductor, it is well known that an increase in this inductance will increase the commutation angle, μ, shown in Figure 11. For constant V_L and I_L this effect can also lead to a reduction in output ripple voltage, as illustrated in Figure 25. Comparing parts (a.) and (b.) of the figure it is seen that the same average output voltage, V_L, is achieved by different combinations of the angle, β and μ. However, the deviation of v_o is less in part (b.). This indicates than an increase in μ requires the bridge firing angle to decrease, resulting in a more level v_o. Therefore, the β_2, μ_2 combination in (b.) produces a lower ripple voltage than the β_1, μ_1 combination in (a.). This implies that at least over a limited range of μ values it is possible to decrease the ripple voltage by increasing μ. *Thus for a fixed load, it is possible to decrease*

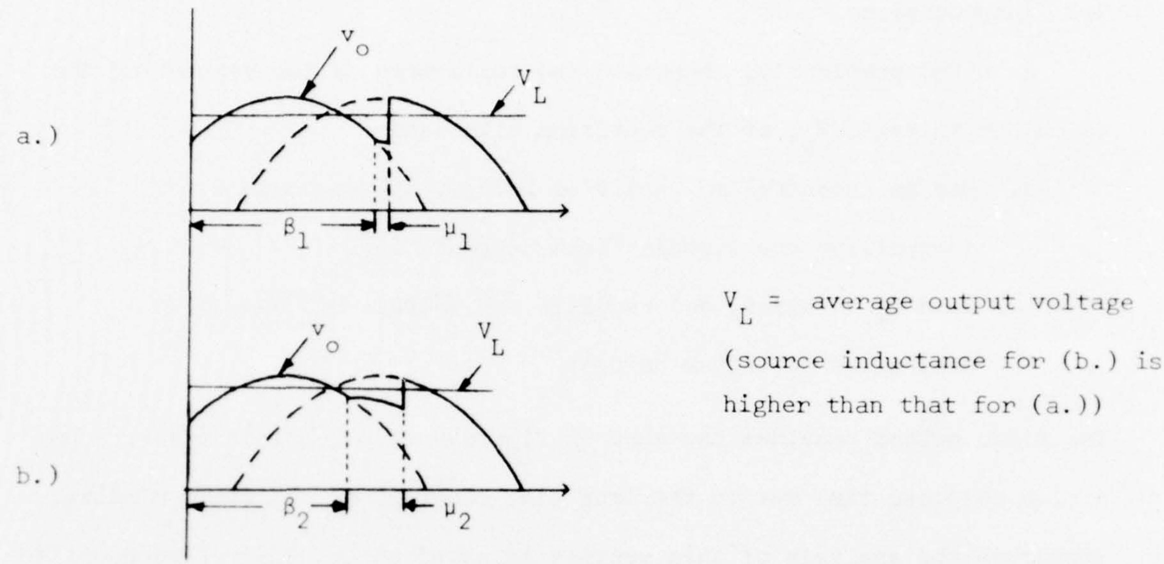

Figure 25. Effect of μ upon output ripple voltage for fixed V_L and I_L.

the ripple by increasing the source inductance since this causes an increase in μ.

The model used in this study was considerably more complicated than the one just described, but it was found that for a constant load the ripple could be decreased if the armature inductance, L_a, was increased beyond its specified value of 0.3 mH. This implies that a lighter weight filter could be used if L_a were increased. A word of caution is in order however, since these gains may be offset by an increase in alternator weight (due to the larger L_a). Ultimately, it would be desirable to develop a procedure that would minimize the combined weight of the alternator and filter. This would require a detailed weight analysis of the superconducting alternator however, and such an effort would be beyond the scope of this present study.

4.2 Effect of L_a on the Output Voltage Harmonics

As discussed in the previous section, it is possible to reduce the full load ripple voltage by changing the output impedance of the alternator. The model used in this study cannot be reduced to a single ac source in series with such an impedance, but a similar effect will occur if the armature self inductance, L_a, is varied. Changes in L_a will, of course, change the armature mutual inductances. To account for this, it is assumed that the coefficient of coupling between L_a and each of the other windings, remains constant while L_a is varied, i.e.,

$$k_{af} = \frac{M_f}{\sqrt{L_a L_f}} = \text{constant} \qquad (87.)$$

$$k_{aa} = \frac{M_a}{L_a} = \text{constant} \tag{88.}$$

$$k_{ad} = \frac{M_d}{\sqrt{L_a L_d}} = \text{constant} \tag{89.}$$

(L_f and L_d also remain constant.)

4.3 Numerical Results

Since k_{af} and L_f are assumed constant, (87.) indicates that an increase in L_a will also increase M_f. Thus an increase in L_a implies that the same magnetic flux linkage from field to armature, $M_f I_f$, can be achieved with a lower I_f (since a thyristor bridge is used for voltage regulation it is assumed that I_f will be held constant at 110% of the minimum allowable value for a given L_a, as discussed in the section on controlled rectifiers). Figure 26 indicates the decrease in the required I_f as L_a is increased for I_L = 1420 A. dc. This decrease in I_f might allow the use of smaller superconducting wire for the rotor winding, thus decreasing the rotor size. An alternate approach would be to hold M_f constant and allow L_f to decrease as L_a increased; thus the field winding would have fewer turns (both effects appear small).

Figure 27 indicates that the 6th harmonic of v_o reaches a minimum at L_a = 0.72 mH. This leads to a decrease in the size of the output filter, $L_o C_o$, since less attenuation is required.

$$\text{Break frequency} = f_b = \frac{1}{\sqrt{L_o C_o}} \tag{90.}$$

Figure 27 also indicates that the 12th and 18th harmonics generally continue to increase with L_a, but their effect is less important since filter attenuation is much greater at these frequencies. Figure 28 shows that the 6th harmonic continues to decrease as L_a increases, indicating that the optimum L_a at 40% of full load lies somewhere above 0.9 mH. Thus the optimum L_a is different for different values of I_L.

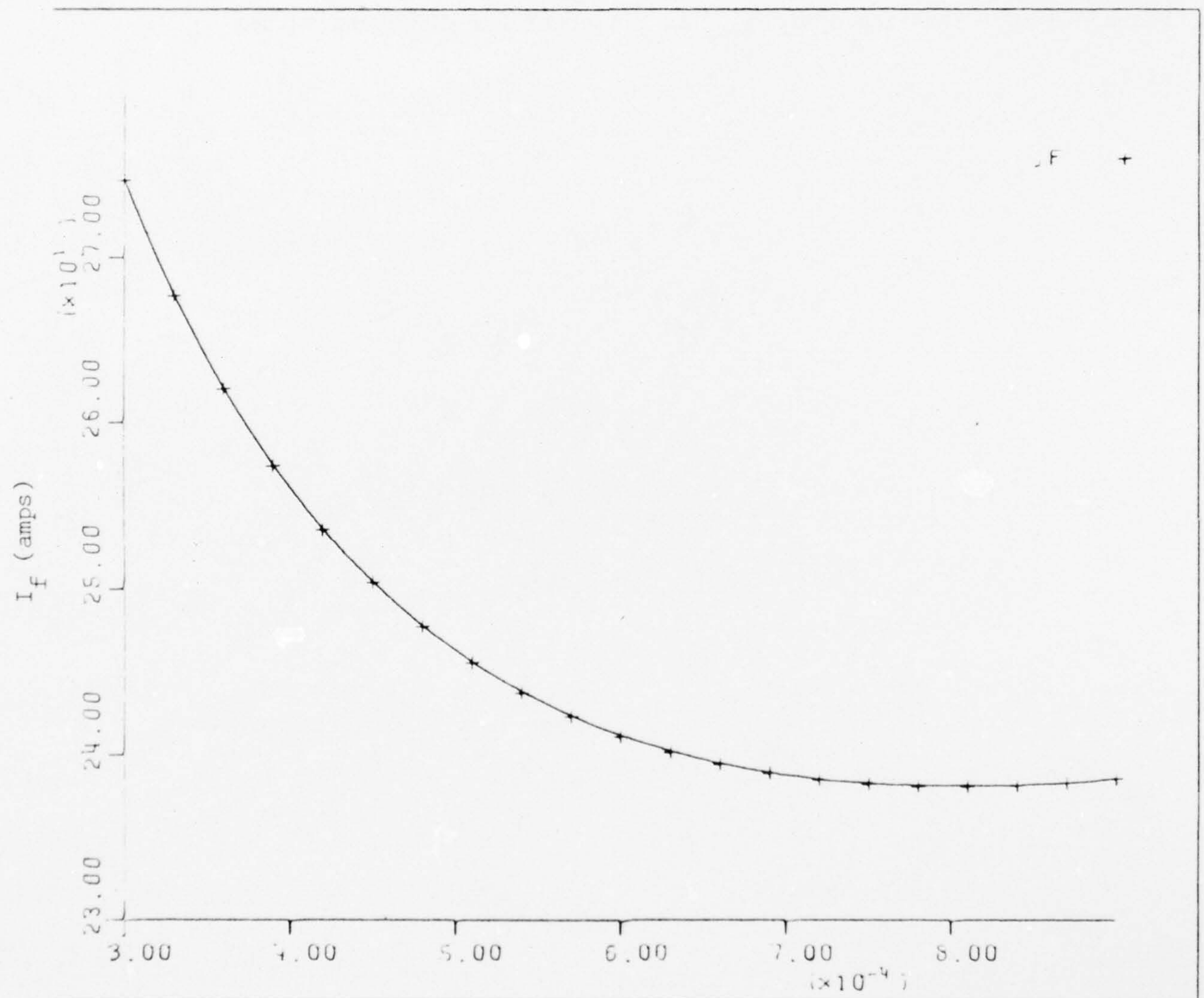

L_a (H.)

Figure 26. I_f vs. L_a for the controlled rectifier bridge. I_L = 1420 A.d.c.

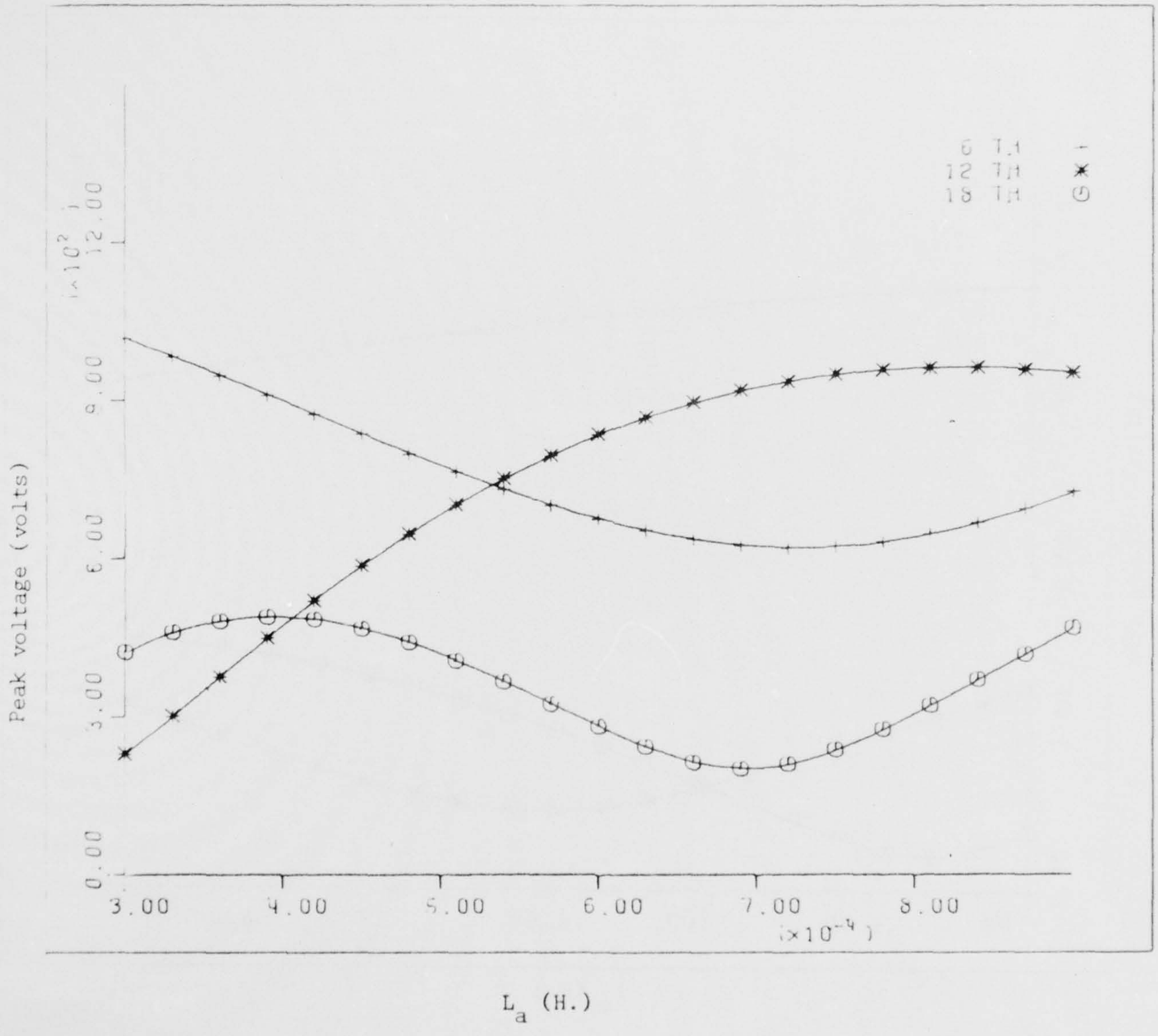

Figure 27. 6th, 12th and 18th harmonics of v_o vs. L_a for the controlled rectifier bridge. I_L = 1420 A.d.c.

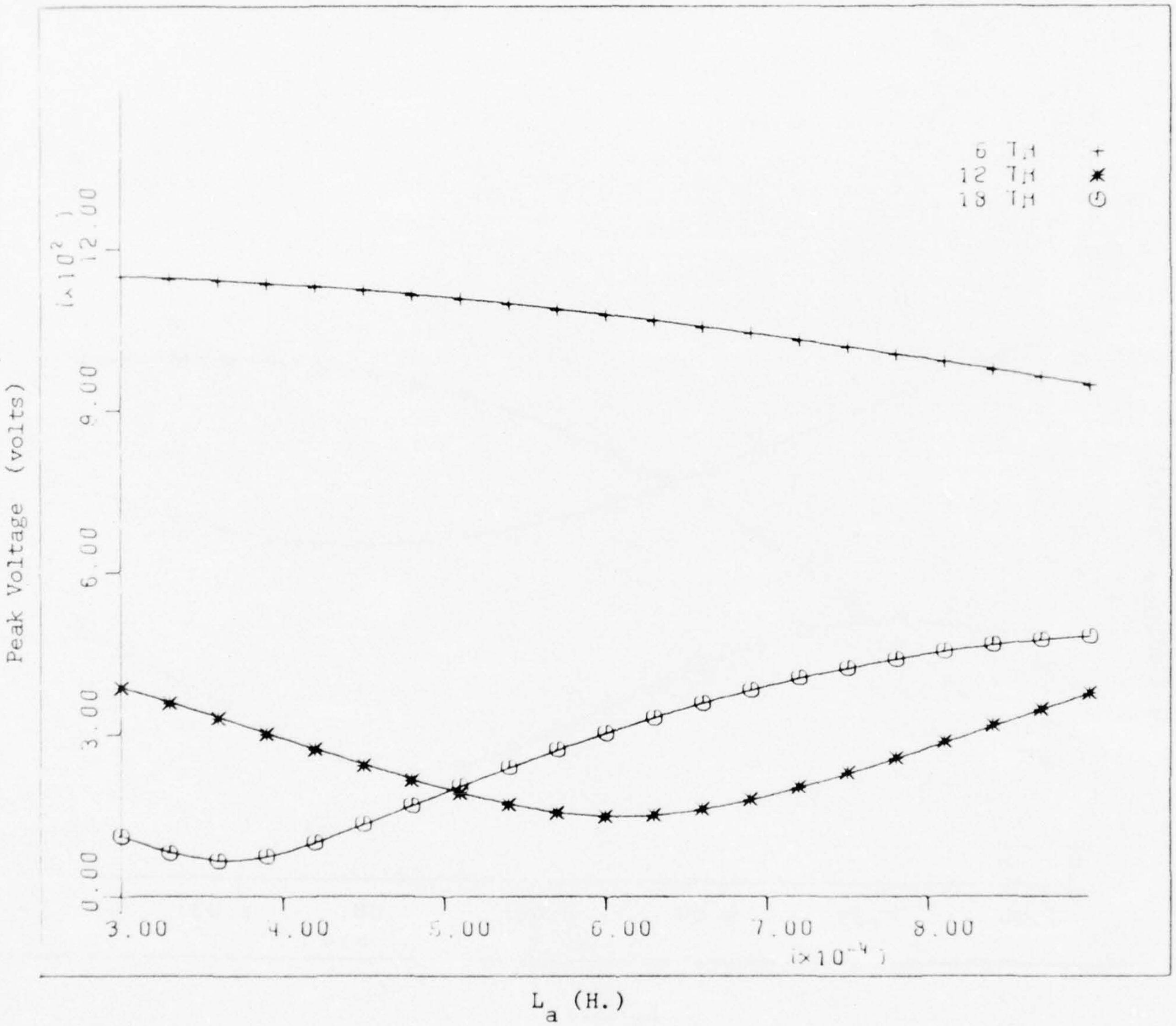

Figure 28. 6th, 12th and 18th harmonics of v_o vs. L_a for the controlled rectifier bridge. I_L = 568 A.d.c.

5. MINIMIZATION OF L_oC_o FILTER WEIGHT

5.1 Introduction

The previous sections have considered the following topics:

1. Steady state behavior with an uncontrolled rectifier bridge.
2. Steady state behavior with a controlled rectifier bridge.
3. Transient currents that occur when a short circuit is placed across the output.
4. Reducing the full load output ripple voltage by increasing L_a.

The results of these studies can now be used in designing an L_oC_o output filter for minimum weight. This analysis assumes the use of a controlled rectifier bridge for voltage regulation. The maximum allowable ripple voltage will be based on the size of the sixth harmonic that is present at full load. It should be noted that this harmonic will actually be greater at minimum load since the firing angle of the thyristors will be greater. This study assumes that the load will be fairly constant however, and that the presence of ripple voltage will be more important at full load than at lighter loads. Hence the filter optimization is based on full load conditions.

5.2 Calculation of L_o and C_o for Minimum Total Filter Weight

In the weight minimization algorithm, L_o and C_o are calculated to provide a given amount of ripple attenuation at full load. This calculation is based only on the sixth harmonic and ignores the harmonic attenuation provided by the load in conjunction with L_o. Therefore,

$$\left| \frac{1}{1-L_o C_o \omega_6^2} \right| \leq k_1 \qquad (91.)$$

where k_1 = specified magnitude of the 6th harmonic attenuation

and ω_6 = 15079.64 radians/sec.

$$\therefore \qquad L_o C_o \geq \frac{k_1 + 1}{k_1 \omega_6^2} \qquad (92.)$$

Due to the high value of the magnetic field and the low weight requirement, it is assumed that L_o will be an air core reactor. Aluminum was chosen for the conductor due to its low weight/conductance ratio. The physical configuration of the inductor is shown in Figure 29. This particular design is chosen to produce the minimum loss for a given amount of material (see [25,26]). The inductance is,

$$L_o = (24.5 \times 10^{-7})\, N^2 a \quad \text{H.} \qquad (93.)$$

and the weight of L_o is given by

$$L_o \text{ wt.} = 3\, \pi\, f\, D_w\, a^3 \text{ lbs.} \qquad (94.)$$

where

N = number of turns

a = thickness of the coil (m.)

D_w = density of Al (5837.8 lbs/m.^{3})

f = filling factor of the conductors (assumed to be 0.7)

The filling factor can be expressed,

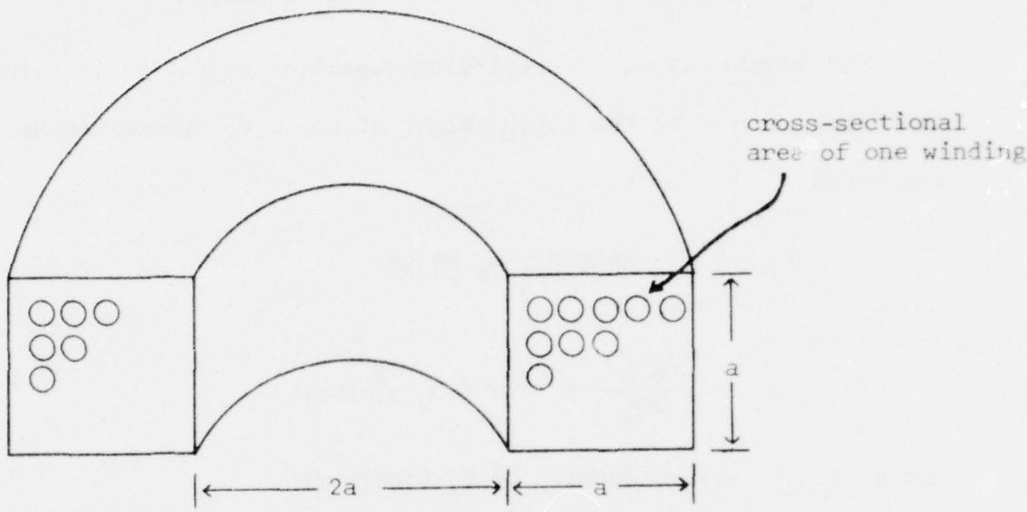

Figure 29. L_o dimensions.

$$f = \frac{NF_w}{a^2} \tag{95.}$$

where F_w = cross sectional area of one winding(m.^{2})

The common method of specifying capacitor weight is in terms of jouls/lb. Therefore the total weight of the L_oC_o filter can be expressed,

$$T_{wt} = C_o \text{ weight} + L_o \text{ weight}$$

$$= \frac{C_o V_L^2}{2D_c} + 3\pi f D_w a^3 \text{ lbs.} \tag{96.}$$

where D_c = energy density of C_o (joules/lb.).

Therefore substituting (92.), (93.) and (95.) into (96.)

$$T_{wt} = k_2/a^5 + k_3 a^3 \tag{97.}$$

where $k_2 = \left(\frac{1}{51.1\text{x}10^{-7}}\right)\left(\frac{F_w V_L}{f}\right)^2\left(\frac{k_1+1}{D_c k_1 \omega_6^2}\right)$

$k_3 = 3\pi f D_w$

To find the minimum value of T_{wt}, set

$$\frac{dT_{wt}}{da} = \frac{-5k_2}{a^6} + 3k_3 a^2 = 0 \tag{98.}$$

$$a = \left(\frac{5k_2}{3k_3}\right)^{1/8} \tag{99.}$$

Once a is determined, N can be found from (95.) , L_o from (93.) and C_o from (92.) .

5.3 L_oC_o Design Algorithm

The flow chart for the L_oC_o filter design program is shown in Figure 30. The following discussion refers to the seven blocks indicated in the figure.

1. Read input data. This includes the following information: C_o energy density (D_c), L_o current density, maximum 6th harmonic ripple voltage at full load, and maximum short circuit current, $I_{L(max.)}$. This particular program assumes that the following quantities are constant:

$$V_L = 6760 \text{ V.dc}$$

$$I_L = 1420 \text{ A.dc}$$

$$\omega_6 = 15079.6 \text{ rad./sec. (line frequency = 400 Hz.)}$$

V_L, I_L and ω_6 could be varied if desired, by making a few minor changes in the program.

2. Set L_a = 0.3 mH, the normal design value specified in [13,14].

3. Assuming that a controlled rectifier bridge is used, the minimum weight L_o and C_o that will meet the 6th harmonic ripple specification are calculated.

4. A transient analysis subroutine to called to determine if the peak short circuit current will exceed the specified value of $I_{L(max.)}$. The details of this analysis are given in section 3.

5. If $I_{L(max.)}$ is exceeded, L_o is increased by 10%, and step 3 is repeated (C_o is simultaneously decreased to maintain a constant L_oC_o product.) If $I_{L(max)}$ is not exceeded, the L_o and C_o design data is printed.

6. The program calculates L_o and C_o, first for the normal and then for the optimum values of L_a. If the calculation for the optimum L_a has

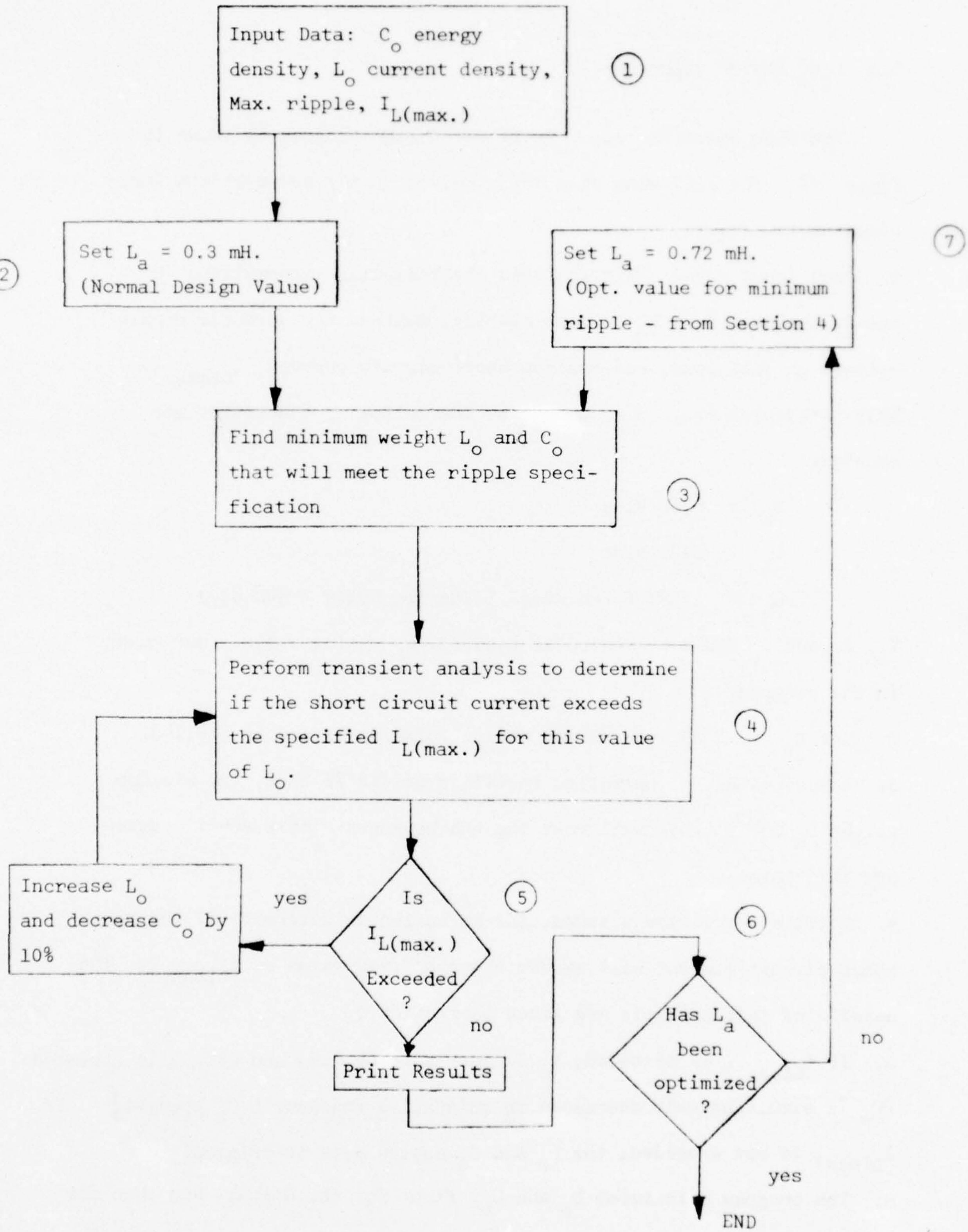

Figure 30. L_oC_o weight minimization flow chart.

been completed the program ends. If not, the program branches to step 7.

7. Set L_a = 0.72 mH., the optimum value for minimum ripple at full load calculated in Section 4. Steps 3 through 6 are then repeated.

5.4 Numerical Results

A sample of the computer results for the optimization program are shown in the following example. Note that use of the optimum L_a decreases the total filter weight by approximately 22%.

The total filter weight will obviously decrease if a higher energy density (D_c) is used for C_o and/or a higher current density is used for L_o. Plots of filter weight vs. energy density and current density are shown in Figures 31 and 32 respectively. The filter weight will also be affected if the allowable $I_{L(max.)}$ is changed. A plot of this is shown in Figure 33.

```
WRITE THE FØLLØWING PARAMETERS FØR THE FILTER

     ALL INPUTS HAVE FØRMAT = F7.2 UNLESS ØTHERWISE SPECIFIED

 CAP. ENERGY DENSITY (JOULES/LB.) =
50.0


 CURRENT DENSITY FØR L WIRE (CIR MIL/AMP) =
90.0


 MAX. RMS VALUE ØF 6TH HARM. ØF VO (VØLTS) =
20.0


 ALLØWABLE PEAK FAULT CURRENT (AMPS) =
2500.0


  THE FØLLØWING VALUES ARE BASED ØN NØRMAL LA = 0.300E-03  H.
  IF= 0.275E+03       BETA= 0.212E+01       MU= 0.307E+00
  IL= 0.142E+04       VL= 0.676E+04      V1= 0.120E+04

 ØPT.VALUES BEFØRE FAULT TEST ARE LO= 0.422E-02 H.,   CO= 0.636E-04 FD. R
ES= 0.547E-01
  MAX LØAD CURRENT FRØM FAULT = 0.250E+04

 FAULT CURRENT TØØ LARGE, LO INCREASED
  MAX LØAD CURRENT FRØM FAULT = 0.250E+04
  MAX LØAD CURRENT FRØM FAULT = 0.245E+04

 LO= 0.511E-02      CO= 0.525E-04      ILF= 0.245E+04    RES= 0.615E-01

 LWT= 0.542E+02      CWT= 0.240E+02       TØTAL WT = 0.781E+02

 NØ. TURNS = 134      L RADIUS = 0.223E+00M       L LENGTH = 0.111E+00M

  THE FØLLØWING VALUES ARE BASED ØNØPTIMUM LA = 0.720E-03  H.
  IF= 0.239E+03       BETA= 0.223E+01       MU= 0.604E+00
  IL= 0.142E+04       VL= 0.676E+04      V1= 0.620E+03

 ØPT.VALUES BEFØRE FAULT TEST ARE LO= 0.282E-02 H.,   CO= 0.499E-04 FD. R
ES= 0.428E-01
  MAX LØAD CURRENT FRØM FAULT = 0.250E+04

 FAULT CURRENT TØØ LARGE, LO INCREASED
  MAX LØAD CURRENT FRØM FAULT = 0.250E+04
  MAX LØAD CURRENT FRØM FAULT = 0.250E+04

 LO= 0.341E-02      CO= 0.412E-04      ILF= 0.250E+04    RES= 0.432E-01

 LWT= 0.425E+02      CWT= 0.188E+02       TØTAL WT = 0.613E+02

 NØ. TURNS = 114      L RADIUS = 0.206E+00M       L LENGTH = 0.103E+00M

 WRITE "0" TØ END, ØR "1" FØR ANØTHER RUN

     FØRMAT=I2
0
```



```
STØP --
```

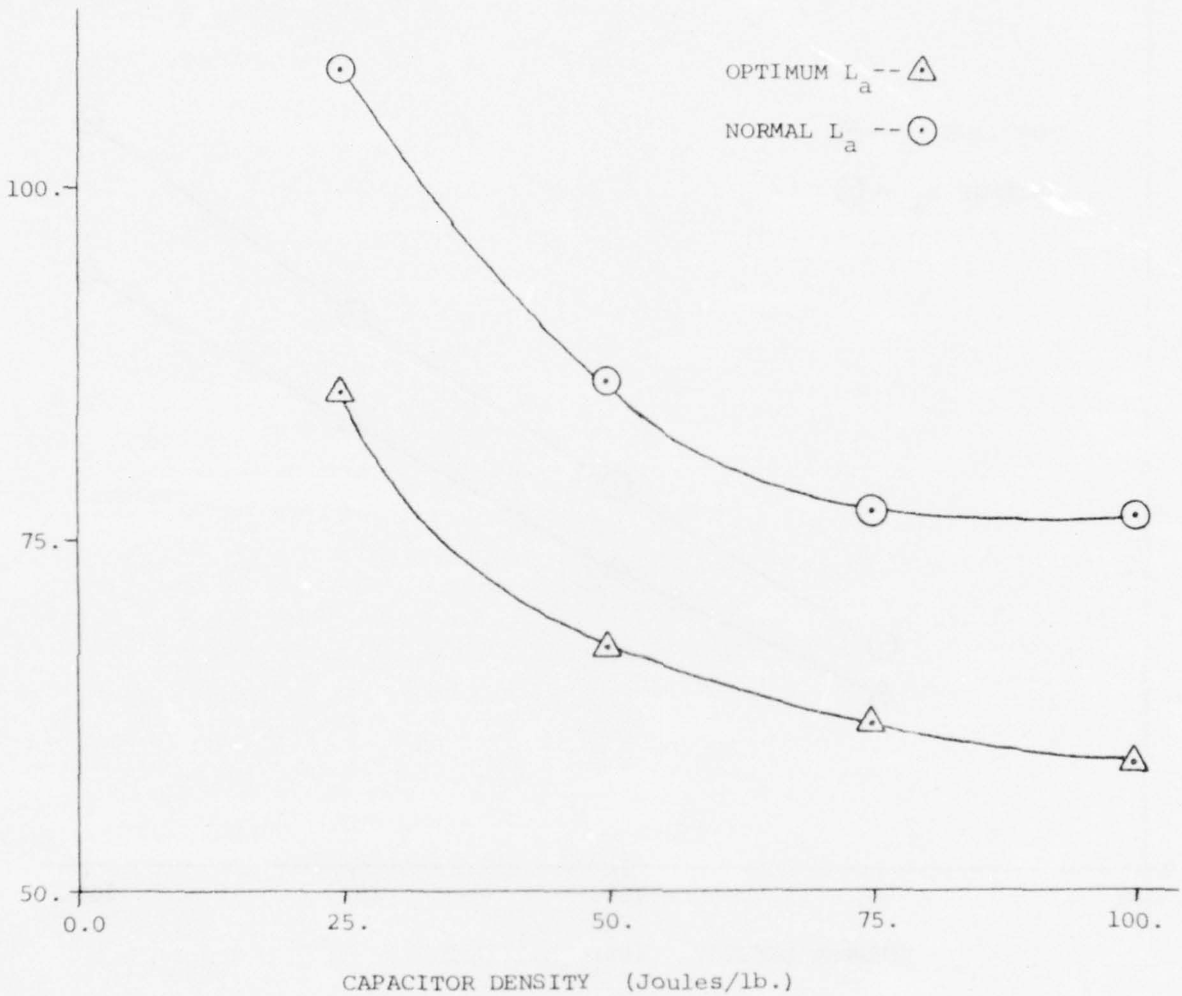

Figure 31. Filter weight vs. C_o energy density. Current density = 100 cir. mile/amp, all other variables are the same as in the example run.

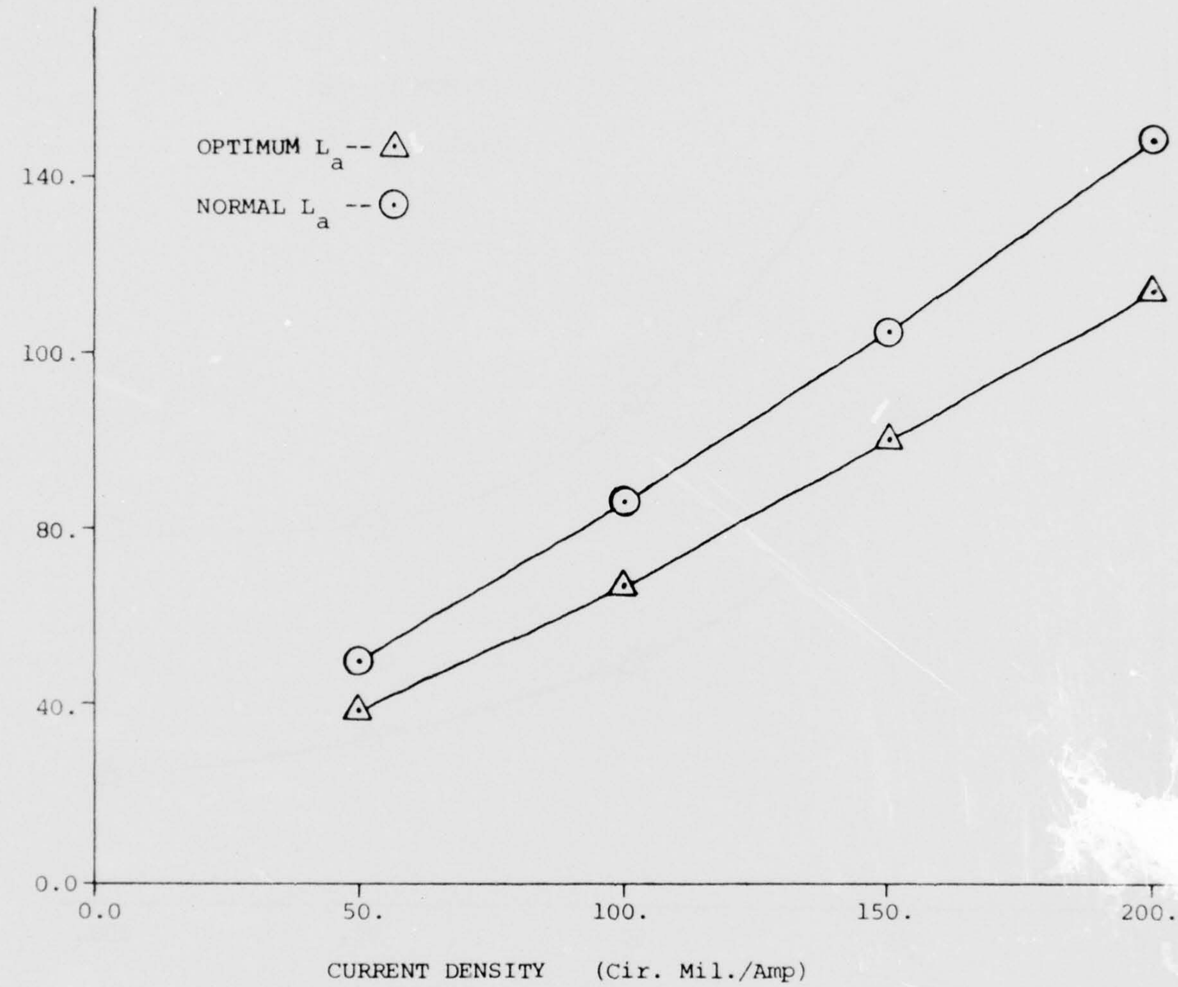

Figure 32. Filter weight vs. L_o current density. All other variables are the same as in the example run.

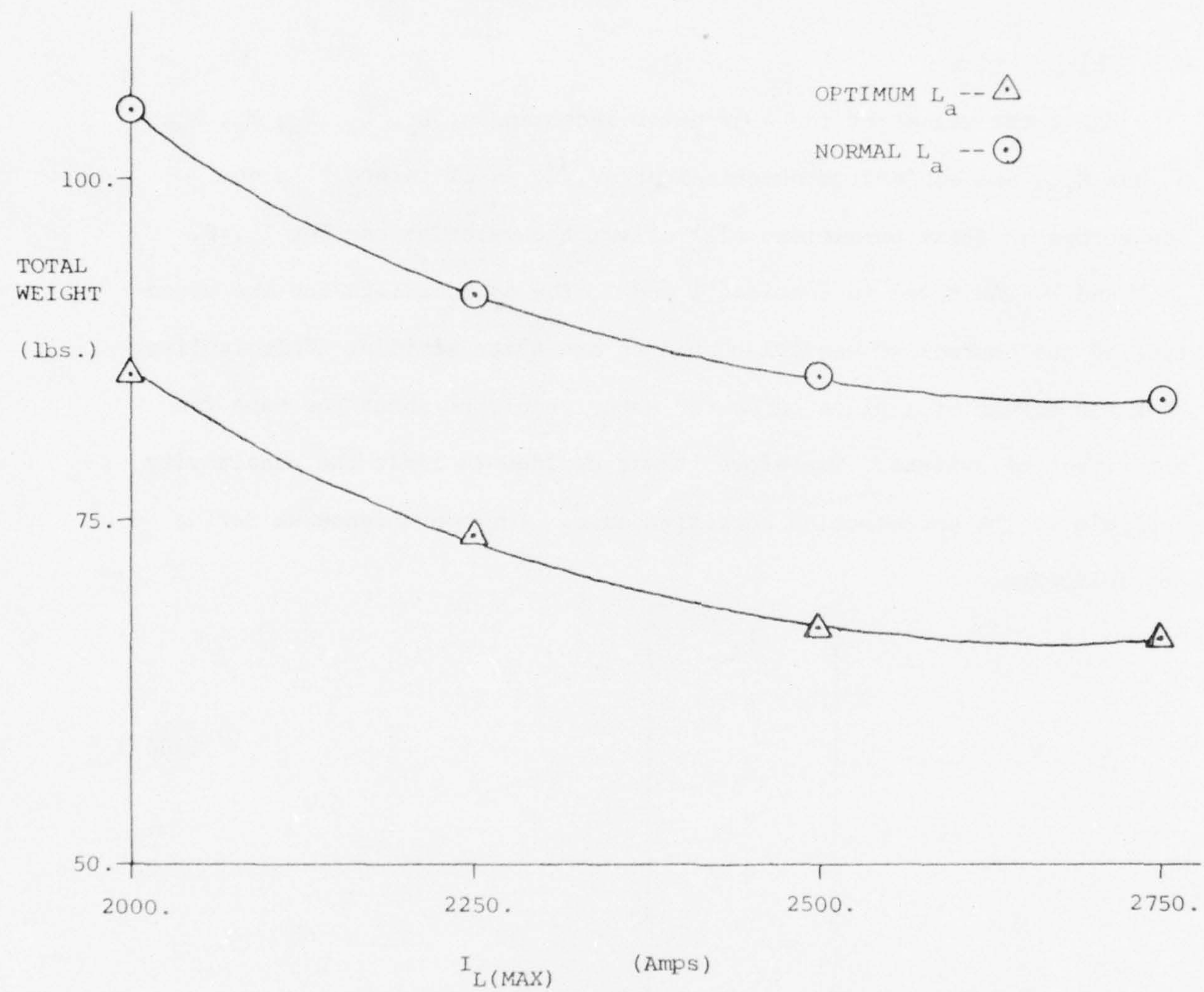

Figure 33. Filter weight vs. maximum allowable short circuit current. Current density = 100 cir. mils/amp, all other variables are the same as in the example run.

6. SENSITIVITY ANALYSIS

6.1 Introduction

Since the values of the alternator inductances, L_a, L_f, L_d, M_a, M_f, M_d and M_{fd}, are subject to numerical error, it is of interest to see how errors in these parameters will affect the calculations for I_f, β, μ, V and W. As noted in Sections 1 and 2, the calculations for the uncontrolled and controlled rectifier bridges are quite similar. This implies that the effect of a given parameter error should be about the same for both types of systems. Therefore it was decided to limit the sensitivity analysis to the uncontrolled rectifier case. For convenience we define the following,

$$\underline{x} \equiv \begin{bmatrix} I_f \\ \beta \\ \mu \\ V \\ W \end{bmatrix} \qquad (100.)$$

$$\underline{y} \equiv \begin{bmatrix} L_a \\ L_f \\ L_d \\ M_a \\ M_f \\ M_d \\ M_{fd} \end{bmatrix} \qquad (101.)$$

$$\underline{f}(\underline{x},\underline{y}) = \text{R.H.S. of} \begin{bmatrix} (44.) \\ (45.) \\ (46.) \\ (47.) \\ (48.) \end{bmatrix} = \underline{0} \qquad (102.)$$

Theoretically, this analysis could be performed by either of two methods:

1. Use (102.) to find $\frac{\partial \underline{x}}{\partial \underline{y}}$ and solve for $\Delta\underline{x}$ for a given $\Delta\underline{y}$, i.e., $\Delta\underline{x} = \frac{\partial \underline{x}}{\partial \underline{y}} \Delta\underline{y}$. This will be referred to as the differential method.

2. Simply replace $\underline{y}$ by $\underline{y} + \Delta\underline{y}$ and use the Newton Raphson method to find the resulting $\underline{x} + \Delta\underline{x}$. This will be referred to as the deliberate error method.

The differential method is certainly the more elegant of the two, so this was investigated first. Unfortunately this approach depends on solving sets of simultaneous equations that have ill-conditioned coefficient matrices. Two algorithms were used for solving these equations, but both failed due to excessive round-off errors. Therefore it was necessary to resort to the deliberate error method. This second approach worked satisfactorily even though it is rather inefficient in terms of computation time. Both methods will be discussed for completeness, even though the first did not produce satisfactory results.

6.2 Differential Method

One usually does not bother to describe methods that do not work, but this analysis is interesting from a conceptual standpoint, so it is included for that reason. It is also possible that the problems with this method may eventually be solved, even though it was unsuccessful in this present research.

Taking the partial derivative of (102.) produces an equation of the form,

$$\frac{\partial f(\underline{x},\underline{y})}{\partial y_i} = [C]\frac{\partial \underline{x}}{\partial y_i} + \underline{r} = \underline{0} \qquad (103.)$$

where [C] is a (5x5) coefficient matrix, and $\underline{r}$ is a (5x1) vector.

$$\therefore \quad \frac{\partial \underline{x}}{\partial y_i} = -[C]^{-1}\,\underline{r} \qquad (104.)$$

which is the ith column of $\frac{\partial \underline{x}}{\partial \underline{y}}$, a (5x7) matrix. Therefore it is conceptually possible to use (104.) for all seven elements of $\underline{y}$ to find $\frac{\partial \underline{x}}{\partial \underline{y}}$. $\Delta\underline{x}$ for a given $\Delta\underline{y}$ is then,

$$\Delta\underline{x} = \frac{\partial \underline{x}}{\partial \underline{y}}\,\Delta\underline{y} \qquad (105.)$$

Unfortunately, the [C] matrices indicated by (103.) are very ill conditioned in this application, and this prevented finding a solution for $\frac{\partial \underline{x}}{\partial \underline{y}}$. Two methods of solution were attempted, the first being the DGELG double precision subroutine from the IBM Scientific Subroutine Package and the second being a Shipley-Coleman inversion algorithm to find $[C]^{-1}$. Both of these programsuse pivoting for size, but they were still incapable of finding the correct solution. Therefore this approach was abandoned in favor of the deliberate error method.

6.3 Deliberate Error Method

In this method a given error, Δy_i, is added to y_i and the resulting $\underline{x} + \Delta\underline{x}$ is calculated by the equations described in section 1. The terms of $\underline{y}$ are not independent however, since mutual inductance terms are present, and this must be accounted for in the analysis. Therefore, the approach used in this particular study was to assume that the following terms can be varied independently of one another: L_a, L_f, L_d, k_{aa}, k_{af}, k_{ad}, and k_{fd}, where the last four terms are the coefficients of coupling, i.e.,

$$k_{aa} = \frac{M_a}{L_a}, \quad k_{af} = \frac{M_f}{\sqrt{L_a L_f}}, \quad k_{ad} = \frac{M_d}{\sqrt{L_a L_d}}, \quad k_{fd} = \frac{M_{fd}}{\sqrt{L_f L_d}} \qquad (106.)$$

The independent and dependent parameters are listed as follows:

Independent	Dependent
L_a	M_a, M_f, M_d
L_f	M_f, M_{fd}
L_d	M_d, M_{fd}
k_{aa}	M_a
k_{af}	M_f
k_{ad}	M_d
k_{fd}	M_{fd}

For example, a 10% increase in L_a implies (new value = 1.1 L_a),

$$M_a = 1.1\, k_{aa}\, L_a, \quad M_f = k_{af}\sqrt{1.1\, L_a L_f}\,, \quad M_d = k_{ad}\sqrt{1.1\, L_a L_d}\,,$$

whereas a 10% increase in k_{af} implies (new value = 1.1 k_{af}),

$$M_{af} = 1.1\, k_{af}\sqrt{L_a L_f}$$

The effect of these errors will be described in the next section on numerical results.

6.4 Numerical Results

The following paragraphs discuss the effects of varying each of the machine inductances, i.e., the effect of a deliberate error. Note that since the algorithm used in Section 1 depends upon the approximation given by (41.), it is necessary to restrict the parameter variations to the range where (41.) is valid. It is assumed that (41.) is satisfied as long as the following condition is met:

$$\left| M_o - M_{oo} \right| < 0.1\, M_{oo}$$

$\underline{\Delta L_a}$: Results are shown in Figures 34 and 35. These figures indicate that all of the $\underline{x}$ variables are quite sensitive with respect to ΔL_a.

$\underline{\Delta L_f}$: Results are shown in Figures 36 and 37. It is noted that β, μ, V and W do not vary with respect to L_f. The reason for this is that the algorithm automatically adjusts I_f to compensate for any L_f changes, so that the $M_f I_f$ flux linkages remain constant (note that M_f is dependent on L_f.) Compare with the M_f results shown in Figures 42 and 43.

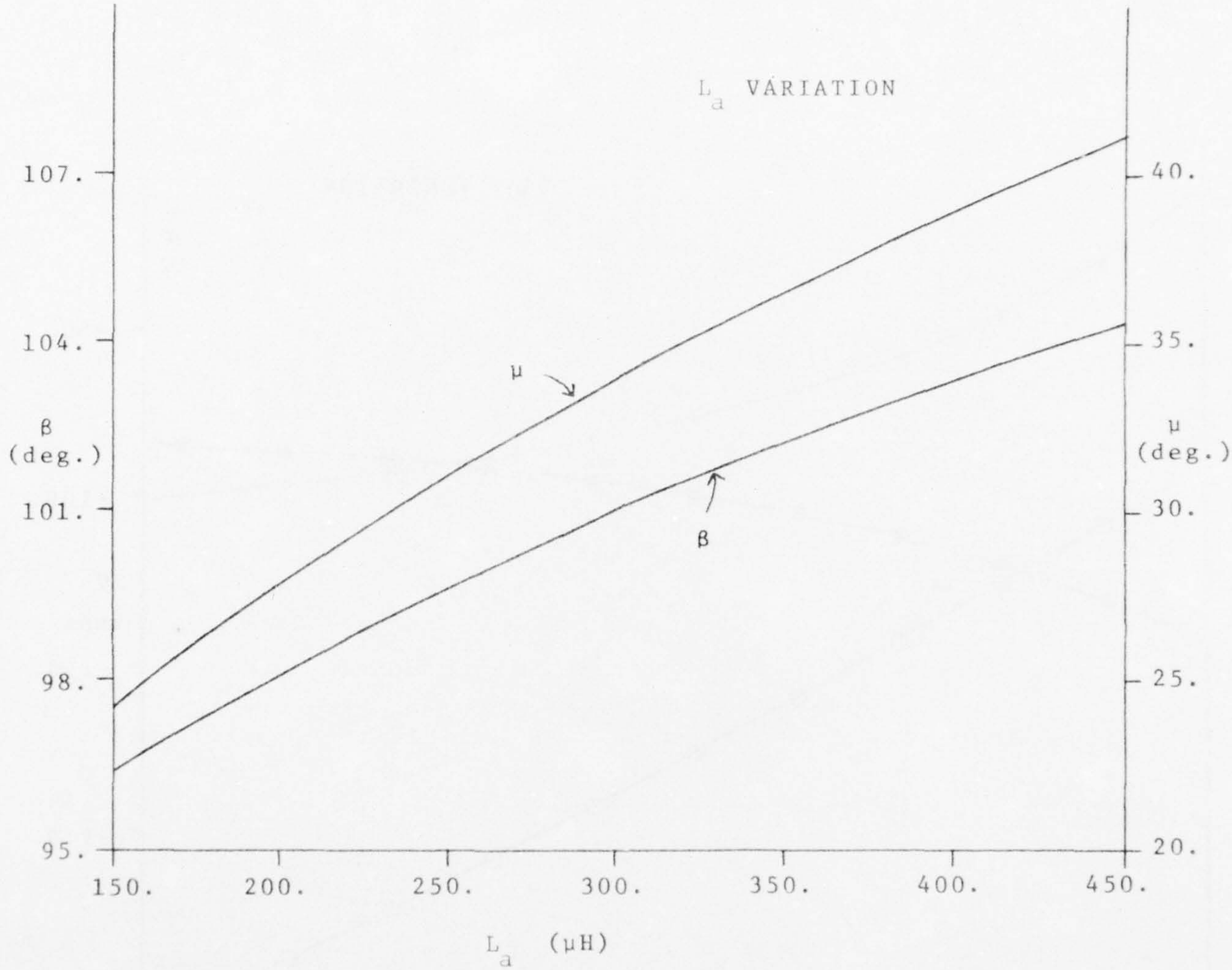

Figure 34. β and μ variation vs. L_a.

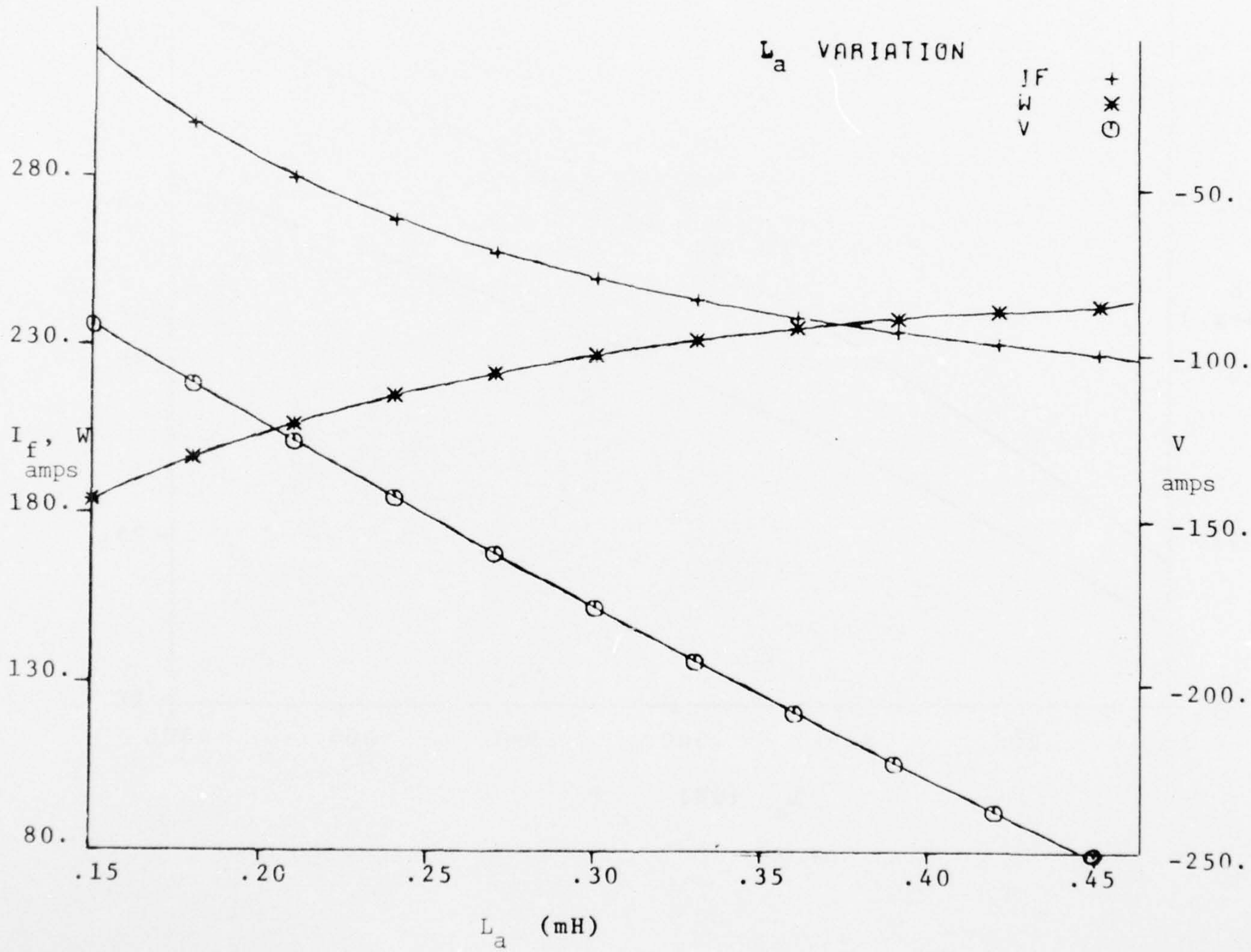

Figure 35. I_f, W and V variation vs. L_a.

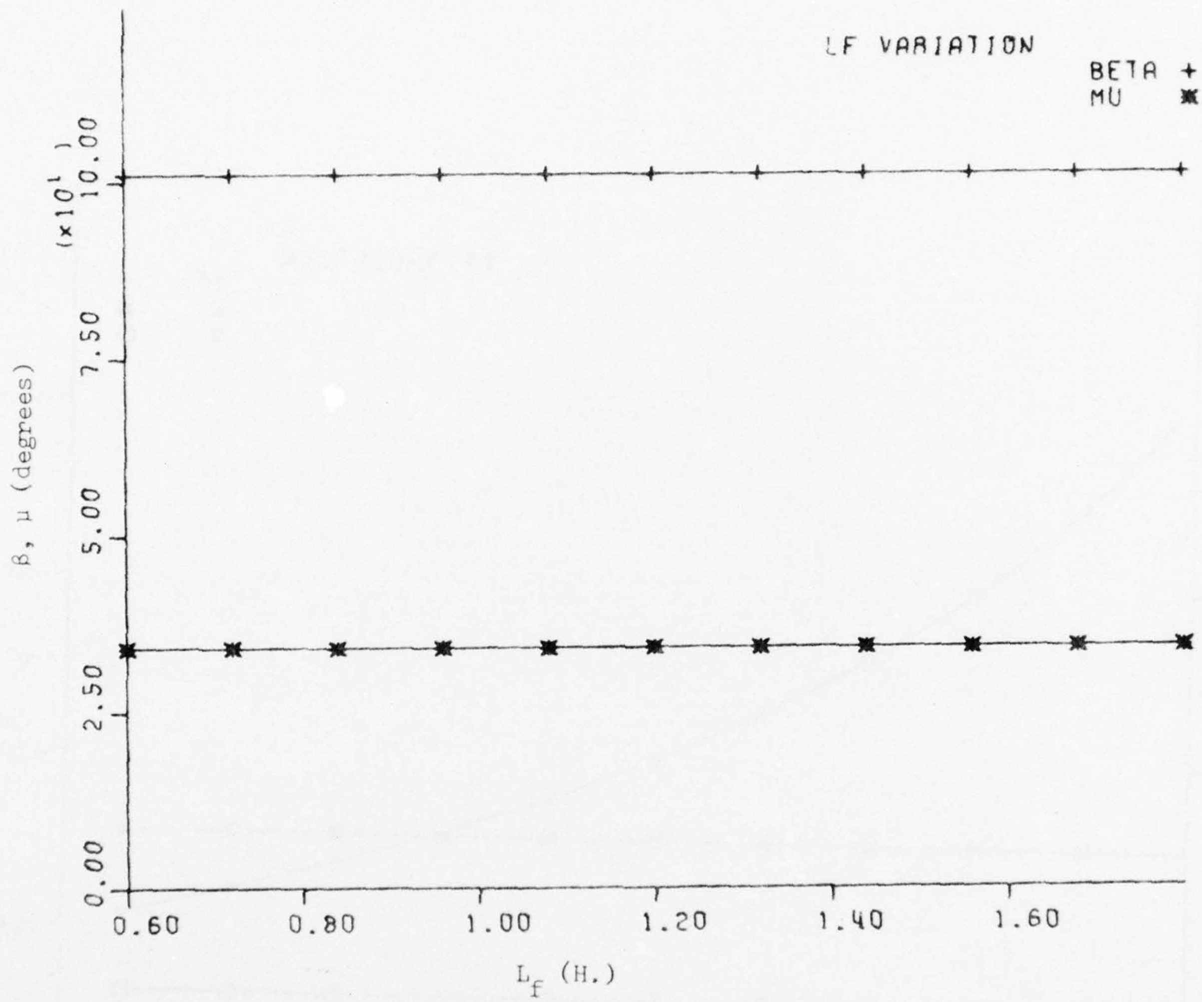

Figure 36. β and μ variation vs. L_f.

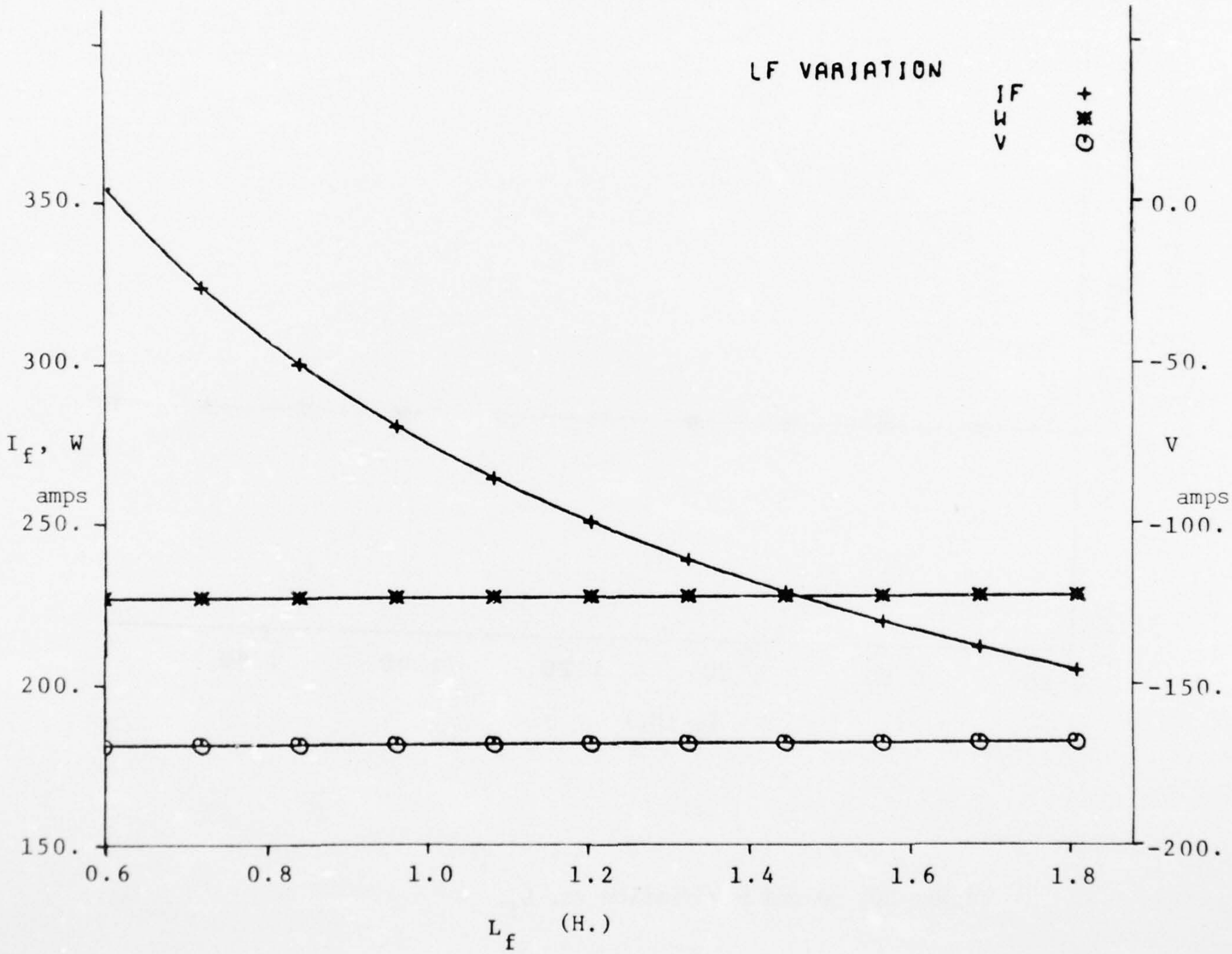

Figure 37. I_f, W and V variation vs. L_f.

$\underline{\Delta L_d}$: Results are shown in Figures 38 and 39. These figures indicate that the calculations are completely insensitive to L_d variations. The reason for this stems from the previously mentioned approximation,

$$M_o \approx M_{oo} \tag{107.}$$

which is given by (41.) in Section 1. Once this approximation is made, M_o is replaced by M_{oo} in all subsequent calculations. The value of M_{oo} is,

$$M_{oo} = \frac{M_d^{\,2}}{Ld} = k_{ad}^{\,2}\, L_a \tag{108.}$$

The result of this is that L_d does not actually appear in (44.)-(51.), which are the equations used to find $\underline{x}$.

$\underline{\Delta k_{aa}\ (\Delta M_a)}$: Results are shown in Figures 40 and 41. The figures indicate that μ is quite sensitive to ΔM_a variations, while I_f and β are less sensitive. W and V also vary considerably with respect to M_a.

$\underline{\Delta k_{af}\ (\Delta M_f)}$: Results are shown in Figures 42 and 43. For an explanation of these results, refer to the discussion for ΔL_f.

$\underline{\Delta k_{ad}\ (\Delta M_d)}$: Results are shown in Figures 44 and 45.

$\underline{\Delta k_{fd}\ (\Delta M_{fd})}$: Results are shown in Figures 46 and 47. These figures indicate that the calculations are insensitive to M_{fd} variations. The reason for this is much the same as for L_d, i.e., once the approximation (107.) is made, M_{fd} does not appear in any of the subsequent equations.

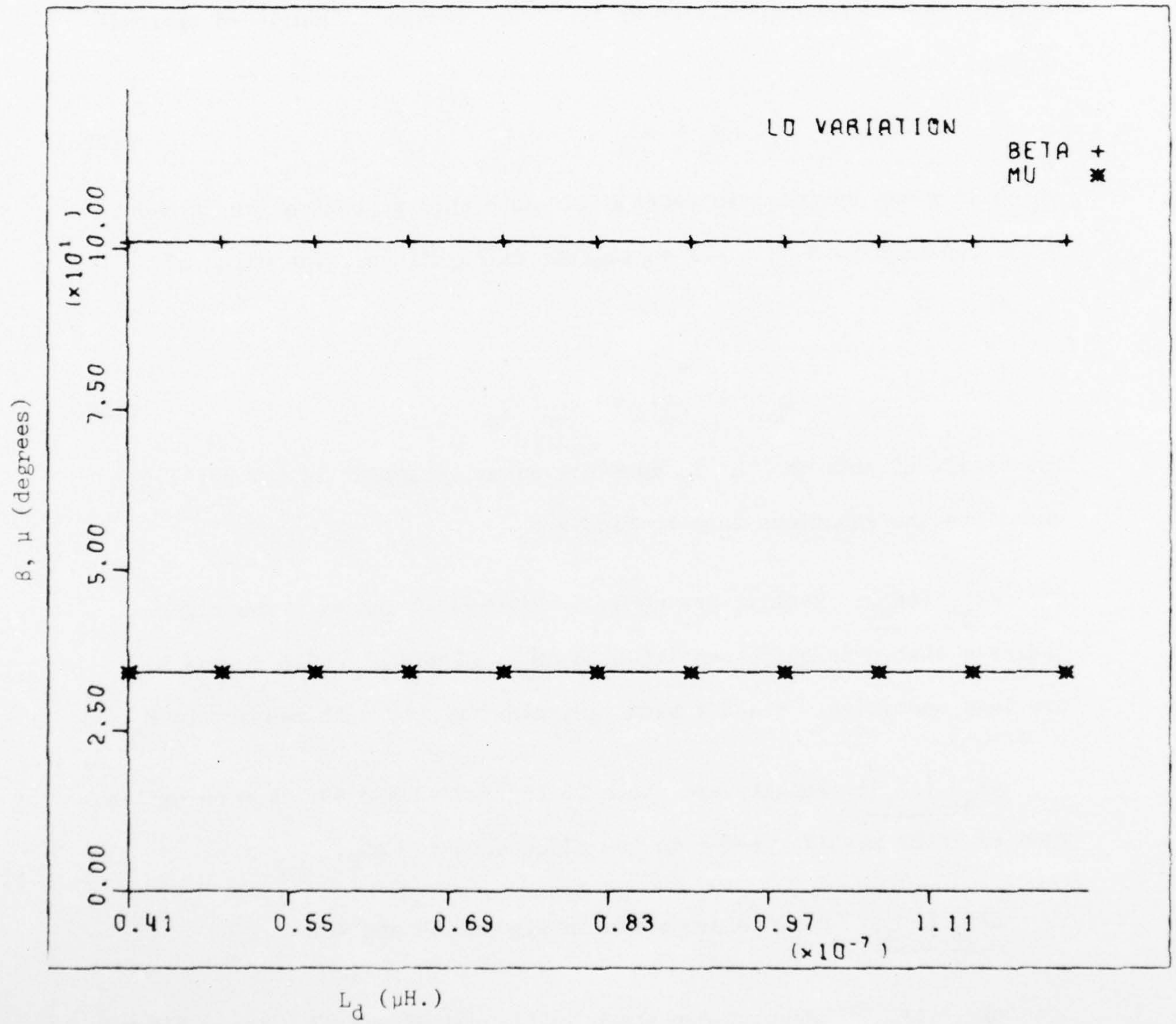

Figure 38. β and μ variation vs. L_d.

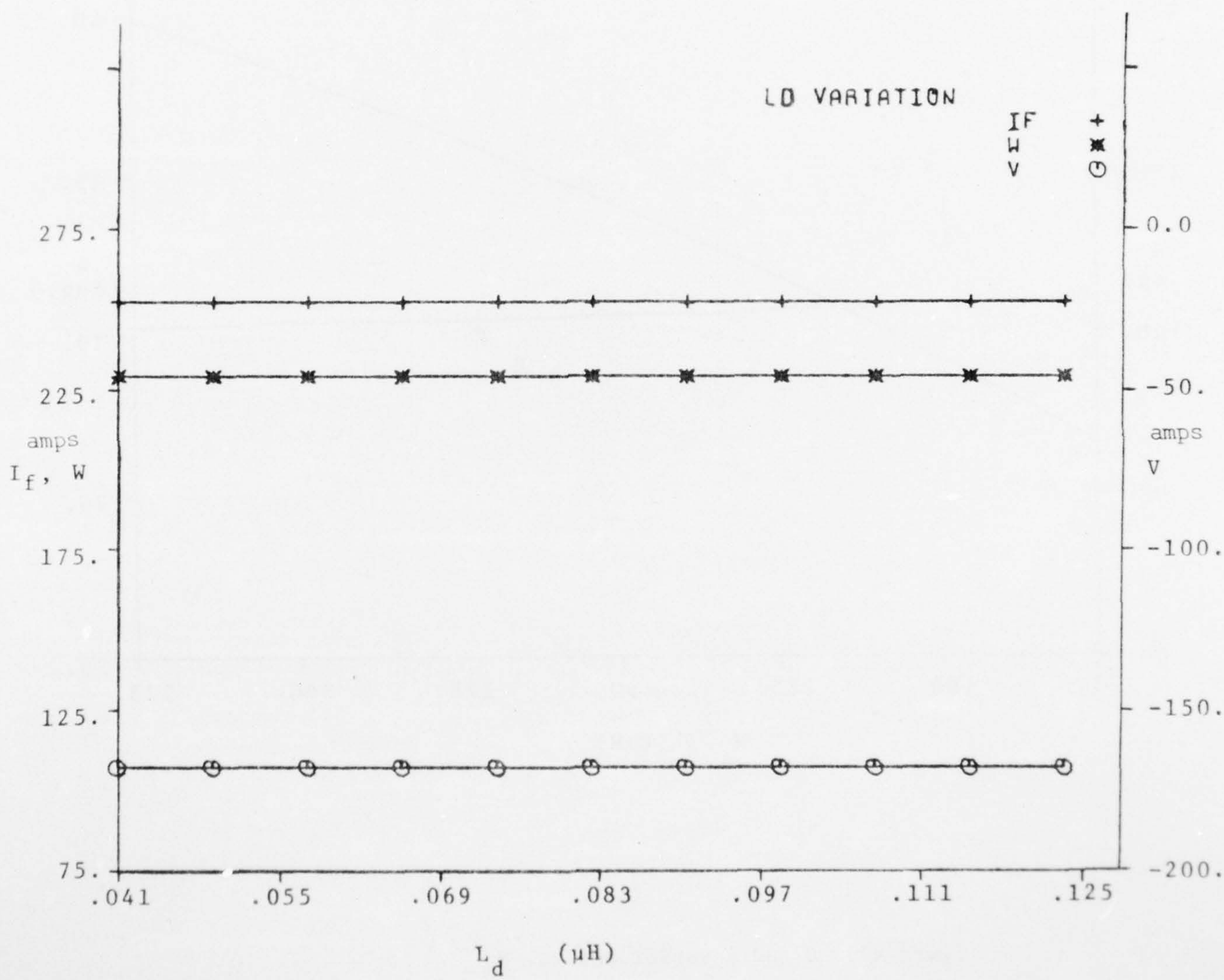

Figure 39. I_f, W and V variation vs. L_d.

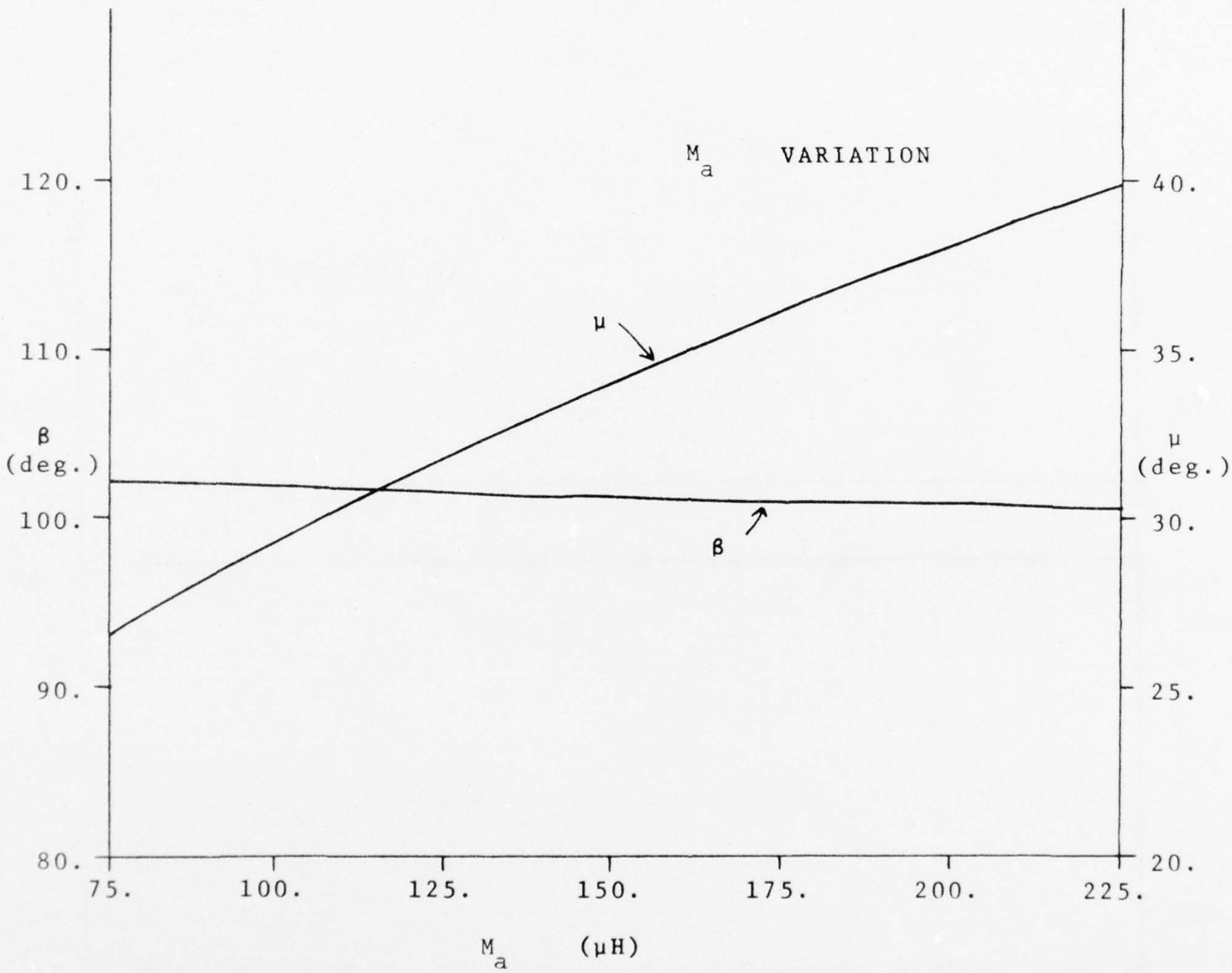

Figure 40. β and μ variations vs. M_a.

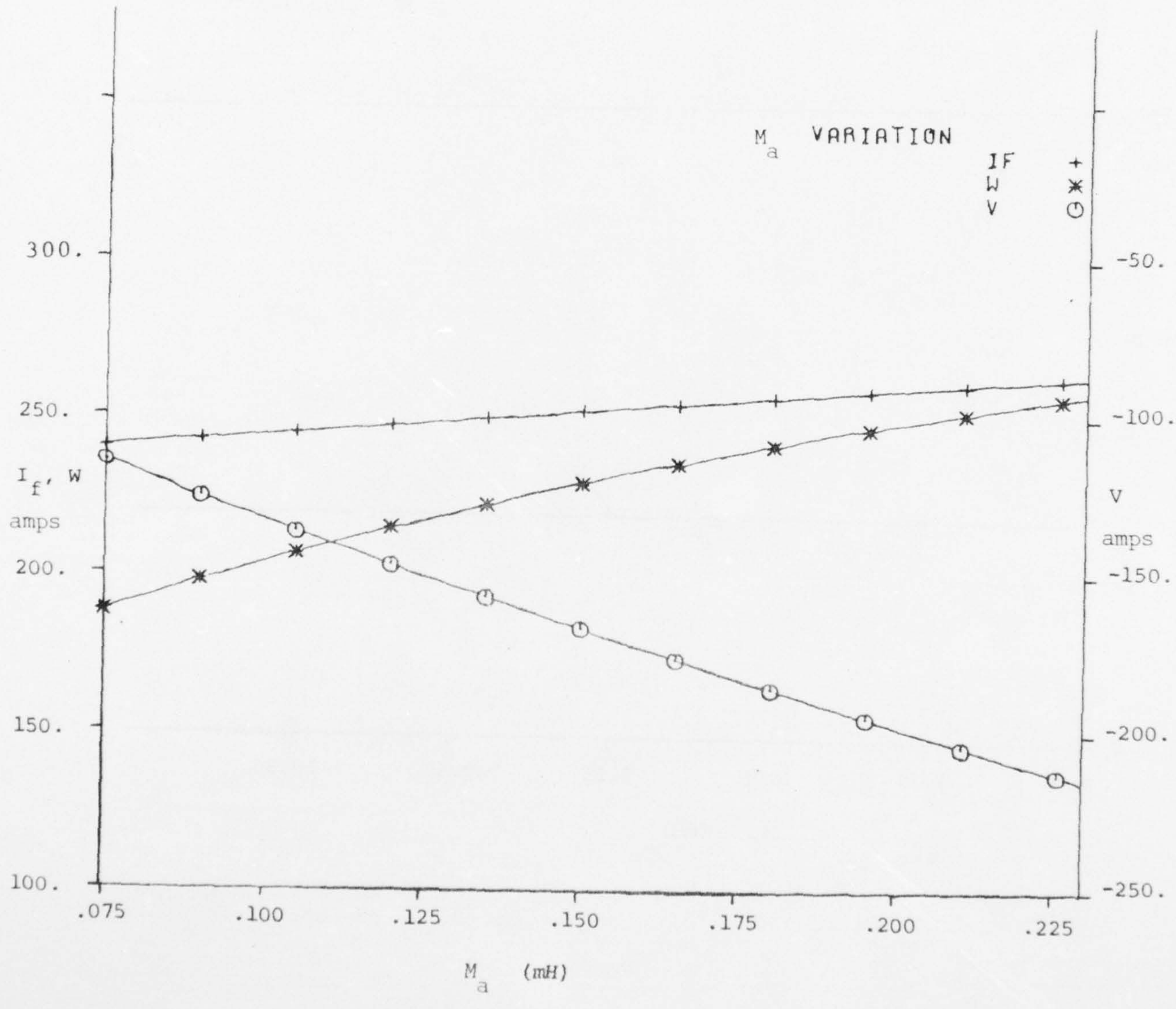

Figure 41. I_f, W and V variation vs. M_a.

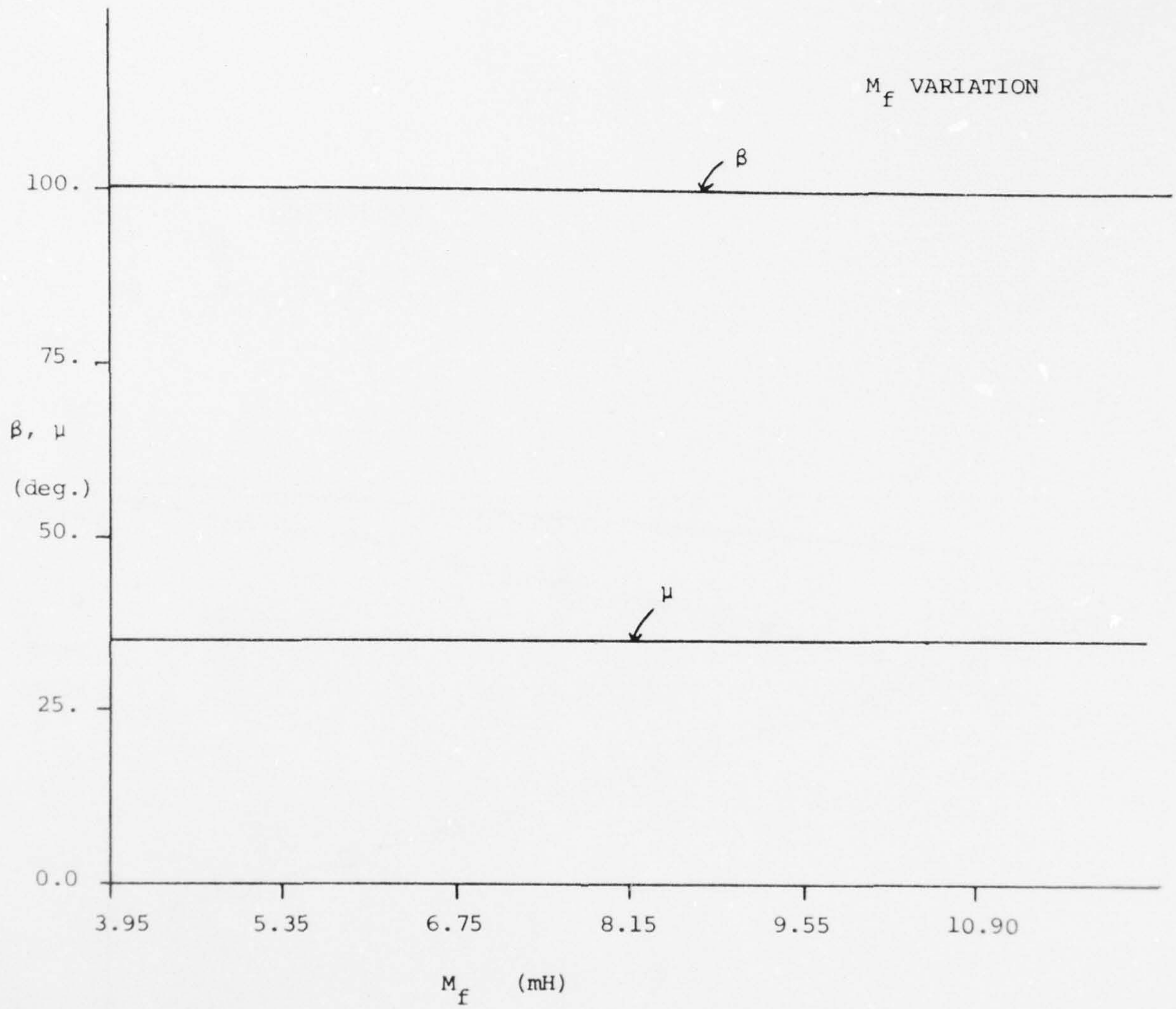

Figure 42. β and μ variation vs. M_f.

AD-A043 432 TOLEDO UNIV OH DEPT OF ELECTRICAL ENGINEERING F/G 9/5
UTILIZATION OF SOURCE IMPEDANCE TO DECREASE THE WEIGHT OF D.C. --ETC(U)
JUL 77 T A STUART AF-AFOSR-2997-76

UNCLASSIFIED AFOSR-TR-77-0985 NL

2 OF 2
AD
A043432

END
DATE
FILMED
9-77
DDC

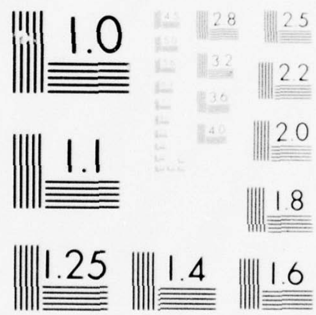

MICROCOPY RESOLUTION TEST CHART
NATIONAL BUREAU OF STANDARDS-1963-A

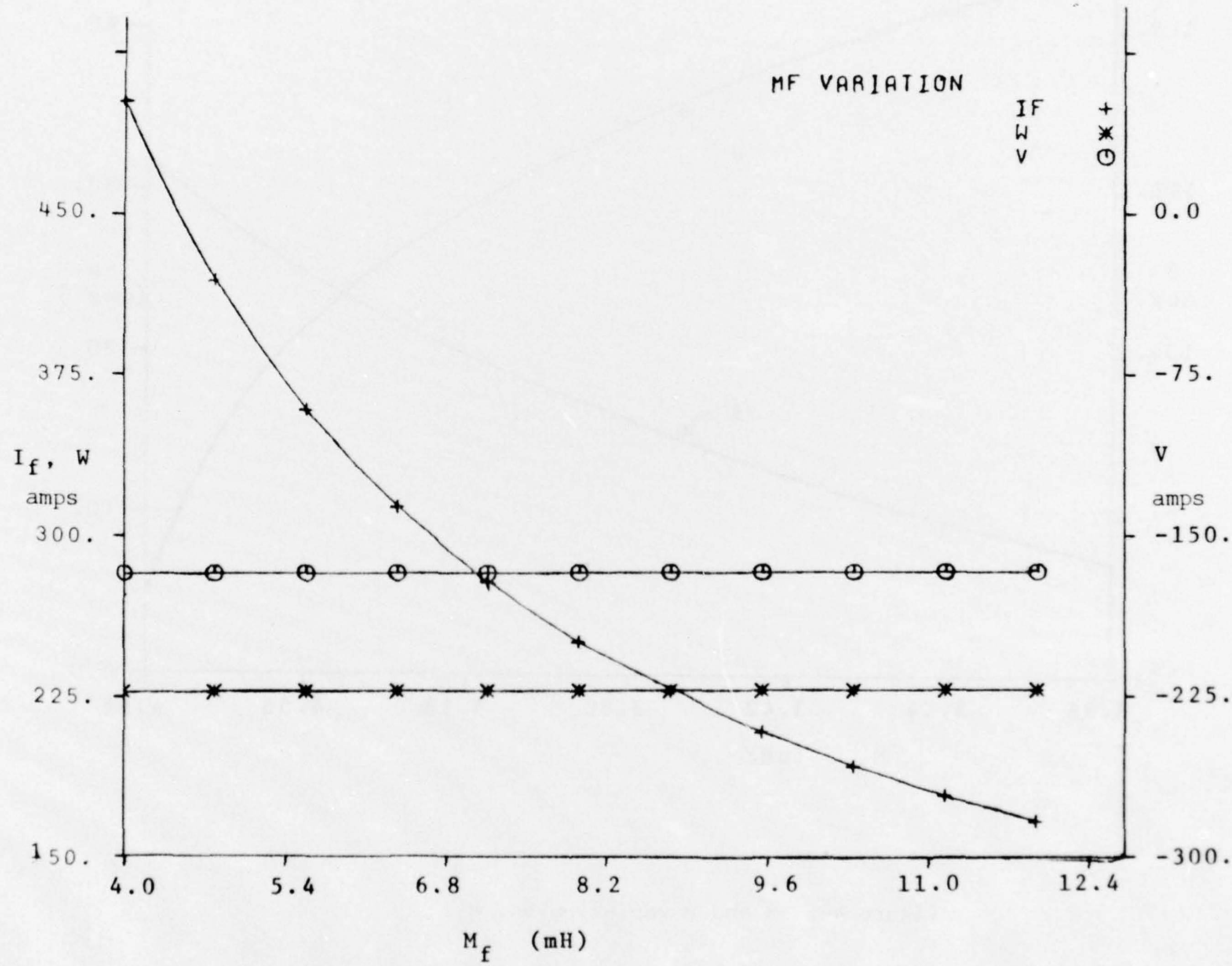

Figure 43. β and μ variation vs. M_f.

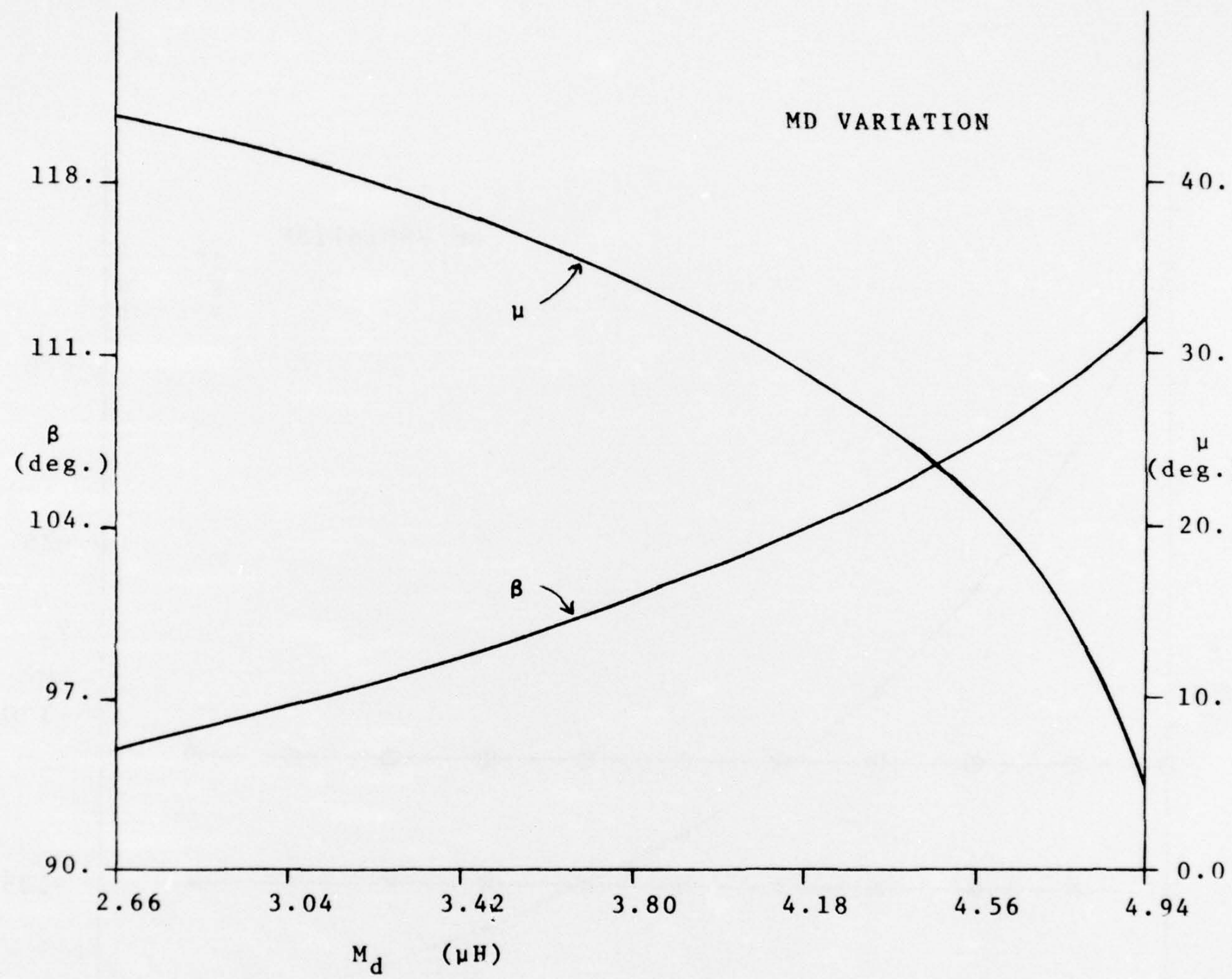

Figure 44. β and μ variation vs. M_d.

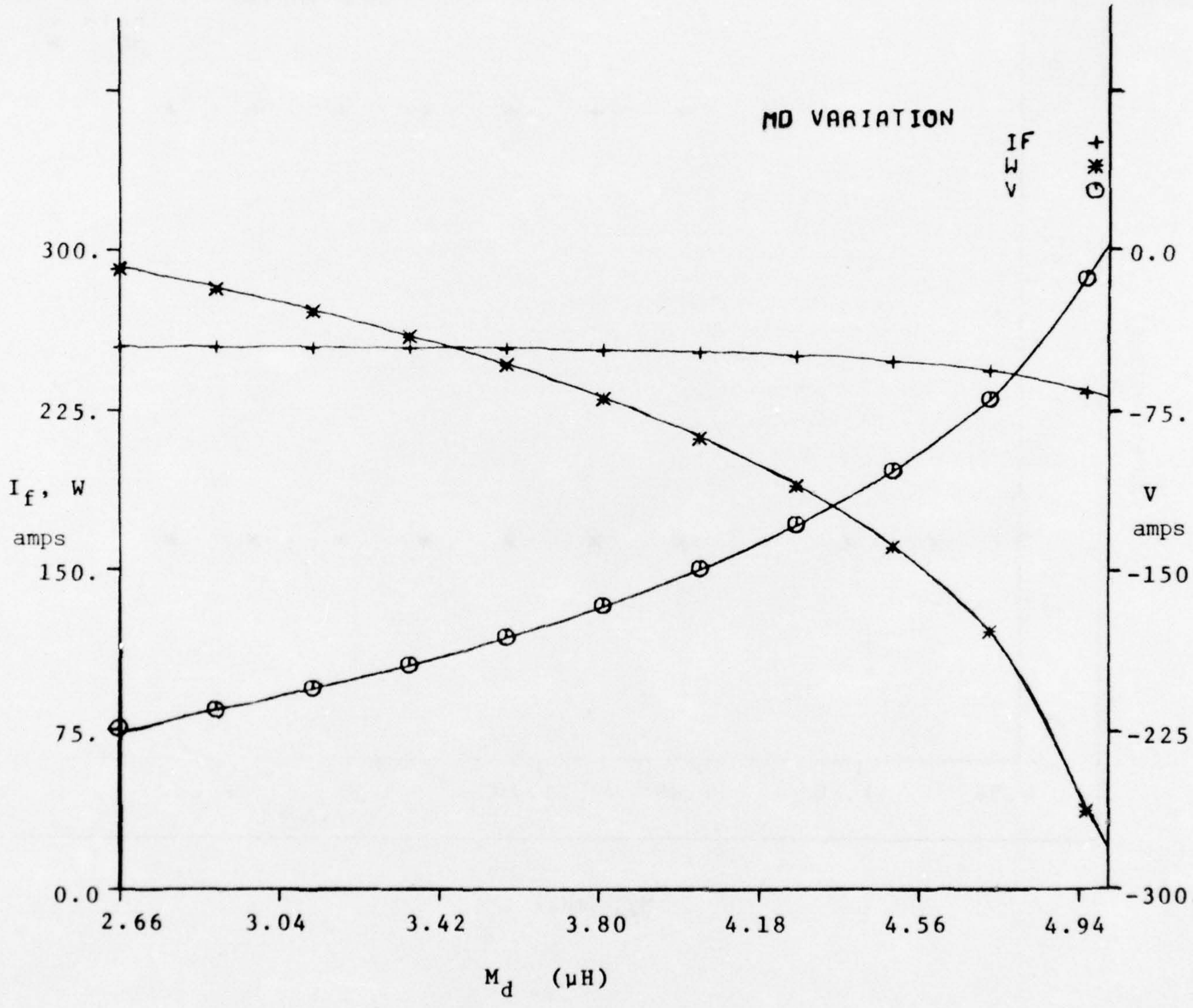

Figure 45. I_f, W and V variation vs. M_d.

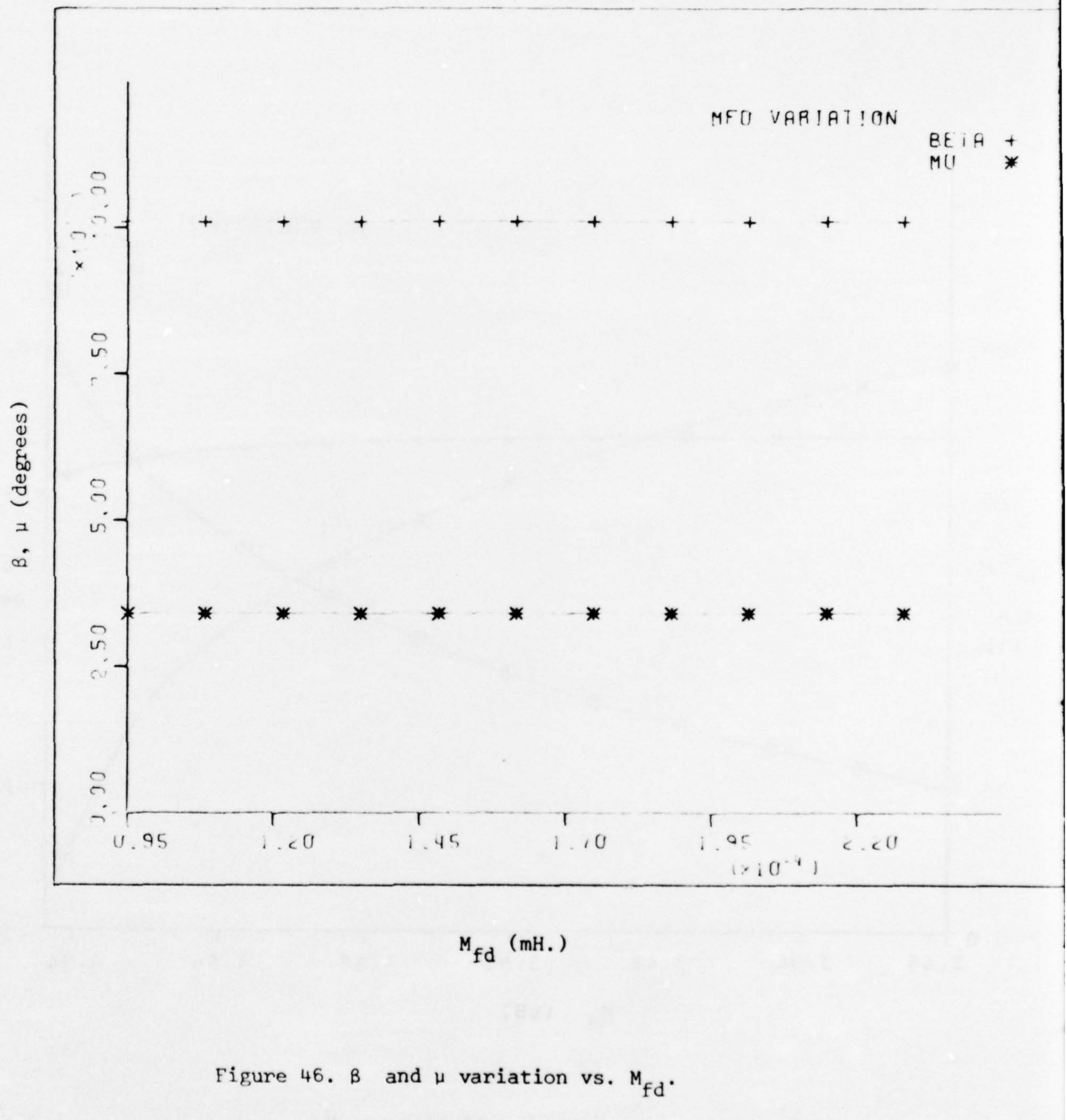

M_{fd} (mH.)

Figure 46. β and μ variation vs. M_{fd}.

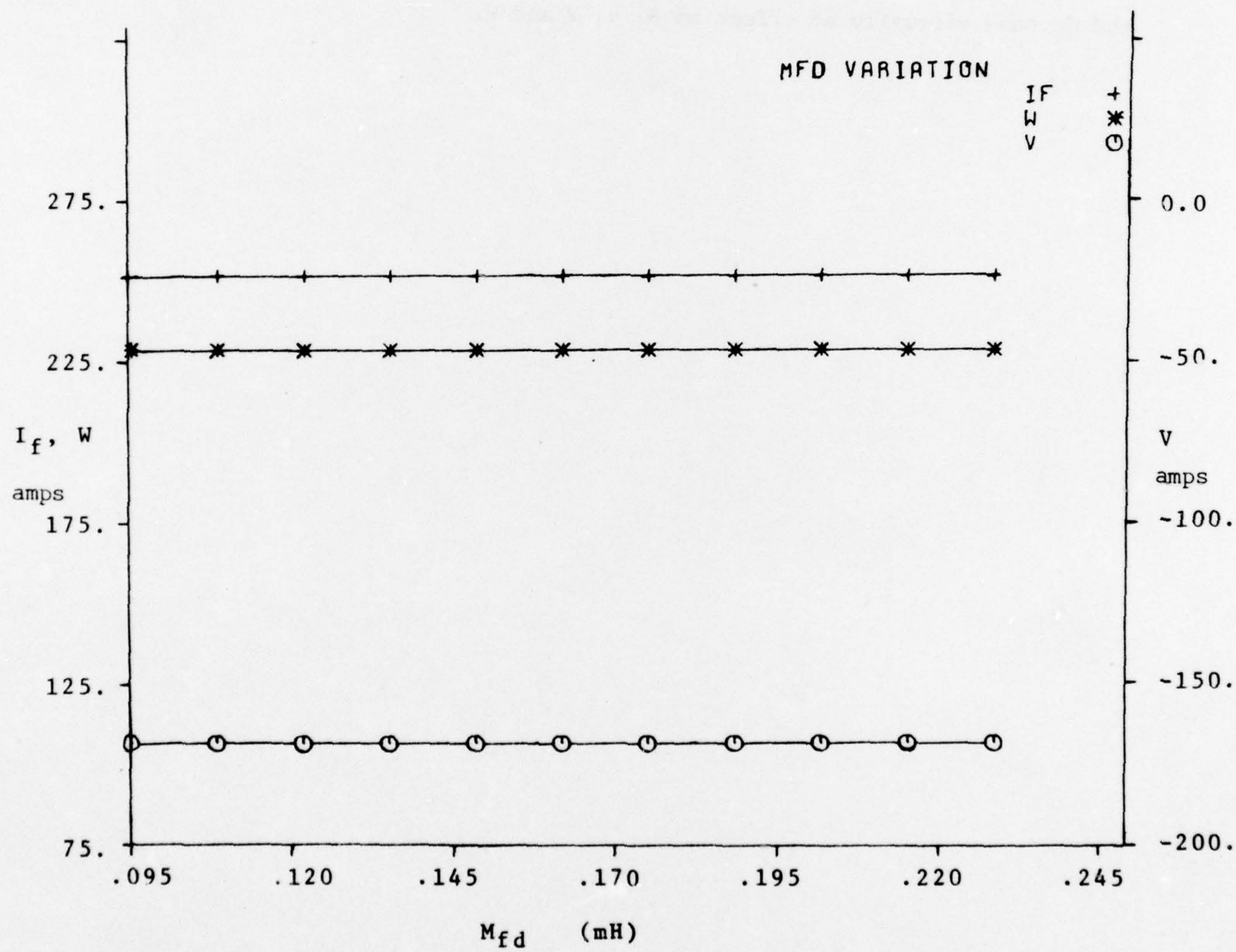

Figure 47. I_f, W and V variation vs. M_{fd}.

To summarize, it can be seen that I_f, β, μ, V and W as a group are most sensitive to errors in L_a, M_a and M_d. I_f is also quite sensitive to errors in L_f and M_f, but since the algorithm adjusts to maintain a constant $M_f I_f$ product (mutual flux linkages) errors in L_f and M_f have virtually no effect on β, μ, V and W.

7. VOLTAGE REGULATOR AND CURRENT OVERLOAD PROTECTION CIRCUITS

7.1 Introduction

The experimental portion of this study consisted of designing and building a phase controlled voltage regulator for eventual testing with an alternator. This circuit was designed and tested early in the project when it was thought that the alternator could be modelled by a voltage source in series with single inductance. Testing the regulator with this type of a source would have been a fairly simple matter, but such a test now appears to have limited value since a more detailed machine model was employed. Therefore it was decided to concentrate more effort on the analytical study and postpone this testing until a conventional alternator with known inductances could be obtained. Schematics of the complete design are shown in Figures 48 and 49. Operation of the voltage regulator circuit in Figure 48 is described in [23], and the operation of the current overload circuit in Figure 49 is described in [22]. The parts list is shown in Table I.

7.2 Experimental Results

As stated above, the experimental results were limited to building and testing a phase controlled voltage regulator circuit with a current overload. This circuit has the following characteristics:

1. The output voltage can be varied continuously from 0 to 290 V.d.c. with a 100 ohm load.
2. The overload circuit turns the regulator off at a load current of approximately 3.5 A.d.c.

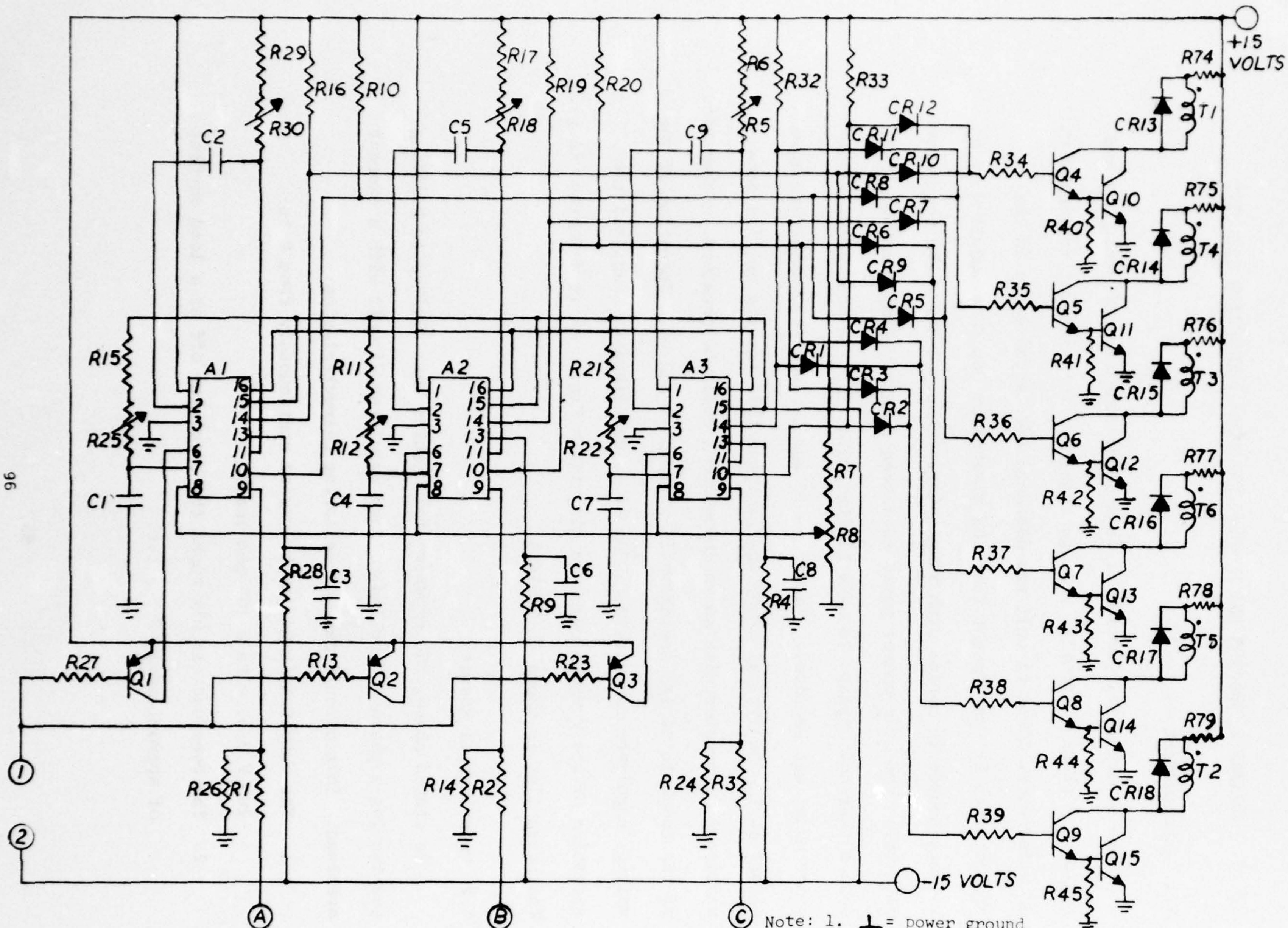

Figure 48. Voltage regulator circuit.

Note: 1. ⏚ = power ground (must be separate from ground in Figure. (49.)
2. Ref. Fig. 49 for 1, 2

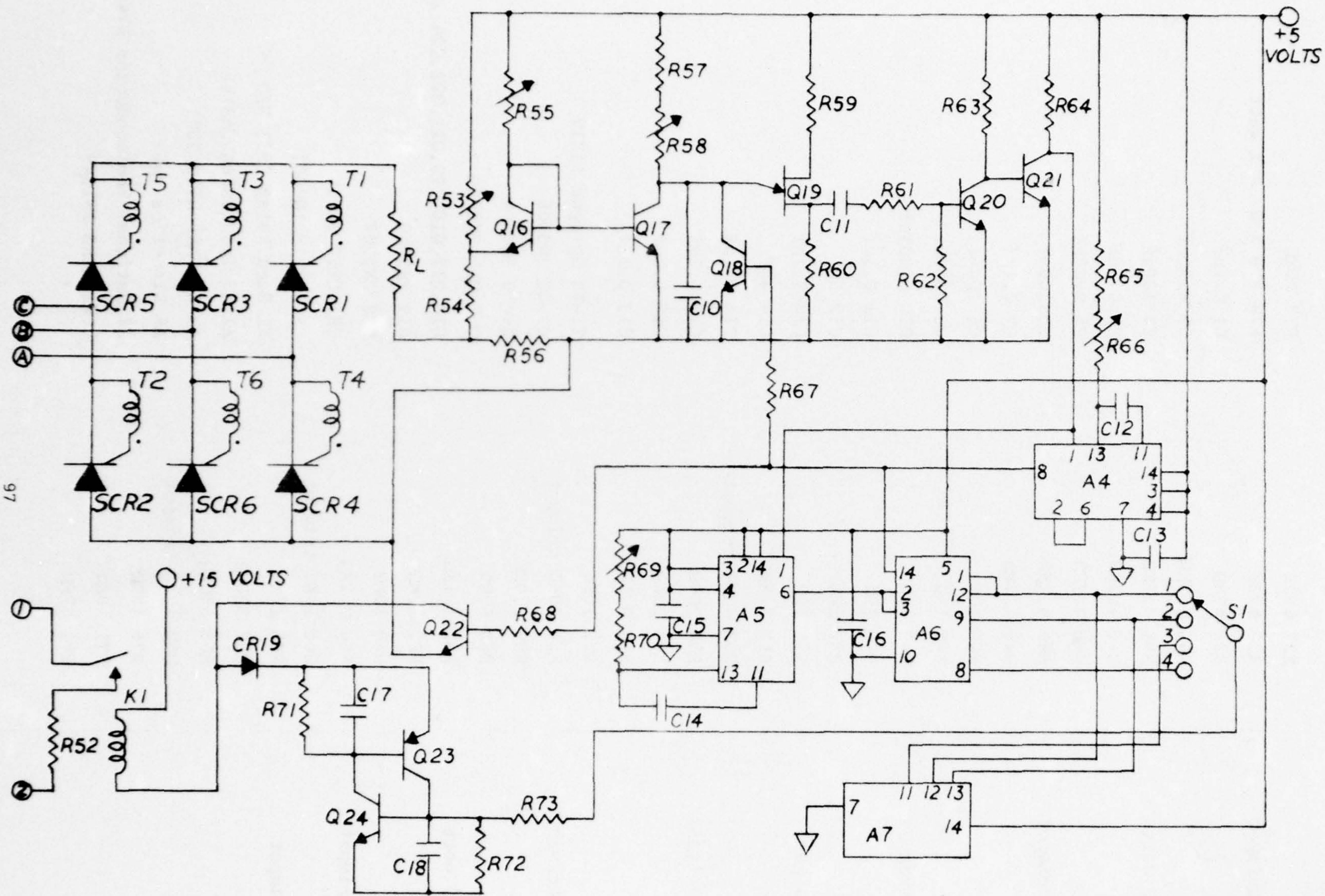

Figure 49. Output stage and current overload circuit.

Note: 1. ⏚ must be separate from power ground in Figure 48

2. Ref. Fig. 48 for 1, 2

TABLE I. PARTS LIST FOR CIRCUITS IN FIGURES 48 AND 49

R15 10KΩ
R25 250KΩ trimpot
R27 4.7KΩ
R26 3.76KΩ
R1 11KΩ - 2 watt
R28 330Ω
R29 5.6KΩ
R30 250KΩ trimpot
R16 1.5KΩ
R10 1.5KΩ
R11 10KΩ
R12 250KΩ trimpot
R13 4.7KΩ
R14 3.76KΩ
R2 11KΩ - 2 watt
R9 330Ω
R17 5.6KΩ
R18 250KΩ trimpot
R19 1.5KΩ
R20 1.5KΩ
R21 10KΩ
R22 250KΩ trimpot
R23 4.7KΩ
R24 3.76KΩ
R3 11KΩ - 2 watt
R4 330Ω
R6 5.6KΩ
R5 250KΩ trimpot
R7 10KΩ
R8 10KΩ trimpot
R31 1.5KΩ
R32 1.5KΩ
R33 1.5KΩ
R34 470Ω
R35 470Ω
R36 470Ω

R37 470Ω
R38 470Ω
R39 470Ω
R40 4.7KΩ
R41 4.7KΩ
R42 4.7KΩ
R43 4.7KΩ
R44 4.7KΩ
R45 4.7KΩ
R46 10Ω
R47 10Ω
R48 10Ω
R49 10Ω
R50 10Ω
R51 10Ω
R52 3.3KΩ
R53 20KΩ trimpot
R54 200Ω
R55 20KΩ
R56 0.04Ω
R57 10KΩ
R58 20KΩ trimpot
R59 2.0KΩ
R60 630Ω
R61 1.1KΩ
R62 10KΩ
R63 10KΩ
R64 2.2KΩ
R65 10KΩ trimpot
R66 15KΩ
R67 330KΩ
R68 330KΩ
R69 10KΩ trimpot
R70 15KΩ
R71 10KΩ
R72 47KΩ

R73 20KΩ
R74-R79 30Ω - 1 watt
C1 0.1μf
C2 0.05μf
C3 100μf
C4 0.1μf
C5 0.05μf
C6 100μf
C7 0.1μf
C8 100μf
C9 0.05μf
C10 0.001μf
C11 0.1μf
C12 2μf
C13 0.1μf
C14 4μf
C15 0.1μf
C16 0.1μf
C17 0.1μf
C18 0.1μf

T1-T6 Sprague 11Z12
Q1-Q3 2N3906
Q4-Q9 2N3904
Q10-Q15 2N2222
Q16,Q17,Q18,Q20,Q21,Q22,Q24 2N2222
Q19 2N2646
Q23 2N2907
CR1-CR12 1N914
CR13-CR18 1N4001
K1 Reed Relay SPST N/O
A1-A3 Telefunken UAA145
A4-A5 Fairchild 9601
A6 Signetics 7493
A7 National Semiconductor N7408
SCR1-SCRG 2N1849

3. No misfiring problems were observed once the final design was complete.

Certain waveforms of interest are shown in Figures 50 through 53.

Figure 50. AC output voltage across the load for a delay angle of 15°. (Scale = 15°/div.)

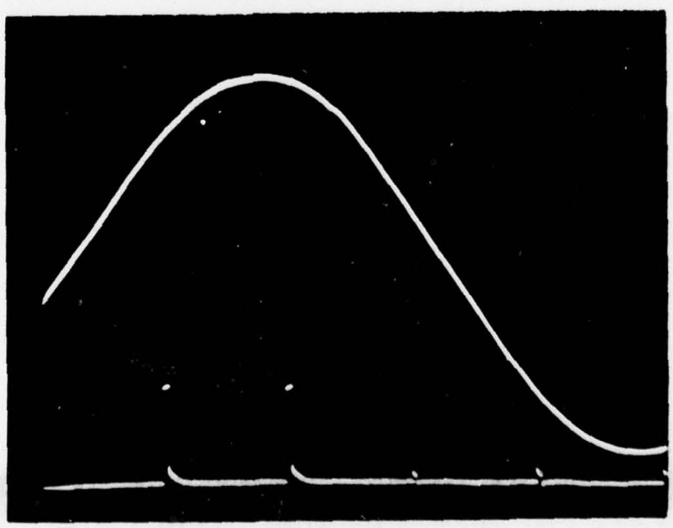

Figure 51. (Top) Line to neutral input voltage. (Bottom) Thyristor firing pulses for a delay angle of 15°. (Note: 0° delay angle corresponds to 30° on the line to neutral voltage waveform. (Scale = 30°/div.)

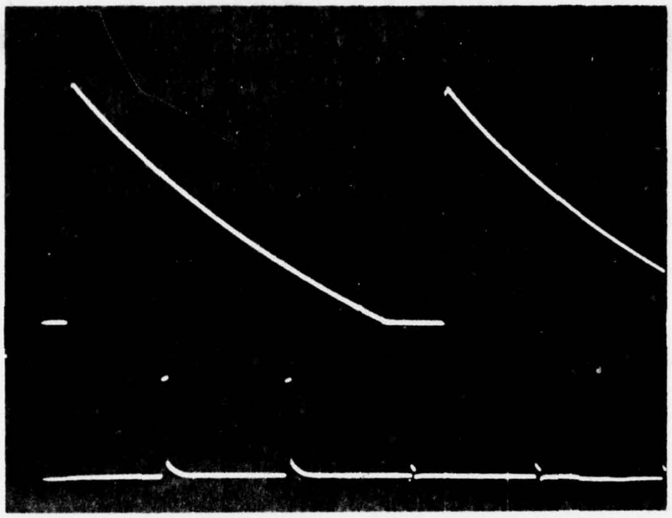

Figure 52. (Top) Ramp voltage at pin 7 of the UAA145.
(Bottom) Thyristor firing pulses for a delay angle of 15°. (Scale = 30°/div.)

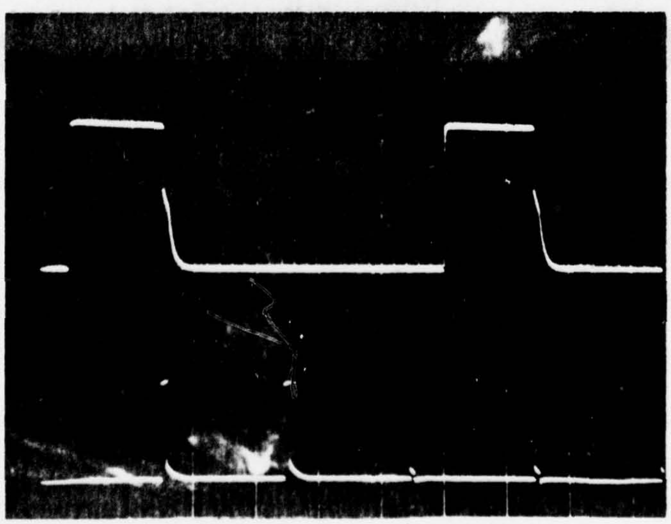

Figure 53. (Top) Pulse formation control signal at pin 11 of UAA145.
(Bottom) Thyristor firing pulses for a delay angle of 15°. (Scale = 30°/div.)

8. CONCLUSIONS

This study indicates that it is possible to utilize L_a to help perform some of the functions normally assigned to the L_oC_o output filter. This implies that a smaller filter can be used, thus decreasing the weight of the L_o and C_o components. For the 10 MVA/5kV example alternator with a controlled rectifier bridge it was shown that an increase in L_a from 0.3 mH. to 0.72 mH decreases the filter weight by about 17 lbs., a 22% reduction. This example also indicated 0.72 mH. to be an optimum value, i.e., filter weight increased for $L_a >$ 0.72 mH. Naturally, this savings may be offset by an increase in alternator weight due to the larger L_a. Therefore any final weight optimization study should consider the alternator and filter as a combined system.

In the course of developing the filter weight minimization program it was necessary to derive both steady state and transient models for the alternator and rectifier bridge. Because of the large amounts of information provided by these models, it appears they may be useful for simulating the system during the design stage. Once experimental data becomes available for comparison, these models may be refined as necessary in order to accurately predict the various winding currents, commutation angles, etc. It is stressed that this experimental verification is necessary, and plans have been made to proceed with this for a system with a conventional alternator.

9. RECOMMENDATIONS

This study indicates that if L_a is increased up to a certain optimum point, it is possible to significantly reduce the size of the output filter. Information of this type should be brought to the attention of machine designers, but it may or may not influence the design of future alternators due to the many other factors which govern the size of L_a. Ultimately the alternator and filter should be considered together in future weight minimization studies.

Perhaps the most pressing need at this point is to obtain some experimental data to compare with the predicted results. Eventually this must be done using a superconducting alternator; however, it is unlikely that such a machine will be available for this purpose for quite some time. In the interim, it is proposed that tests should be conducted on a conventional alternator-rectifier system in order to evaluate the models.

10. REFERENCES

1. H. H. Woodson, Z. J. J. Stekly, and E. Halas, "A Study of Alternators with Superconducting Field Windings: I - Analysis," IEEE Trans. on Power Apparatus and Systems, vol. PAS-95, No. 3, pp. 264-274, March 1966.

2. Z. J. J. Stekly, H. H. Woodson, A. M. Hatch, L. O. Hoppie, and E. Halas, "A Study of Alternators with Superconducting Field Windings: II - Experiment," IEEE Trans. on Power Apparatus and Systems, vol. PAS-95, No. 3, pp. 274-280, March 1966.

3. P. Thullen, J. C. Dudley, D. L. Greene, J. L. Smith, Jr., and H. H. Woodson, "An Experimental Alternator with a Superconducting Rotating Field Winding," IEEE Trans. on Power Apparatus and Systems, vol. PAS-90, No. 2, pp. 611-619, March-April 1971.

4. H. H. Woodson, J. L. Smith, Jr., P. Thullen, and J. L. Kirtley, "The Application of Superconductors in the Field Windings of Large Synchronous Machines," IEEE Trans. on Power Apparatus and Systems, vol. PAS-90, No. 2, pp. 620-627, March-April 1971.

5. J. L. Kirtley, Jr., "Basic Formulas for Air-Core Synchronous Machines," IEEE PES Winter Power Meeting, Paper No. 71 CP 155-PWR, New York, New York, January 1971.

6. J. L. Kirtley, Jr., "Per Unit Reactances of Superconducting Synchronous Machinery," IEEE Trans. on Power Apparatus and Systems, vol. PAS-92, No. 4, pp. 1316-1320, July-August 1973.

7. T. H. Einstein, "Generalized Representation of Generator Excitation Power Requirements," IEEE Trans. Power Apparatus and Systems, vol. PAS-91, No. 5, pp. 1840-1847, September-October 1972.

8. T. H. Einstein, "System Performance Characteristics of Superconducting Alternators for Electric Utility Power Generation," IEEE Trans. Power Apparatus and Systems, vol. PAS-94, No. 2, pp. 310-319, March-April 1975.

9. M. Furuyama and J. L. Kirtley, Jr., "Transient Stability of Superconducting Alternators," IEEE Trans. on Power Apparatus and Systems, vol. PAS-94, No. 2, pp. 320-328, March-April 1975.

10. J. L. Smith, "Superconductors in Large Synchronous Machines," Final Report for EPRI-EEI research project RP-92, Electric Power Research Institute, Palo Alto, California, June 1975.

11. J. L. Kirtley, Jr., and M. Furuyama, "A Design Concept for Large Superconducting Alternators," IEEE Trans. Power Apparatus and Systems, vol. PAS-94, No. 4, pp. 1264-1269, July-August 1975.

12. J. L. Smith, Jr., P. Thullen, "Steady-State Electrical Tests on the MIT-EPRI 3 MVA Superconducting Generator," IEEE Trans. on Power Apparatus and Systems, vol. PAS-95, No. 3, pp. 887-893, May-June 1975.

13. J. L. McCabria, R. D. Blaugher, and J. H. Parker, Jr., "Superconducting Generator Development," NAECON '75 Record, pp. 261-271, Dayton, Ohio, June 1975.

14. A. E. King, C. C. Kouba, J. L. McCabria, and L. D. Smith, "High Power Study - Superconducting Generators," Final Report AFAPL-TR-76-37, USAF Aero Propulsion Laboratory, Wright-Patterson AFB, Ohio, March 1976.

15. W. J. Shilling, "Exciter Armature Reaction and Excitation Requirements in a Brushless Rotating Rectifier Aircraft Alternator," AIEE Trans. Applications and Industry, vol. 79 , Pt. 2, pp. 394-402, 1960.

16. J. Stepina, "Calculation of the R.M.S. Value of the Ampere-Turns Per Unit of Rotor Periphery in the Synchronous Machine Under Rectifier Load," ACTA TECHNICA GSAV, No. 3, pp. 255-280, 1964.

17. P. W. Franklin, "Theory of the Three Phase Salient Pole Type Generator with Bridge Rectified Output - Part I," IEEE Trans. Power Apparatus and Systems, vol. PAS-72, No. 5, pp. 1960-1967, September-October 1972.

18. P. W. Franklin, "Theory of the Three Phase Salient Pole Type Generator with Bridge Rectified Output - Part II," IEEE Trans. Power Apparatus and Systems, vol. PAS-72, No. 5, pp. 1968-1975, September-October 1972.

19. W. J. Bonwick and V. H. Jones, "Performance of a Synchronous Generator with a Bridge Rectifier," Proceedings of IEE, Vol. 119, No. 9, pp. 1338-1342, September 1972.

20. W. J. Bonwick and V. H. Jones, "Rectifier-Loaded Synchronous Generators with Damper Windings," Proceedings of IEE, Vol. 120, No. 6, pp. 659-666, June 1973.

21. P. K. Dash, G. S. Hope and O. P. Malik, "Digital Simulation of a Synchronous Generator Operating with Thyristor Bridge," presented at the 1977 IEEE PES Winter Meeting (Paper No. A77-194-4), New York, New York, February 1977.

22. T. A. Stuart, "Overload Protection and Filtering Requirements for Phase Controlled Voltage Regulators," ASEE-USAF Summer Faculty Research Program Report (sponsored by Auburn University), Wright-Patterson AFB, Ohio, August 15, 1975.

23. "Phase Control Integrated Circuit," (Application Note), AEG-Telefunken Corporation, Heilbronn, West Germany.

24. F. W. Gutzwiller, G. H. Bacon, E. E. Von Zastrow, and R. R. Rottier, "Rectifier Components Guide," General Electric Company, Auburn, New York, 1962.

25. C. C. Damstra and T. Stoop, "A Three Phase Resonant Inverter Circuit for HVDC Valve," Proceedings of the 1977 IEEE/IAS International Semiconductor Power Converter Conference, pp. 164-171, Lake Buena Vista, Florida, March 1977.

26. J. Hak, Eisenlose Drosselspule, Leipzig-Kohler-Verlag, 1938.

27. G. W. Stagg and A. H. El-Abiad, "Computer Methods in Power System Analysis," McGraw-Hill, New York, New York, 1968.

11. RESEARCH PUBLICATIONS

1. T. A. Stuart and M. W. Tripp, "Predicted Characteristics of the Superconducting Alternator with Rectified Load," NAECON '77 Conference Proceedings, Dayton, Ohio, May 1977.

2. T. A. Stuart and M. W. Tripp, "Calculation of Rotor Currents for the Rectified Superconducting Alternator," to be published as a short paper by the Proceedings of the IEEE (accepted February 1977).

3. T. A. Stuart and M. W. Tripp, "A Steady State Analysis of the Superconducting Alternator with Rectified Output," accepted for the July 1977 issue of IEEE Trans. on Aerospace and Electronic Systems.

4. M. W. Tripp, "An Improved Model for Predicting the Output Characteristics of the Superconducting Alternator with Rectified Load," Masters Thesis, Department of Electrical Engineering, The University of Toledo, Toledo, Ohio, May 1977.

APPENDIX I: GLOSSARY OF TERMS

A, B, C = constants defined by (49.), (50.) and (51.)

a = thickness of L_o

C_o = output filter capacitor

D_c = energy density of C_o

D_w = density of aluminum

f = fill-in factor for L_o

f_b = break frequency of output filter

F_w = cross sectional area of one winding of L_o

i_a, i_b, i_c = line currents

i_d, i_q = currents in the equivalent direct and quadrature windings used to represent the damper shield

I_f = average field current

i_f = time varying component of field current

i_k = commutation current

i_{LF} = load current with short circuit across load

i_{kF} = commutation current with short circuit across load

i_{fo}, i_{do}, i_{qo} = field and damper currents at $\theta = \beta+\mu-\pi/3$

K_q, K_f, K_d = constants defined by (15.) and (18.)

k_{aa} = coefficient of coupling between armature phase windings

k_{ad} = coefficient of coupling between armature and equivalent damper windings

k_{af} = coefficient of coupling between field and armature

k_{fd} = coefficient of coupling between field and equivalent direct axis damper windings

k_1 = specified harmonic attenuation factor of output filter

k_2, k_3 = constants defined just below (97.)

I_L = load current

L_a = self inductance of each armature winding

L_d = self inductance of the direct and quadrature axis windings

L_f = self inductance of the field winding

L_o = output filter inductor

M_a = magnitude of mutual inductance between armature windings

M_d = magnitude of mutual inductance between damper and armature windings

M_f = magnitude mutual inductance between field and armature windings

M_{fd} = mutual inductance between field and direct axis damper windings

M_o, M_{∞} = constants defined by (33.) and (34.)

N = number of turns for L_o

R_a = resistance of one armature winding

R_p = resistance of inductor, L_o

v_f, v_d, v_q = voltages across rotor windings

v_{ab}, v_{bc}, v_{ca} = phase to phase armature voltages

v_o = instantaneous rectifier output voltage

V_L = average output voltage

V = variable defined by (21.)

W = variable defined by (20.)

β = angle at which commutation starts

Λ_o = constant defined by (36.)

Λ_f, Λ_d = constants defined by (36.)

λ_a, λ_b, λ_c, λ_f, λ_d, λ_q = flux linkages

θ = time angle

μ = commutation angle

ω = electrical angular velocity

APPENDIX II: TRANSIENT MATRICES

$$[A] = \left[\begin{array}{c|c} A_{11} & A_{12} \\ \hline A_{21} & A_{22} \end{array}\right] = \left[\begin{array}{cccc|c} (L_o + 2L_a + 2M_a) & \sqrt{3}M_f \cos(\omega t + \frac{\pi}{6}) & \sqrt{3}\, M_d \cos(\omega t + \frac{\pi}{6}) & -\sqrt{3}M_d \sin(\omega t + \frac{\pi}{6}) & -(L_a + M_a) \\ \sqrt{3}\, K_f \cos(\omega t + \frac{\pi}{6}) & 1 & 0 & 0 & \sqrt{3}\, K_f \sin(\omega t) \\ \sqrt{3}\, K_d \cos(\omega t + \frac{\pi}{6}) & 0 & 1 & 0 & \sqrt{3}\, K_d \sin(\omega t) \\ -\sqrt{3}\, K_q \sin(\omega t + \frac{\pi}{6}) & 0 & 0 & 1 & \sqrt{3}\, K_q \cos(\omega t) \\ \hline -(L_a + M_a) & \sqrt{3}\, M_f \sin(\omega t) & \sqrt{3}\, M_d \sin(\omega t) & \sqrt{3}\, M_d \cos(\omega t) & 2(L_a + M_a) \end{array}\right]$$

$$[B] = \left[\begin{array}{c|c} B_{11} & B_{12} \\ \hline B_{21} & B_{22} \end{array}\right] = \left[\begin{array}{cccc|c} -(R_p + 2R_a) & \sqrt{3}\, M_f\, \omega \sin(\omega t+\pi/6) & \sqrt{3}\, M_d\, \omega \sin(\omega t+\pi/6) & \sqrt{3}\, M_d\, \omega \cos(\omega t+\pi/6) & R_a \\ \sqrt{3}\, K_f\, \omega \sin(\omega t+\pi/6) & 0 & 0 & 0 & -\sqrt{3}\, K_f\, \omega \cos(\omega t) \\ \sqrt{3}\, K_d\, \omega \sin(\omega t+\pi/6) & 0 & 0 & 0 & -\sqrt{3}\, K_d\, \omega \cos(\omega t) \\ \sqrt{3}\, K_q\, \omega \cos(\omega t+\pi/6) & 0 & 0 & 0 & \sqrt{3}\, K_q\, \omega \sin(\omega t) \\ \hline R_a & -\sqrt{3}\, M_f\, \omega \cos(\omega t) & -\sqrt{3}\, M_d\, \omega \cos(\omega t) & \sqrt{3}\, M_d\, \omega \sin(\omega t) & -2R_a \end{array}\right]$$

APPENDIX III: MAIN PROGRAMS

The following programs are listed in alphabetical order. All subroutines except GELG and ARCSIN are listed in APPENDIX IV. It should be noted that the notation in the programs occasionally differs from that in the text:

Text	Program
L_a	L_o
M_a	L_{ab}

1. CONT: Finds the solution for the controlled rectifier bridge case.
2. MACH2: Finds the value of L_a which produces the minimum value of the 6th harmonic of v_o.
3. MAST: Finds the minimum filter weight for a given set of specifications
4. PLTDAT: General purpose program that includes various simulations for both the controlled and uncontrolled rectifier bridge.
5. SENSI3: Sensitivity analysis program.
6. TABLE: Determines the harmonics of v_o and $i_{f(rms)}$ for various values of L_a.
7. TESTR2: Calling program for fault current simulation.
8. UNCONT: Finds the solution for the uncontrolled rectifier bridge case.

```
C      MAIN PLOTTER PROGRAM
       DIMENSION FD(5),F(5,1),FF(5,5),MUS(50),RMSIF(50),
      1XRMS(50),ALIF(21),TBETA(21),TMU(21),FF1(4,4),F1(4,1),
      1FD1(4),ILS(50),BETAS(50),IFS(50),APIL(50),APBETA(50),
      1APMU(50),APIF(50),AHAR6(50),AHAR12(50),AHAR18(50),
      1AHAR24(50),AHAR30(50),APRMS(50),HAR6(50),HAR12(50),
      1HAR18(50),HAR24(50),HAR30(50),ALO(21),XHAR6(21),XHAR12(50),
      1XHAR18(21),XHAR24(21),XHAR30(21),AIQ(60),AID(60),AIF(60),
      1AIK(60),THETA(60)
       REAL*4 MO,MOO,MU,IF,IL,K1,LD,LF,MF,MFD,LAB,LO,MD,KQ,
      1NN1,NP2,OMEGA,LA,MUP,MUF,KFO,KAB,KOD,ILS,IFS,MUS,KF,KD
C      INPUT MACHINE PARAMETERS
       WRITE(7,50)
50     FORMAT('0',2X,' THIS IS THE DATA FOR THE PHASE CONTROLLED
      1 BRIDGE RECTIFIER')
       LF=0.12E 01
       LD=0.82E-07
       MF=0.79E-02
       MD=0.38E-05
       MFD=0.19E-03
       LAB=0.15E-03
       LO=0.3E-03
C      LO=LA  AND LAB=MA
       K1=1.0
       VL=6760.0
       IL=1420.0
       OMEGA=2513.27
       FREQ=400.0
       KF=(MF*LD-MD*MFD)/(LF*LD-(MFD)**2)
       KD=(MD*LF-MF*MFD)/(LF*LD-(MFD)**2)
       KQ=MD/LD
       MOO=MD**2/LD
       MO=MOO
       DELTAF=MO+MOO
       DELTAO=(1.333*(LO+LAB))-DELTAF
       DIL=1420.0/15.0
       KFO=MF/SQRT(LF*LO)
       KAB=LAB/LO
       KOD=MD/SQRT(LO*LD)
       DLO=0.0
       IL=1420.0
       KKK=0
       MF=KFO*SQRT(LF*LO)
       LAB=KAB*LO
       MD=KOD*SQRT(LO*LD)
       MOO=MD**2/LD
       MO=MOO
       DELTAF=MO+MOO
       DELTAO=(1.3333*(LO+LAB))-DELTAF
       KF=(MF*LD-MD*MFD)/(LF*LD-(MFD)**2)
       CALL NEWTON(MU,BETA,IF,W,V,FREQ,DELTAO,IL,VL,MOO,K1,
      1MF,MO,OMEGA,DELTAF,ZETA)
       IL=0.0
       IF=1.1*IF
       DO 100 LLL=1,17
       KKK=0
```

```
      CALL PHACON(IF,MF,BETA,MO,W,V,IL,MU,DELTAO,OMEGA,VL,MOO)
      APIL(LLL)=IL
      APBETA(LLL)=BETA*180.0/3.1416
      APMU(LLL)=MU*180.0/3.1416
      CALL FS(MU,BETA,OMEGA,IL,IF,MO,DELTAO,MF,W,V,LO,LAB,
     1DELTAF,LLL,AHAR6,AHAR12,AHAR18,AHAR24,AHAR30)
      CALL RMS(BETA,LLL,MU,APRMS,IL,DELTAO,MF,MO,W,V,MOO,IF,
     1KF,DELTAF)
      IL=IL+DIL
100   CONTINUE
      WRITE(7,300)LO,IF
300   FORMAT('0',5X,'LO=',E10.3,5X,'IF=',E10.3)
      WRITE(7,203)
203   FORMAT('0',5X,'IL,IFRMS,6TH,12TH,18TH,BETA,MU')
      DO 201 KK=1,17
       WRITE(7,202)APIL(KK),APRMS(KK),AHAR6(KK),AHAR12(KK),
     1AHAR18(KK),APBETA(KK),APMU(KK)
201   CONTINUE
202   FORMAT(' ',2X,F7.1,2X,F7.3,2X,E10.3,2X,E10.3,2X,
     1E10.3,2X,F7.1,2X,F5.2)
      STOP
      END
```

```
      DIMENSION FD(5),F(5,1),FF(5,5),MUS(50),RMSIF(50),
     1XRMS(50),ALIF(21),TBETA(21),TMU(21),FF1(4,4),F1(4,1),
     1FD1(4),ILS(50),BETAS(50),IFS(50),APIL(50),APBETA(50),
     1APMU(50),APIF(50),AHAR6(50),AHAR12(50),AHAR18(50),
     1AHAR24(50),AHAR30(50),APRMS(50),HAR6(50),HAR12(50),
     1HAR18(50),HAR24(50),HAR30(50),ALO(21),XHAR6(21),XHAR12(50),
     1XHAR18(21),XHAR24(21),XHAR30(21),AIQ(60),AID(60),AIF(60),
     1AIK(60),THETA(60)
      REAL*4 MO,MOO,MU,IF,IL,K1,LD,LF,MF,MFD,LAB,LO,MD,KQ,
     1NN1,NP2,OMEGA,LA,MUP,MUF,KFO,KAB,KOD,ILS,IFS,MUS,KF,KD
C     INPUT MACHINE PARAMETERS
      LF=0.12E 01
      LD=0.82E-07
      MF=0.79E-02
      MD=0.38E-05
      MFD=0.19E-03
      LAB=0.15E-03
      LO=0.3E-03
C     LO=LA AND LAB=MA
      K1=1.0
      VL=6760.0
      IL=1420.0
      OMEGA=2513.27
      FREQ=400.0
      KF=(MF*LD-MD*MFD)/(LF*LD-(MFD)**2)
      KD=(MD*LF-MF*MFD)/(LF*LD-(MFD)**2)
      KQ=MD/LD
      MOO=MD**2/LD
      MO=MOO
      DELTAF=MO+MOO
      DELTAO=(1.333*(LO+LAB))-DELTAF
      KFO=MF/SQRT(LF*LO)
      KAB=LAB/LO
      KOD=MD/SQRT(LO*LD)
      DLO=0.0
      H6M=9999.0
      DO 200 L=1,21
      LO=LO+DLO
      KKK=0
      MF=KFO*SQRT(LF*LO)
      LAB=KAB*LO
      MD=KOD*SQRT(LO*LD)
      MOO=MD**2/LD
      MO=MOO
      DELTAF=MO+MOO
      DELTAO=(1.3333*(LO+LAB))-DELTAF
      KF=(MF*LD-MD*MFD)/(LF*LD-(MFD)**2)
      CALL NEWTON(MU,BETA,IF,W,V,FREQ,DELTAO,IL,VL,MOO,K1,
     1MF,MO,OMEGA,DELTAF,ZETA)
      DLO=0.03E-03
       IF=1.1*IF
      CALL PHACON(IF,MF,BETA,MO,W,V,IL,MU,DELTAO,OMEGA,VL,MOO)
      CALL FS(MU,BETA,OMEGA,IL,IF,MO,DELTAO,MF,W,V,LO,LAB,
     1DELTAF,L,AHAR6,AHAR12,AHAR18,AHAR24,AHAR30)
      CALL RMS(BETA,L,MU,APRMS,IL,DELTAO,MF,MO,W,V,MOO,IF,
     1KF,DELTAF)
      WRITE(7,302)LO,AHAR6(L),APRMS(L)
```

```
302    FORMAT('0',2X,'LA = ',E10.3,5X,'6 TH HARMONIC OF VO = ',
      1E10.3,5X,'IF RMS = ',E10.3)
       IF(H6M.LT.AHAR6(L)) GO TO 200
       H6M=AHAR6(L)
       BLA=LO
        BAPRMS=APRMS(L)
200    CONTINUE
       WRITE(7,301)
301    FORMAT('0',5X,'THIS IS THE OPTIMUM ARMATURE INDUCTANCE')
       WRITE(7,300)BLA,H6M,BAPRMS
300    FORMAT('0',2X,'BEST LA =',E10.3,5X,'PEAK 6TH HARM. OF VO =',
      1E10.3,1X,'PEAK IF RMS=',E10.3)
       LO=BLA
       MF=KFO*SQRT(LF*LO)
       LAB=KAB*LO
       MD=KOD*SQRT(LO*LD)
       LAB=KAB*LO
       MD=KOD*SQRT(LO*LD)
       MOO=MD*MD/LD
       MO=MOO
       DELTAF=MO+MOO
       DELTAO=(1.3333*(LO+LAB))-DELTAF
       KF=(MF*LD-MD*MFD)/(LF*LD-MFD*MFD)
       RETURN
       END
```

```
C       MASTER OPTOMIZATION OF L-C FILTER DESIGN
        REAL*4 K1,K2,ILFMAX,IF,MU,LA,LAB,LF,LD,MD,MF,MFD,
       1IL,MO,LWT,LEN,N1,LO
21      CONTINUE
        WRITE(7,1)
        WRITE(7,104)
104     FORMAT('0',5X,'ALL INPUTS HAVE FORMAT = F7.2 UNLESS
       1 OTHERWISE SPECIFIED')
1       FORMAT('0',1X,'WRITE THE FOLLOWING PARAMETERS FOR THE FILTER')
        WRITE(7,2)
2       FORMAT('0',1X,'CAP. ENERGY DENSITY (JOULES/LB.) =')
100     FORMAT(F7.2)
103        FORMAT('0',5X,'FORMAT=I2')
101     FORMAT(I2)
        READ(5,100)DC
        WRITE(7,4)
4       FORMAT('0',1X,'CURRENT DENSITY FOR L WIRE (CIR MIL/AMP) =')
        READ(5,100)CMA
        WRITE(7,6)
6       FORMAT('0',1X,'MAX. RMS VALUE OF 6TH HARM. OF VO (VOLTS) =')
        READ(5,100)V2
        WRITE(7,7)
7       FORMAT('0',1X,'ALLOWABLE PEAK FAULT CURRENT (AMPS) =')
        READ(5,100)ILFMAX
        IL=1420.0
        VL=6760.0
        LF=1.2
        LD=0.82E-07
        MFD=0.19E-03
        OMEGA=2513.27
        DO 50 IZ=1,2
C       IZ=1 IS FOR LA NORMAL
C       IZ=2 IS OR LA OPTIMUM
        IF(IZ.EQ.2) GO TO 51
        IF=275.0
        BETA=2.12
        MU=0.307
        LA=0.300E-03
        LAB=0.15E-03
C       LAB=MA
        MD=0.38E-05
        MF=0.79E-02
        W=144.0
        V=-138.0
        DELTAO=0.248E-03
        MO=0.176E-03
        V1=0.120E 04
        WRITE(7,53)LA
53      FORMAT('0',2X,'THE FOLLOWING VALUES ARE BASED ON NORMAL
       1LA =',E10.3,2X,'H.')
        GO TO 52
51       CONTINUE
        IL=1420.0
        IF=239.0
        BETA=2.28
        MU=0.604
        LA=0.720E-03
```

```
      LAB=0.360E-03
C     LAB=MA
      MD=0.589E-05
      MF=0.122E-01
      W=164.0
      V=-340.0
      DELTA0=0.595E-03
      M0=0.423E-03
      V1=620.0
      WRITE(7,54)LA
54    FORMAT('0',2X,'THE FOLLOWING VALUES ARE BASED ON
     1OPTIMUM LA =',E10.3,2X,'H.')
52    WRITE(7,300)IF,BETA,MU
300   FORMAT(' ',2X,'IF=',E10.3,5X,'BETA=',E10.3,5X,'MU=',E10.3)
      WRITE(7,305)IL,VL,V1
305   FORMAT(' ',2X,'IL=',E10.3,5X,'VL=',E10.3,5X,'V1=',E10.3)
      K1=V2/V1
C     FIND CONDUCTOR AREA IN CIR MILS & SQ. CM.
      CM=CMA*IL
      A16=(1+K1)/(K1*36*OMEGA**2)
       AM=CM*5.07E-10
       FW=AM
       F=0.7
       DW=5937.8
       A2=(VL*FW)**2*(K1+1)/(DC*51.1E-07*K1*36*(OMEGA**2)*F*F)
       A3=3*3.1416*F*DW
       A=(5*A2/(3*A3))**0.125
       N=A**2*F/FW
       L0=(25.5E-07)*((F/FW)**2)*(A)**5
      C0=A16/L0
         RES=N*3*3.1416*A*(2.83E-08)/FW
      WRITE(7,55)L0,C0,RES
55    FORMAT('0',1X,'OPT.VALUES BEFORE FAULT TEST
     1 ARE L0=',E10.3,1X,'H.,  C0=',E10.3,1X,'FD.',1X,'RES=',E10.3)
       K=1
  15      RES=N*3*3.1416*A*(2.83E-08)/FW
      CALL FAULT2(IF,BETA,MU,LA,LAB,LF,LD,MD,MF,MFD,W,V,IL,
     1OMEGA,DELTA0,M0,VL,L0,ILFMAX,RES)
      WRITE(7,345)IL
345   FORMAT(' ',2X,'MAX LOAD CURRENT FROM FAULT =',E10.3)
      IF(IL.LT.ILFMAX) GO TO 14
      K=K+1
      L0=L0*1.1
      C0=A16/L0
       A=((L0*(FW/F)**2)/25.5E-07)**0.2
       N=(A**2)*F/FW
      IF(K.GT.100) GO TO 14
      IL=1420.0
      IF(K.GT.2) GO TO 15
      WRITE(7,16)
16    FORMAT('0',1X,'FAULT CURRENT TOO LARGE, L0 INCREASED')
      GO TO 15
14    CONTINUE
       LWT=A3*A**3
       CWT=A2/(A**5)
      WT=LWT+CWT
      WRITE(7,17)L0,C0,IL,RES
```

```
17     FORMAT('0',1X,'LO=',E10.3,5X,'CO=',E10.3,5X,'ILF=',E10.3,1X,'
      1  RES=',E10.3)
       WRITE(7,18)LWT,CWT,WT
18     FORMAT('0',1X,'LWT=',E10.3,5X,'CWT=',E10.3,5X,'TOTAL WT =',E10.3)
       RAD=2*A
       WRITE(7,19)N,RAD,A
19     FORMAT('0',1X,'NO. TURNS =',I4,5X,'L RADIUS =',
      1E10.3,'M',5X,'L LENGTH =',E10.3,'M')
50     CONTINUE
       WRITE(7,20)
20     FORMAT('0',1X,'WRITE "0" TO END, OR "1" FOR ANOTHER RUN')
       WRITE(7,103)
       READ(5,101)KEY
       IF(KEY.GT.0) GO TO 21
       STOP
       END
```

```
C     MAIN PLOTTER PROGRAM
      DIMENSION FD(5),F(5,1),FF(5,5),MUS(50),RMSIF(50),
     1XRMS(50),ALIF(21),TBETA(21),TMU(21),FF1(4,4),F1(4,1),
     1FD1(4),ILS(50),BETAS(50),IFS(50),APIL(50),APBETA(50),
     1APMU(50),APIF(50),AHAR6(50),AHAR12(50),AHAR18(50),
     1AHAR24(50),AHAR30(50),APRMS(50),HAR6(50),HAR12(50),
     1HAR18(50),HAR24(50),HAR30(50),ALO(21),XHAR6(21),XHAR12(50),
     1XHAR18(21),XHAR24(21),XHAR30(21),AIQ(60),AID(60),AIF(60),
     1AIK(60),THETA(60)
      REAL*4 MO,MOO,MU,IF,IL,K1,LD,LF,MF,MFD,LAB,LO,MD,KQ,
     1NN1,NP2,OMEGA,LA,MUP,MUF,KFO,KAB,KOD,ILS,IFS,MUS,KF,KD
C     INPUT MACHINE PARAMETERS
      LF=0.12E 01
      LD=0.82E-07
      MF=0.79E-02
      MD=0.38E-05
      MFD=0.19E-03
      LAB=0.15E-03
      LO=0.3E-03
C     LO=LA  AND  LAB=MA
      K1=1.0
      VL=6760.0
      IL=1420.0
      OMEGA=2513.27
      FREQ=400.0
      KF=(MF*LD-MD*MFD)/(LF*LD-(MFD)**2)
      KD=(MD*LF-MF*MFD)/(LF*LD-(MFD)**2)
      KQ=MD/LD
      MOO=MD**2/LD
      MO=MOO
      DELTAF=MO+MOO
      DELTAO=(1.333*(LO+LAB))-DELTAF
      DIL=2130.0/50.0
      CALL NEWTON(MU,BETA,IF,W,V,FREQ,DELTAO,IL,VL,MOO,K1,
     1MF,MO,OMEGA,DELTAF,ZETA)
      CALL LITLI(DELTAO,MF,IF,BETA,MO,W,
     1MOO,V,IL,DELTAF,MU,AID,AIQ,AIF,AIK,THETA,KQ,KF,KD)
      KFO=MF/SQRT(LF*LO)
      KAB=LAB/LO
      KOD=MD/SQRT(LO*LD)
      DLO=0.0
      IL=1420.0
      DO 200 L=1,21
      LO=LO+DLO
      KKK=0
      MF=KFO*SQRT(LF*LO)
      LAB=KAB*LO
      MD=KOD*SQRT(LO*LD)
      MOO=MD**2/LD
      MO=MOO
      DELTAF=MO+MOO
      DELTAO=(1.3333*(LO+LAB))-DELTAF
      KF=(MF*LD-MD*MFD)/(LF*LD-(MFD)**2)
      CALL NEWTON(MU,BETA,IF,W,V,FREQ,DELTAO,IL,VL,MOO,K1,
     1MF,MO,OMEGA,DELTAF,ZETA)
      IF=1.1*IF
      CALL PHACON(IF,MF,BETA,MO,W,V,IL,MU,DELTAO,OMEGA,VL,MOO)
```

```
      ALO(L)=LO
      CALL FS(MU,BETA,OMEGA,IL,IF,MO,DELTAO,MF,W,V,LO,LAB,
     1DELTAF,L,XHAR6,XHAR12,XHAR18,XHAR24,XHAR30)
      CALL RMS(BETA,L,MU,XRMS,IL,DELTAO,MF,MO,W,V,MOO,IF,
     1KF,DELTAF)
      ALIF(L)=IF
      TBETA(L)=BETA*180./3.1416
      TMU(L)=MU*180./3.1416
      DLO=0.03E-03
200   CONTINUE
      WRITE(7,201)
      DO 202 L=1,21
      WRITE(7,203)ALO(L),XRMS(L),XHAR6(L),XHAR12(L),XHAR18(L),
     1TBETA(L),TMU(L)
202   CONTINUE
201   FORMAT(' ',5X,'LO',10X,'IF',10X,'6TH',10X,'12TH',10X,'18TH',
     112X,'BETA',12X,'MU')
203   FORMAT(' ',1X,7E13.4)
      LO=0.3E-03
      LAB=0.15E-03
      MD=0.38E-05
      MOO=MD*MD/LD
      MO=MOO
      MF=0.79E-02
      KF=(MF*LD-MD*MFD)/(LF*LD-MFD*MFD)
      DELTAF=MO+MOO
      DELTAO=(1.3333*(LO+LAB))-DELTAF
      IL=0.0
      WRITE(7,2800)
      DO 100 LLL=1,50
      KKK=0
      CALL NEWTON(MU,BETA,IF,W,V,FREQ,DELTAO,IL,VL,MOO,K1,
     1MF,MO,OMEGA,DELTAF,ZETA)
      ILS(LLL)=IL
      BETAS(LLL)=BETA*180.0/3.1416
      MUS(LLL)=MU*180.0/3.1416
      IFS(LLL)=IF
2800  FORMAT(' ',4X,'IL',8X,'BETA',7X,'MU',8X,'IF')
2801  FORMAT('0',2X,F7.1,4X,F6.2,4X,F6.3,4X,F6.1,4X,F6.1,4X,F6.1)
      CALL FS(MU,BETA,OMEGA,IL,IF,MO,DELTAO,MF,W,V,LO,LAB,
     1DELTAF,LLL,HAR6,HAR12,HAR18,HAR24,HAR30)
      CALL RMS(BETA,LLL,MU,RMSIF,IL,DELTAO,MF,MO,W,V,MOO,IF,
     1KF,DELTAF)
      IF=1.1*IF
      CALL PHACON(IF,MF,BETA,MO,W,V,IL,MU,DELTAO,OMEGA,VL,MOO)
      APIL(LLL)=IL
      APBETA(LLL)=BETA
      APMU(LLL)=MU
      APIF(LLL)=IF
      CALL FS(MU,BETA,OMEGA,IL,IF,MO,DELTAO,MF,W,V,LO,LAB,
     1DELTAF,LLL,AHAR6,AHAR12,AHAR18,AHAR24,AHAR30)
      CALL RMS(BETA,LLL,MU,APRMS,IL,DELTAO,MF,MO,W,V,MOO,IF,
     1KF,DELTAF)
      IL=IL+DIL
      IF(LLL.EQ.1) IL=35.0
100   CONTINUE
      DO 101 LLL=1,50
```

```
      WRITE(7,2801)ILS(LLL),BETAS(LLL),MUS(LLL),IFS(LLL)
101   CONTINUE
      DO 102 LLL=1,50
      WRITE(7,2802)LLL,HAR6(LLL),HAR12(LLL),HAR18(LLL),HAR24(LLL),
     1HAR30(LLL)
2802  FORMAT(' ',1X,I3,5E13.4)
102   CONTINUE
      DO 103 LLL=1,50
      WRITE(7,2803)LLL,RMSIF(LLL)
2803  FORMAT(' ',1X,I4,E20.5)
103   CONTINUE
      DO 104 L=1,50
      WRITE(7,2802)L,AHAR6(L),AHAR12(L),AHAR18(L),AHAR24(L),AHAR30(L)
 104  CONTINUE
      DO 105 L=1,50
      WRITE(7,2803)L,APRMS(L)
105   CONTINUE
      WRITE(7,110)
110   FORMAT('0',1X,'IL,BETA,MU,IF--WITH PHASE CONT')
      DO 106 L=1,50
      WRITE(7,107)APIL(L),APBETA(L),APMU(L),APIF(L)
107   FORMAT('0',1X,4E13.4)
106   CONTINUE
      STOP
      END
```

```
C       TEST PROGRAM FOR NEWTON SENSITIVITY ANALYSIS
        DIMENSION FD(5),F(5,1),FF(5,5),AIF(11),ABETA(11),AMU(11),
       1AW(11),AV(11),A1(11),AMO(11),AMOO(11),ALAMD(11)
        REAL*4 MO,MOO,MU,IF,IL,K1,LD,LF,MF,MFD,LAB,LO,MD,KQ,ILFMAX,
       1LA,KFO,KAB,KOD,KF,KD,IK,MA,IFT,IQ,LAMQ,LAMD,ILO,ILC,IKO,IKC
        DO 34 I1=1,7
        LF=0.12E 01
        LD=0.82E-07
        MF=0.79E-02
        MD=0.38E-05
        MFD=0.19E-03
        LAB=0.15E-03
        LO=0.3E-03
C       LO=LA  AND  LAB=MA
        CAF=MF/SQRT(LO*LF)
        CAB=LAB/LO
        CAD=MD/SQRT(LO*LD)
        CFD=MFD/SQRT(LF*LD)
        DO 35 I2=1,11
        IF(I1.GT.6) GO TO 36
        IF(I1.GT.5) GO TO 37
        IF(I1.GT.4) GO TO 38
        IF(I1.GT.3) GO TO 39
        IF(I1.GT.2) GO TO 40
        IF(I1.GT.1) GO TO 41
        LF=0.6+0.12*(I2-1)
        MF=CAF*SQRT(LO*LF)
        MFD=CFD*SQRT(LF*LD)
        A1(I2)=LF
        GO TO 42
41       LD=0.41E-07+(0.082E-07)*(I2-1)
        MD=CAD*SQRT(LO*LD)
        MFD=CFD*SQRT(LF*LD)
        A1(I2)=LD
        GO TO 42
40      MF=0.395E-02+(0.079E-02)*(I2-1)
        A1(I2)=MF
        GO TO 42
39      MFD=0.095E-03+(0.019E-03)*(I2-1)
        A1(I2)=MFD
        GO TO 42
38      MD=0.19E-05+(0.038E-05)*(I2-1)
        A1(I2)=MD
        GO TO 42
37      LAB=0.075E-03+(0.015E-03)*(I2-1)
        A1(I2)=LAB
        GO TO 42
36      LO=0.15E-03+(0.03E-03)*(I2-1)
        MF=CAF*SQRT(LO*LF)
        MD=CAD*SQRT(LO*LD)
        LAB=CAB*LO
        A1(I2)=LO
42      CONTINUE
        K1=1.0
        VL=6760.0
        IL=1420.0
        OMEGA=2513.27
```

```
      FREQ=400.0
      KF=(MF*LD-MD*MFD)/(LF*LD-MFD*MFD)
      KD=(MD*LF-MF*MFD)/(LF*LD-MFD*MFD)
      KQ=MD/LD
      M00=MD**2/LD
      AM00(I2)=M00
      AM0(I2)=KF*MF+KD*MD
      ALAMD(I2)=AM0(I2)-M00
      M0=M00
      DELTAF=M0+M00
      DELTA0=(1.3333*(L0+LAB))-DELTAF
1      CONTINUE
      CALL NEW3ON(MU,BETA,IF,W,V,FREQ,DELTA0,IL,VL,M00,K1,
     1MF,M0,OMEGA,DELTAF,ZETA,K)
      IF(K.LT.200) GO TO 80
5     AIF(I2)=0.0
      ABETA(I2)=0.0
      AMU(I2)=0.0
      AW(I2)=0.0
      AV(I2)=0.0
      GO TO 35
0     CONTINUE
      AIF(I2)=IF
      ABETA(I2)=BETA
      AMU(I2)=MU
      AW(I2)=W
      AV(I2)=V
5     CONTINUE
      IF(I1.GT.6) GO TO 46
      IF(I1.GT.5) GO TO 47
      IF(I1.GT.4) GO TO 48
      IF(I1.GT.3) GO TO 49
      IF(I1.GT.2) GO TO 50
      IF(I1.GT.1) GO TO 51
      WRITE(7,100)
00    FORMAT('0',5X,'LF VARIATION')
      GO TO 52
1      WRITE(7,101)
01    FORMAT('0',5X,'LD VARIATION')
      GO TO 52
0     WRITE(7,102)
02    FORMAT('0',5X,'MF VARIATION')
      GO TO 52
9     WRITE(7,103)
03    FORMAT('0',5X,'MFD VARIATION')
      GO TO 52
8     WRITE(7,104)
04    FORMAT('0',5X,'MD VARIATION')
      GO TO 52
7     WRITE(7,105)
05    FORMAT('0',5X,'LAB VARIATION')
      GO TO 52
6     WRITE(7,106)
06    FORMAT('0',5X,'L0 VARIATION')
2     CONTINUE
      WRITE(7,120)
20    FORMAT('0',7X,'PARAMETER'8X,'IF',11X,'BETA',11X,'MU',
```

```
      113X,'W',13X,'V',11X,'MOO',12X,'MO',11X,'LAMD')
       DO 55 L=1,11
       WRITE(7,110)A1(L),AIF(L),ABETA(L),AMU(L),AW(L),AV(L),
      1AMOO(L),AMO(L),ALAMD(L)
110    FORMAT(' ',2X,9E14.4)
55     CONTINUE
34     CONTINUE
       STOP
       END
```

```
C       PROGRAM TABLE.FOR
C      MAIN PLOTTER PROGRAM
       DIMENSION FD(5),F(5,1),FF(5,5),MUS(50),RMSIF(50),
      1XRMS(50),ALIF(21),TBETA(21),TMU(21),FF1(4,4),F1(4,1),
      1FD1(4),ILS(50),BETAS(50),IFS(50),APIL(50),APBETA(50),
      1APMU(50),APIF(50),AHAR6(50),AHAR12(50),AHAR18(50),
      1AHAR24(50),AHAR30(50),APRMS(50),HAR6(50),HAR12(50),
      1HAR18(50),HAR24(50),HAR30(50),ALO(21),XHAR6(21),XHAR12(50),
      1XHAR18(21),XHAR24(21),XHAR30(21),AIQ(60),AID(60),AIF(60),
      1AIK(60),THETA(60)
       REAL*4 MO,MOO,MU,IF,IL,K1,LD,LF,MF,MFD,LAB,LO,MD,KQ,
      1NN1,NP2,OMEGA,LA,MUP,MUF,KFO,KAB,KOD,ILS,IFS,MUS,KF,KD
C      INPUT MACHINE PARAMETERS
       LF=0.12E 01
       LD=0.82E-07
       MF=0.79E-02
       MD=0.38E-05
       MFD=0.19E-03
       LAB=0.15E-03
       LO=0.3E-03
       K1=1.0
       VL=6760.0
       IL=1420.0
       OMEGA=2513.27
       FREQ=400.0
       KF=(MF*LD-MD*MFD)/(LF*LD-(MFD)**2)
       KD=(MD*LF-MF*MFD)/(LF*LD-(MFD)**2)
       KQ=MD/LD
       MOO=MD**2/LD
       MO=MOO
       DELTAF=MO+MOO
       DELTAO=(1.333*(LO+LAB))-DELTAF
       DIL=1420.0/15.0
       KFO=MF/SQRT(LF*LO)
       KAB=LAB/LO
       KOD=MD/SQRT(LO*LD)
       DLO=0.0
       DO 200 L=1,21
       IL=1420.0
       LO=LO+DLO
       KKK=0
       MF=KFO*SQRT(LF*LO)
       LAB=KAB*LO
       MD=KOD*SQRT(LO*LD)
       MOO=MD**2/LD
       MO=MOO
       DELTAF=MO+MOO
       DELTAO=(1.3333*(LO+LAB))-DELTAF
       KF=(MF*LD-MD*MFD)/(LF*LD-(MFD)**2)
       CALL NEWTON(MU,BETA,IF,W,V,FREQ,DELTAO,IL,VL,MOO,K1,
      1MF,MO,OMEGA,DELTAF,ZETA)
       DLO=0.03E-03
       IL=0.0
       IF=1.1*IF
       DO 100 LLL=1,17
       KKK=0
       CALL PHACON(IF,MF,BETA,MO,W,V,IL,MU,DELTAO,OMEGA,VL,MOO)
```

```
      APIL(LLL)=IL
      APBETA(LLL)=BETA*180.0/3.1416
      APMU(LLL)=MU*180.0/3.1416
      CALL FS(MU,BETA,OMEGA,IL,IF,MO,DELTAO,MF,W,V,LO,LAB,
     1DELTAF,LLL,AHAR6,AHAR12,AHAR18,AHAR24,AHAR30)
      CALL RMS(BETA,LLL,MU,APRMS,IL,DELTAO,MF,MO,W,V,MOO,IF,
     1KF,DELTAF)
      IL=IL+DIL
100   CONTINUE
      WRITE(7,300)LO,IF
300   FORMAT('0',5X,'LO=',E10.3,5X,'IF=',E10.3)
      WRITE(7,203)
203   FORMAT('0',5X,'IL,IFRMS,6TH,12TH,18TH,BETA,MU')
      DO 201 KK=1,17
       WRITE(7,202)APIL(KK),APRMS(KK),AHAR6(KK),AHAR12(KK),
     1AHAR18(KK),APBETA(KK),APMU(KK)
201   CONTINUE
200    CONTINUE
202   FORMAT(' ',2X,F7.1,2X,F7.3,2X,E10.3,2X,E10.3,2X,
     1E10.3,2X,F7.1,2X,F5.2)
      STOP
      END
```

```
C       TEST PROGRAM FOR FAULT
        DIMENSION FD(5,1),F(5,1),FF(5,5),A(4,4),B(5,5),RH(5,1),CIL(300),
       1CIK(300),CWT(300)
        REAL*4 MO,MOO,MU,IF,IL,K1,LD,LF,MF,MFD,LAB,LO,MD,KQ,ILFMAX,
       1LA,KFO,KAB,KOD,KF,KD,IK,MA,IFT,IQ,LAMQ,LAMD,ILO,ILC,IKO,IKC
        LF=0.12E 01
        LD=0.82E-07
        MF=0.79E-02
        MD=0.38E-05
        MFD=0.19E-03
        LAB=0.15E-03
        LO=0.3E-03
        LA=LO
        ILFMAX=0.1E 06
        WRITE(7,200)
200     FORMAT('0',2X,'TYPE THE VALUE OF RP DESIRED')
        READ(5,201)RP
201     FORMAT(E20.10)
        K1=1.0
        VL=6760.0
        IL=1420.0
        OMEGA=2513.27
        FREQ=400.0
        KF=(MF*LD-MD*MFD)/(LF*LD-MFD*MFD)
        KD=(MD*LF-MF*MFD)/(LF*LD-MFD*MFD)
        KQ=MD/LD
        MOO=MD**2/LD
        MO=MOO
        DELTAF=MO+MOO
        DELTAO=(1.3333*(LO+LAB))-DELTAF
        CALL NEWTON(MU,BETA,IF,W,V,FREQ,DELTAO,IL,VL,MOO,K1,
       1MF,MO,OMEGA,FELTAF,ZETA)
500     WRITE(7,299)
299     FORMAT('0',1X,'ENTER VALUE OF LO DESIRED---FORMAT E10.3')
        READ(5,298)LO
298     FORMAT(E10.3)
10      FORMAT(' ',1X,5E13.4)
        IL=1420.0
        CALL FAULT2(IF,BETA,MU,LA,LAB,LF,LD,MD,MF,MFD,W,V,IL,
       1OMEGA,DELTAO,MO,VL,LO,ILFMAX,RP)
        WRITE(7,300)IL
300     FORMAT('0',3X,'ILMAX FROM FAULT =',E10.3)
        WRITE(7,600)
600     FORMAT('0',3X,'TYPE "0" TO END, OR "1" FOR ANOTHER RUN')
        READ(5,700)KEY
700     FORMAT(I4)
        IF(KEY.GT.0) GO TO 500
        STOP
        END
```

UNCONT

```
C       MAIN PLOTTER PROGRAM
        DIMENSION FD(5),F(5,1),FF(5,5),MUS(50),RMSIF(50),
       1XRMS(50),ALIF(21),TBETA(21),TMU(21),FF1(4,4),F1(4,1),
       1FD1(4),ILS(50),BETAS(50),IFS(50),APIL(50),APBETA(50),
       1APMU(50),APIF(50),AHAR6(50),AHAR12(50),AHAR18(50),
       1AHAR24(50),AHAR30(50),APRMS(50),HAR6(50),HAR12(50),
       1HAR18(50),HAR24(50),HAR30(50),ALO(21),XHAR6(21),XHAR12(50),
       1XHAR18(21),XHAR24(21),XHAR30(21),AIQ(60),AID(60),AIF(60),
       1AIK(60),THETA(60)
        REAL*4 MO,MOO,MU,IF,IL,K1,LD,LF,MF,MFD,LAB,LO,MD,KQ,
       1NN1,NP2,OMEGA,LA,MUP,MUF,KFO,KAB,KOD,ILS,IFS,MUS,KF,KD
C       INPUT MACHINE PARAMETERS
        WRITE(7,50)
50      FORMAT('0',2X,' THIS IS THE DATA FOR THE UNCONTROLLED
       1 BRIDGE RECTIFIER')
        LF=0.12E 01
        LD=0.82E-07
        MF=0.79E-02
        MD=0.38E-05
        MFD=0.19E-03
        LAB=0.15E-03
        LO=0.3E-03
C       LO=LA  AND  LAB=MA
        K1=1.0
        VL=6760.0
        IL=1420.0
        OMEGA=2513.27
        FREQ=400.0
        KF=(MF*LD-MD*MFD)/(LF*LD-(MFD)**2)
        KD=(MD*LF-MF*MFD)/(LF*LD-(MFD)**2)
        KQ=MD/LD
        MOO=MD**2/LD
        MO=MOO
        DELTAF=MO+MOO
        DELTAO=(1.333*(LO+LAB))-DELTAF
        DIL=1420.0/15.0
        KFO=MF/SQRT(LF*LO)
        KAB=LAB/LO
        KOD=MD/SQRT(LO*LD)
        DLO=0.0
        IL=1420.0
        KKK=0
        MF=KFO*SQRT(LF*LO)
        LAB=KAB*LO
        MD=KOD*SQRT(LO*LD)
        MOO=MD**2/LD
        MO=MOO
        DELTAF=MO+MOO
        DELTAO=(1.3333*(LO+LAB))-DELTAF
        KF=(MF*LD-MD*MFD)/(LF*LD-(MFD)**2)
        IL=0.0
        DO 100 LLL=1,17
        KKK=0
        CALL NEWTON(MU,BETA,IF,W,V,FREQ,DELTAO,IL,VL,MOO,K1,
       1MF,MO,OMEGA,DELTAF,ZETA)
        APIL(LLL)=IL
```

```
      APIF(LLL)=IF
      APBETA(LLL)=BETA*180.0/3.1416
      APMU(LLL)=MU*180.0/3.1416
      CALL FS(MU,BETA,OMEGA,IL,IF,MO,DELTAO,MF,W,V,LO,LAB,
     1DELTAF,LLL,AHAR6,AHAR12,AHAR18,AHAR24,AHAR30)
      CALL RMS(BETA,LLL,MU,APRMS,IL,DELTAO,MF,MO,W,V,MOO,IF,
     1KF,DELTAF)
      IL=IL+DIL
100   CONTINUE
      WRITE(7,300)LO
300   FORMAT('0',5X,'LO=',E10.3)
      WRITE(7,203)
203   FORMAT('0',5X,'IL,IFRMS,6TH,12TH,18TH,BETA,MU,IF')
      DO 201 KK=1,17
       WRITE(7,202)APIL(KK),APRMS(KK),AHAR6(KK),AHAR12(KK),
     1AHAR18(KK),APBETA(KK),APMU(KK),APIF(KK)
201   CONTINUE
202   FORMAT(' ',2X,F7.1,2X,F7.3,2X,E10.3,2X,E10.3,2X,
     1E10.3,2X,F7.1,2X,F5.2,3X,F6.2)
      STOP
      END
```

APPENDIX IV. SUBROUTINES

The following subroutines for the main programs of Appendix III are listed in alphabetical order. Subroutines GELG and ARSIN are not included. GELG is a program for solving simultaneous equations that is part of the IBM Scientific Subroutine Package. ARSIN is a series for the arcsin function. It should be noted that the notation in the programs occasionally varies from that in the text:

Text	Program
L_a	L_o
M_a	L_{ab}

1. FS: Finds the harmonics of v_o.
2. FAULT2: Calculates the fault current.
3. JACOB: Calculates the Jacobian matrix for the uncontrolled rectifier bridge.
4. JACOB4: Calculates the Jacobian matrix for the controlled rectifier bridge.
5. LITLI: Calculates i_d, i_q, i_f and i_k vs. θ.
6. NEWTON: Newton-Raphson algorithm for the uncontrolled rectifier bridge.
7. NEW3ON: Same as NEWTON except variable K is included in argument list to test for convergence. Used only with SENSI3.
8. PHACON: Newton-Raphson algorithm for the controlled rectifier bridge.

9. RHS: Calculates right hand side vector for NEWTON.

10. RHS4B4: Calculates right hand side vector for PHACON.

11. RMS: Find rms value of i_f.

12. TERMA: Performs repetitive calculation for FS.

```
      SUBROUTINE FS(MU,BETA,OMEGA,IL,IF,MO,DELTAO,MF,W,V,LO,LAB,
     1DELTAF,LLL,HAR6,HAR12,HAR18,HAR24,HAR30)
      DIMENSION CN(5),HAR6(50),HAR12(50),HAR18(50),HAR24(50),HAR30(50)
      REAL*4 MU,IL,IF,MO,MF,LO,LAB
      A=-OMEGA*(1.732*IF*MF+2.865*MO*W)*1.91
      B=2.865*OMEGA*MO*V*1.91
      C=-2.865*OMEGA*IL*MO*1.91
      DD=(OMEGA/DELTAO)*(1.5*MO-LO-LAB)
      D=DD*(1.155*MF*IF+1.91*MO*W)*1.91
      E=+1.91*MO*V*DD*1.91
      F=0.955*IL*DELTAF*DD*1.91
      DO 10 K=1,5
      B1=BETA+MU-1.047
      B2=B1+1.047
      N=K*6
      CALL TERMA(N,A,2.094,B2,AN1,BN1)
      AN=AN1
      BN=BN1
      CALL TERMA(N,A,2.094,B1,AN1,BN1)
      AN=AN-AN1
      BN=BN-BN1
      CALL TERMA(N,B,0.524,B2,AN1,BN1)
      AN=AN+AN1
      BN=BN+BN1
      CALL TERMA(N,B,0.524,B1,AN1,BN1)
      AN=AN-AN1
      BN=BN-BN1
      ANG=2.094-BETA-MU
      CALL TERMA(N,C,ANG,B2,AN1,BN1)
      AN=AN+AN1
      BN=BN+BN1
      CALL TERMA(N,C,ANG,B1,AN1,BN1)
      AN=AN-AN1
      BN=BN-BN1
      B1=BETA
      B2=BETA+MU
      CALL TERMA(N,D,0.0,B2,AN1,BN1)
      AN=AN+AN1
      BN=BN+BN1
      CALL TERMA(N,D,0.0,B1,AN1,BN1)
      AN=AN-AN1
      BN=BN-BN1
      CALL TERMA(N,E,1.571,B2,AN1,BN1)
      AN=AN+AN1
      BN=BN+BN1
      CALL TERMA(N,E,1.571,B1,AN1,BN1)
      AN=AN-AN1
      BN=BN-BN1
      ANG=-BETA-MU
      CALL TERMA(N,F,ANG,B2,AN1,BN1)
      AN=AN+AN1
      BN=BN+BN1
      CALL TERMA(N,F,ANG,B1,AN1,BN1)
      AN=AN-AN1
      BN=BN-BN1
      CN(K)=SQRT(AN**2+BN**2)
```

```
10      CONTINUE
        HAR6(LLL)=CN(1)
        HAR12(LLL)=CN(2)
        HAR18(LLL)=CN(3)
        HAR24(LLL)=CN(4)
        HAR30(LLL)=CN(5)
        RETURN
        END
```

```
      SUBROUTINE FAULT2(IF,BETA,MU,LA,LAB,LF,LD,MD,MF,MFD,W,V,IL,
     1OMEGA,DELTAO,MO,VL,LO,ILFMAX,RP)
C     ROTOR FLUX LINKAGES ASSUMED CONSTANT
      DIMENSION A(4,4),B(5,5),CIL(300),CIK(300),CWT(300),
     1ARH(4,1),BRH(5,1)
      REAL*4 LO,KD,KF,KQ,IK,IF,MU,LA,LAB,LF,LD,MD,MF,MFD,IL,IFT,
     1ID,IQ,LAMQ,LAMF,LAMD,ILO,ILC,IKO,IKC,MO,ILFMAX
      KK=0
      JJ=0
C     SPECIFY INITIAL CONDITIONS FOR CONDUCTION PERIOD
      WT=BETA+MU-1.047
C     LO=0.1
      KD=(MD*LF-MF*MFD)/(LF*LD-MFD*MFD)
      KF=(MF*LD-MD*MFD)/(LF*LD-MFD*MFD)
      KQ=MD/LD
      IFT=IF+1.732*KF*((3/3.1416)*(W+IL*
     1COS(BETA+MU))-(IL*COS(WT+0.524)))
      ID=(IFT-IF)*KD/KF
      IQ=1.732*KQ*((3/3.1416)*(V-IL*SIN(BETA+MU))
     1+IL*SIN(WT+0.524))
      F1=1/(LF*LD-MFD*MFD)
      LAMQ=-1.732*MD*IL*SIN(WT+0.524)+LD*IQ
      LAMF=1.732*IL*MF*COS(WT+0.524)+LF*IFT+MFD*ID
      LAMD=1.732*IL*MD*COS(WT+0.524)+MFD*IFT+LD*ID
      SF=F1*(LAMF*LD-LAMD*MFD)
      SD=F1*(LAMD*LF-LAMF*MFD)
      SQ=LAMQ/LD
      A(1,1)=LO+2*(LA+LAB)
      A(2,2)=1.0
      A(3,3)=1.0
      A(4,4)=1.0
      A(2,3)=0.0
      A(2,4)=0.0
      A(3,2)=0.0
      A(3,4)=0.0
      A(4,2)=0.0
      A(4,3)=0.0
      B(1,1)=LO+2*(LA+LAB)
      B(2,2)=1.0
      B(3,3)=1.0
      B(4,4)=1.0
      B(2,3)=0.0
      B(2,4)=0.0
      B(3,2)=0.0
      B(3,4)=0.0
      B(4,2)=0.0
      B(4,3)=0.0
      B(5,1)=-LA-LAB
      B(5,5)=2*(LA+LAB)
      B(1,5)=-LA-LAB
C     GO INTO CONDUCTION DO LOOP
      DWT=3.1416/150
      DT=DWT/2513.3
      WT=WT+0.524
      JUMP=0
110   WT=WT-1.047*JUMP
      JUMP=JUMP+1
```

```
      IF(JUMP.GE.4) GO TO 99
      RA=0.0164
      DO 1 K=1,3000
      KEY=0
      ILO=IL
12    KEY=KEY+1
      IF(KEY.GT.2) GO TO 71
C     FIND DY/DX AT 0
      A(1,2)=1.732*MF*COS(WT)
      A(1,3)=1.732*MD*COS(WT)
      A(1,4)=-1.732*MD*SIN(WT)
      A(2,1)=1.732*KF*COS(WT)
      A(3,1)=+1.732*KD*COS(WT)
      A(4,1)=-1.732*KQ*SIN(WT)
71    CONTINUE
      ARH(1,1)=-(RP+2*RA)*IL+1.732*MF*OMEGA*SIN(WT)*
     1IFT+1.732*MD*OMEGA*SIN(WT)*ID
     1+1.732*MD*OMEGA*COS(WT)*IQ
      ARH(2,1)=1.732*KF*OMEGA*SIN(WT)*IL
      ARH(3,1)=+1.732*KD*OMEGA*SIN(WT)*IL
      ARH(4,1)=1.732*KQ*OMEGA*COS(WT)*IL
      ARH(1,1)=(ARH(1,1)-A(1,2)*ARH(2,1)-A(1,3)*ARH(3,1)
     1-A(1,4)*ARH(4,1))/(A(1,1)-A(1,2)*A(2,1)
     1-A(1,3)*A(3,1)-A(1,4)*A(4,1))
      ARH(2,1)=ARH(2,1)-A(2,1)*ARH(1,1)
      ARH(3,1)=ARH(3,1)-A(3,1)*ARH(1,1)
      ARH(4,1)=ARH(4,1)-A(4,1)*ARH(1,1)
C     ARH(1,1)=DIL/DT AT 0
      IF(KEY.GT.1) GO TO 2
      WT=WT+DWT
      IL=IL+ARH(1,1)*DT
      ILC=IL
      DILDT=ARH(1,1)
      GO TO 3
2     CONTINUE
      IL=ILO+((DILDT+ARH(1,1))*DT)/2
3     CONTINUE
      IFT=SF-1.732*IL*COS(WT)*KF
      ID=SD-1.732*IL*COS(WT)*KD
      IQ=SQ+1.732*KQ*IL*SIN(WT)
      IF(KEY.LT.2) GO TO 12
      IF(ABS(IL-ILC).LE.1.0) GO TO 10
      ILC=IL
      IF(KEY.GT.50) GO TO 997
      GO TO 12
10    CONTINUE
      KK=KK+1
      CIL(KK)=IL
      IF(IL.GT.ILFMAX) GO TO 997
      CIK(KK)=0.0
      IF(KK.GE.299) GO TO 997
301   CONTINUE
C     TEST FOR END OF CONDUCTION PERIOD
      VBCT=RA*IL+(LAB+LA)*ARH(1,1)-1.732*MF*SIN(WT-0.524)*ARH(2,1)
     1-1.732*OMEGA*COS(WT-0.524)*(MF*IFT+MD*ID)
     1-1.732*MD*SIN(WT-0.524)*ARH(3,1)-1.732*MD*COS(WT-0.524)*ARH(4,1)
     1+1.732*MD*OMEGA*SIN(WT-0.524)*IQ
```

```
C      FAULT IS PRESENT FOR 1 CONDUCTION PERIOD PLUS 1
C      COMMUTATION PERIOD + 1 COMMUTATION PERIOD WHERE NEXT SCRS
C      ARE BLANKED--PROGRAM ENDS WHEN PEAD IL IS PAST
       IF((JUMP.GE.2).AND.(IL.LT.CIL(KK-1))) GO TO 99
       IF(JUMP.GE.2) GO TO 1
       IF(VBCT.GT.0.0) GO TO 11
1      CONTINUE
       WRITE(7,720)
720    FORMAT(' ',5X,'CONDUCTION PERIOD DOES NOT END')
       GO TO 997
11      CONTINUE
C      CALCULATE COMMUTATION INTERVAL
       IK=0.0
       DO 26 K=1,200
       KEY=0
       ILO=IL
       IKO=IK
120    KEY=KEY+1
       IF(KEY.GT.2) GO TO 70
C      FIND DY/DX AT 0
       B(1,2)=1.732*MF*COS(WT)
       B(1,3)=1.732*MD*COS(WT)
       B(1,4)=-1.732*MD*SIN(WT)
       B(2,1)=1.732*KF*COS(WT)
       B(2,5)=1.732*KF*SIN(WT-0.524)
       B(3,1)=+1.732*KD*COS(WT)
       B(3,5)=+1.732*KD*SIN(WT-0.524)
       B(4,1)=-1.732*KQ*SIN(WT)
       B(4,5)=1.732*KQ*COS(WT-0.524)
       B(5,2)=1.732*MF*SIN(WT-0.524)
       B(5,3)=1.732*MD*SIN(WT-0.524)
       B(5,4)=1.732*MD*COS(WT-0.524)
70     CONTINUE
       BRH(1,1)=-(RP+2*RA)*IL+RA*IK+1.732*MF*OMEGA*SIN(WT)
      1*IFT+1.732*MD*OMEGA*SIN(WT)*ID
      1+1.732*MD*OMEGA*COS(WT)*IQ
       BRH(2,1)=1.732*KF*OMEGA*(SIN(WT)*IL-IK*COS(WT-0.524))
       BRH(3,1)=+1.732*KD*OMEGA*(IL*SIN(WT)-IK*COS(WT-0.524))
       BRH(4,1)=1.732*KQ*OMEGA*(IL*COS(WT)+IK*SIN(WT-0.524))
       BRH(5,1)=RA*IL-2*RA*IK-1.732*MF*OMEGA*IFT*
      1COS(WT-0.524)-1.732*MD*OMEGA*ID*
      1COS(WT-0.524)+1.732*MD*OMEGA*IQ*
      1SIN(WT-0.524)
       H=B(1,1)-B(1,2)*B(2,1)-B(1,3)*B(3,1)-B(1,4)*B(4,1)
       C=B(1,5)-B(1,2)*B(2,5)-B(1,3)*B(3,5)-B(1,4)*B(4,5)
       D=BRH(1,1)-B(1,2)*BRH(2,1)-B(1,3)*BRH(3,1)-B(1,4)*BRH(4,1)
       E=B(5,1)-B(5,2)*B(2,1)-B(5,3)*B(3,1)-B(5,4)*B(4,1)
       F=B(5,5)-B(2,5)*B(5,2)-B(5,3)*B(3,5)-B(5,4)*B(4,5)
       G=BRH(5,1)-B(5,2)*BRH(2,1)-B(5,3)*BRH(3,1)-B(5,4)*BRH(4,1)
       BRH(1,1)=(D*F-C*G)/(H*F-C*E)
       BRH(5,1)=(H*G-D*E)/(H*F-C*E)
C      BRH(1,1)=DIL/DT, BRH(5,1)=DIK/DT  AT 0
       IF(KEY.GT.1) GO TO 20
       WT=WT+DWT
       IL=IL+BRH(1,1)*DT
       IK=IK+BRH(5,1)*DT
       ILC=IL
```

```
      IKC=IK
      DILDT=BRH(1,1)
      DIKDT=BRH(5,1)
      GO TO 30
20    CONTINUE
      IL=ILO+((DILDT+BRH(1,1))*DT)/2
      IK=IKO+((DIKDT+BRH(5,1))*DT)/2
30    CONTINUE
      IFT=SF-1.732*KF*(IL*COS(WT)+IK*SIN(WT-0.524))
      ID=SD-1.732*KD*(IL*COS(WT)+IK*SIN(WT-0.524))
      IQ=SQ+1.732*KQ*(IL*SIN(WT)-IK*COS(WT-0.524))
      IF(KEY.LT.2) GO TO 120
      IF((ABS(IL-ILC).LE.1.0).AND.(ABS(IK-IKC).LE.1.0)) GO TO 100
      ILC=IL
      IKC=IK
      IF(KEY.GT.50) GO TO 997
      GO TO 120
100   CONTINUE
      KK=KK+1
      CIL(KK)=IL
      CIK(KK)=IK
300   CONTINUE
      IF(IL.GT.ILFMAX) GO TO 997
C     TEST FOR END OF COMMUTATION PERIOD
      IF(IK.GE.IL) GO TO 110
26    CONTINUE
      WRITE(7,721)
721   FORMAT(' ',5X,'COMMUTATION PERIOD DOES NOT END')
      GO TO 997
99    CONTINUE
      DUM=BETA+MU-1.047
997   DO 86 K=1,KK
      DUM=DUM+DWT
      CWT(K)=DUM
86    CONTINUE
      DO 144 L=1,KK
C     WRITE(7,145)CIL(L),CIK(L),CWT(L)
145   FORMAT(' ',2X,'IL=',E10.3,5X,'IK=',E10.3,5X,'WT=',E10.3)
144   CONTINUE
      RETURN
      END
```

```
      SUBROUTINE JACOB(MF,BETA,IF,W,V,IL,MO,MU,DELTAO,OMEGA,FF,A,B,C)
      DIMENSION FF(5,5)
      REAL*4 MO,MOO,MU,MF,IL,IF,K1,OMEGA
      PAIF=1.155*MF*SIN(BETA)
      PBIF=1.155*MF
      PABETA=1.155*IF*MF*COS(BETA)+1.91*MO*(W*COS(BETA)-V*SIN(BETA))
      PBBETA=-1.91*MO*IL*SIN(BETA+MU)
      PCBETA=-1.91*MO*IL*COS(BETA+MU)
      PAMU=-1.91*MO*IL*COS(MU)
      PWMU=0.0
      PVMU=0.0
      PBMU=-1.91*MO*IL*SIN(BETA+MU)
      PCMU=-1.91*MO*IL*COS(BETA+MU)
      PAW=1.91*MO*SIN(BETA)
      PBW=1.91*MO
      PAV=1.91*MO*COS(BETA)
      PCV=1.91*MO
      FF(1,1)=(COS(BETA+MU)-COS(BETA))*PAIF
     1+0.25*(2*MU-SIN(2*(BETA+MU))+SIN(2*BETA))*PBIF
      FF(1,2)=(COS(BETA+MU)-COS(BETA))*PABETA
     1-A*(SIN(BETA+MU)-SIN(BETA))-0.25*(2*MU
     1-SIN(2*(BETA+MU))+SIN(2*BETA))*PBBETA
     1+0.5*B*(-COS(2*(BETA+MU))+COS(2*BETA))
     1+0.5*((SIN(BETA+MU))**2-(SIN(BETA))**2)
     1*PCBETA+C*(SIN(BETA+MU)*COS(BETA+MU)-SIN(BETA)*COS(BETA))
      FF(1,3)=PAMU*(COS(BETA+MU)-COS(BETA))-A*SIN(BETA+MU)
     1+0.25*(2*MU-SIN(2*(BETA+MU))+SIN(2*BETA))*
     1PBMU+(B/2)*(1-COS(2*(BETA+MU)))+0.5*((SIN(BETA+MU))**2
     1-(SIN(BETA))**2)*PCMU+C*(SIN(BETA+MU)*COS(BETA+MU))
      FF(1,4)=PAV*(COS(BETA+MU)-COS(BETA))+0.5*((SIN(BETA+MU))**2
     1-(SIN(BETA))**2)*PCV
      FF(1,5)=DELTAO+PAW*(COS(BETA+MU)-COS(BETA))
     1+0.25*(2*MU-SIN(2*(BETA+MU))+SIN(2*BETA))*PBW
      FF(2,1)=PAIF*(SIN(BETA)-SIN(BETA+MU))
     1+0.5*((SIN(BETA+MU))**2-(SIN(BETA))**2)*PBIF
      FF(2,2)=PABETA*(SIN(BETA)-SIN(BETA+MU))
     1+A*(COS(BETA)-COS(BETA+MU))
     1+0.5*((SIN(BETA+MU))**2-(SIN(BETA))**2)*PBBETA
     1+B*(SIN(BETA+MU)*COS(BETA+MU)-SIN(BETA)*COS(BETA))
     1+0.25*PCBETA*(2*MU+SIN(2*(BETA+MU))-SIN(2*BETA))
     1+0.5*C*(COS(2*(BETA+MU))-COS(2*BETA))
      FF(2,3)=PAMU*(SIN(BETA)-SIN(BETA+MU))
     1-A*COS(BETA+MU)+0.5*PBMU*((SIN(BETA+MU))**2
     1-(SIN(BETA))**2)+B*(SIN(BETA+MU)*COS(BETA+MU))
     1+0.25*PCMU*(2*MU+SIN(2*(BETA+MU))-SIN(2*BETA))
     1+0.5*C*(1+COS(2*(BETA+MU)))
      FF(2,4)=DELTAO+PAV*(SIN(BETA)-SIN(BETA+MU))
     1+0.25*PCV*(2*MU+SIN(2*(BETA+MU))-SIN(2*BETA))
      FF(2,5)=PAW*(SIN(BETA)-SIN(BETA+MU))
     1+0.5*PBW*((SIN(BETA+MU))**2-(SIN(BETA))**2)
      FF(3,1)=(3.*OMEGA/3.1416)*(1.732*MF*SIN(BETA+MU))
      FF(3,2)=(3.*OMEGA/3.1416)*((1.732*IF*MF*COS(BETA+MU))
     1+((9.*MO/3.1416)*(W*COS(BETA+MU)-V*SIN(BETA+MU))))
      FF(3,3)=(3.*OMEGA/3.1416)*((1.732*IF*MF*COS(BETA+MU))
     1+((9.*MO/3.1416)*(W*COS(BETA+MU)-V*SIN(BETA+MU))))
      FF(3,4)=27.*OMEGA*MO*COS(BETA+MU)/((3.1416)**2)
```

```
      FF(3,5)=27.*OMEGA*MO*SIN(BETA+MU)/((3.1416)**2)
      FF(4,1)=MF*COS(BETA)/1.732
      FF(4,2)=(-IF*MF*SIN(BETA)/1.732)
     1+((3.*MO/3.1416)*(-W*SIN(BETA)-V*COS(BETA)))
      FF(4,3)=-3.*MO*IL*SIN(MU)/3.1416
      FF(4,4)=-3.*MO*SIN(BETA)/3.1416
      FF(4,5)=3.*MO*COS(BETA)/3.1416
      FF(5,1)=-4.*MF*COS(BETA+MU/2)*SIN(MU/2)/1.732
      FF(5,2)=(4.*IF*MF*SIN(BETA+MU/2)*SIN(MU/2)/1.732)
     1+((6.*MO/3.1416)*(W*(COS(BETA)-COS(BETA+MU))
     1-V*(SIN(BETA)-SIN(BETA+MU))))
      FF(5,3)=(-4.*IF*MF/1.732)*(-0.5*SIN(BETA+MU/2)*SIN(MU/2)
     1+0.5*COS(BETA+MU/2)*COS(MU/2))
     1+(6.*MO/3.1416)*(-W*COS(BETA+MU)+V*SIN(BETA+MU))
     1-6.*IL*MO*COS(MU)/3.1416
      FF(5,4)=6.*MO*(COS(BETA)-COS(BETA+MU))/3.1416
      FF(5,5)=6.*MO*(SIN(BETA)-SIN(BETA+MU))/3.1416
      DO 2 II=1,5
      FF(1,II)=FF(1,II)*1.0E 04
 2    CONTINUE
      DO 3 II=1,5
      FF(2,II)=FF(2,II)*1.0E 04
 3    CONTINUE
      DO 4 II=1,5
      FF(4,II)=FF(4,II)*1.0E 04
 4    CONTINUE
      DO 5 II=1,5
      FF(5,II)=FF(5,II)*1.0E 04
 5    CONTINUE
      RETURN
      END
```

```
      SUBROUTINE JACOB4(MF,BETA,IF,W,V,IL,MO,MU,DELTAO,OMEGA,FF,
     1A,B,C)
      DIMENSION FF(4,4)
      REAL*4 MO,MOO,MU,MF,IL,IF,K1,OMEGA
      PAIF=1.155*MF*SIN(BETA)
      PBIF=1.155*MF
      PABETA=1.155*IF*MF*COS(BETA)+1.91*MO*(W*COS(BETA)-V*SIN(BETA))
      PBBETA=-1.91*MO*IL*SIN(BETA+MU)
      PCBETA=-1.91*MO*IL*COS(BETA+MU)
      PAMU=-1.91*MO*IL*COS(MU)
      PWMU=0.0
      PVMU=0.0
      PBMU=-1.91*MO*IL*SIN(BETA+MU)
      PCMU=-1.91*MO*IL*COS(BETA+MU)
      PAW=1.91*MO*SIN(BETA)
      PBW=1.91*MO
      PAV=1.91*MO*COS(BETA)
      PCV=1.91*MO
      FF(1,1)=(COS(BETA+MU)-COS(BETA))*PABETA
     1-A*(SIN(BETA+MU)-SIN(BETA))-0.25*(2.*MU
     1-SIN(2.*(BETA+MU))+SIN(2.*BETA))*PBBETA
     1+0.5*B*(-COS(2.*(BETA+MU))+COS(2.*BETA))
     1+0.5*((SIN(BETA+MU))**2-(SIN(BETA))**2)
     1*PCBETA+C*(SIN(BETA+MU)*COS(BETA+MU)-SIN(BETA)*COS(BETA))
      FF(1,2)=PAMU*(COS(BETA+MU)-COS(BETA))-A*SIN(BETA+MU)
     1+0.25*(2.*MU-SIN(2.*(BETA+MU))+SIN(2.*BETA))*
     1PBMU+(B/2.)*(1-COS(2.*(BETA+MU)))+0.5*((SIN(BETA+MU))**2
     1-(SIN(BETA))**2)*PCMU+C*(SIN(BETA+MU)*COS(BETA+MU))
      FF(1,3)=PAV*(COS(BETA+MU)-COS(BETA))+0.5*((SIN(BETA+MU))**2
     1-(SIN(BETA))**2)*PCV
      FF(1,4)=DELTAO+PAW*(COS(BETA+MU)-COS(BETA))
     1+0.25*(2.*MU-SIN(2.*(BETA+MU))+SIN(2.*BETA))*PBW
      FF(2,1)=PABETA*(SIN(BETA)-SIN(BETA+MU))
     1+A*(COS(BETA)-COS(BETA+MU))
     1+0.5*((SIN(BETA+MU))**2-(SIN(BETA))**2)*PBBETA
     1+B*(SIN(BETA+MU)*COS(BETA+MU)-SIN(BETA)*COS(BETA))
     1+0.25*PCBETA*(2.*MU+SIN(2.*(BETA+MU))-SIN(2.*BETA))
     1+0.5*C*(COS(2.*(BETA+MU))-COS(2.*BETA))
      FF(2,2)=PAMU*(SIN(BETA)-SIN(BETA+MU))
     1-A*COS(BETA+MU)+0.5*PBMU*((SIN(BETA+MU))**2
     1-(SIN(BETA))**2)+B*(SIN(BETA+MU)*COS(BETA+MU))
     1+0.25*PCMU*(2.*MU+SIN(2.*(BETA+MU))-SIN(2.*BETA))
     1+0.5*C*(1+COS(2.*(BETA+MU)))
      FF(2,3)=DELTAO+PAV*(SIN(BETA)-SIN(BETA+MU))
     1+0.25*PCV*(2.*MU+SIN(2.*(BETA+MU))-SIN(2.*BETA))
      FF(2,4)=PAW*(SIN(BETA)-SIN(BETA+MU))
     1+0.5*PBW*((SIN(BETA+MU))**2-(SIN(BETA))**2)
      FF(3,1)=(3.*OMEGA/3.1416)*((1.732*IF*MF*COS(BETA+MU))
     1+((9.*MO/3.1416)*(W*COS(BETA+MU)-V*SIN(BETA+MU))))
      FF(3,2)=(3.*OMEGA/3.1416)*((1.732*IF*MF*COS(BETA+MU))
     1+((9.*MO/3.1416)*(W*COS(BETA+MU)-V*SIN(BETA+MU))))
      FF(3,3)=27.*OMEGA*MO*COS(BETA+MU)/((3.1416)**2)
      FF(3,4)=27.*OMEGA*MO*SIN(BETA+MU)/((3.1416)**2)
      FF(4,1)=(4.*IF*MF*SIN(BETA+MU/2.)*SIN(MU/2.)/1.732)
     1+((6.*MO/3.1416)*(W*(COS(BETA)-COS(BETA+MU))
     1-V*(SIN(BETA)-SIN(BETA+MU))))
      FF(4,2)=(-4.*IF*MF/1.732)*(-0.5*SIN(BETA+MU/2.)*SIN(MU/2.)
```

```
     1+0.5*COS(BETA+MU/2.)*COS(MU/2.))
     1+(6.*MO/3.1416)*(-W*COS(BETA+MU)+V*SIN(BETA+MU))
     1-6.*MO*COS(MU)*IL/3.1416
      FF(4,3)=6.*MO*(COS(BETA)-COS(BETA+MU))/3.1416
      FF(4,4)=6.*MO*(SIN(BETA)-SIN(BETA+MU))/3.1416
      DO 2 II=1,4
      FF(1,II)=FF(1,II)*1.0E 04
2     CONTINUE
      DO 3 II=1,4
      FF(2,II)=FF(2,II)*1.0E 04
3     CONTINUE
      DO 4 II = 1,4
      FF(4,II)=FF(4,II)*1.0E 04
4     CONTINUE
      RETURN
      END
```

```
      SUBROUTINE LITLI(DELTAO,MF,IF,BETA,MO,W,
     1MOO,V,IL,DELTAF,MU,AID,AIQ,AIF,AIK,THETA,KQ,KF,KD)
      DIMENSION AIF(60),AID(60),AIQ(60),AIK(60),THETA(60)
      REAL*4 MF,IF,MO,MOO,IL,MU,MD,KQ,KD,KF
      WRITE(7,10)KF,KQ,KD
10    FORMAT(' ',1X,'KF =',E15.3,'KQ =',E15.3,'KD =',E15.3)
      WRITE(7,11)IL
      WRITE(7,12)BETA
      WRITE(7,13)MU
      WRITE(7,14)IF
      WRITE(7,15)V
      WRITE(7,16)W
11    FORMAT(' ',1X,'IL =',F10.2)
12    FORMAT(' ',1X,'BETA =',F10.3)
13    FORMAT(' ',1X,'MU =',F10.3)
14    FORMAT(' ',1X,'IF =',F10.3)
15    FORMAT(' ',1X,'V =',F10.3)
16    FORMAT(' ',1X,'W =',F10.3)
      WRITE(7,9)
9     FORMAT(' ',9X,'THETA',9X,'IK',12X,'IQ',12X,'ID',12X,'IF')
      ANG=BETA+MU-1.0472
      DO 100 L=1,60
      X=ANG-BETA
      Y=ANG-(BETA+MU)
      Z=ANG-(BETA+1.0472)
      IF(X) 2,2,3
3     IF(Y) 5,2,4
4     IF(Z) 2,2,5
2     AIK(L)=0.0
      GO TO 6
5     AIK(L)=(1./DELTAO)*(1.155*MF*IF*(SIN(BETA)-SIN(ANG))
     1+1.91*MO*W*(SIN(BETA)-SIN(ANG))+1.91*MOO*V*(COS(BETA)
     1-COS(ANG))-0.955*IL*DELTAF*(SIN(MU)+SIN(ANG-BETA-MU)))
6     AIQ(L)=1.732*KQ*(0.955*(V-IL*SIN(BETA+MU))
     1+(IL*SIN(ANG+0.524)-AIK(L)*COS(ANG)))
      AID(L)=1.732*KD*(0.955*(W+IL*COS(BETA+MU))
     1-(IL*COS(ANG+0.524)+AIK(L)*SIN(ANG)))
      AIF(L)=AID(L)*KF/KD
      THETA(L)=ANG*180.0/3.1416
      AIK(L)=-AIK(L)
      ANG=ANG+0.01745
      WRITE(7,200)THETA(L),AIK(L),AIQ(L),AID(L),AIF(L)
200   FORMAT(' ',1X,F14.2,4E14.3)
100   CONTINUE
      RETURN
      END
```

```
      SUBROUTINE NEWTON(MU,BETA,IF,W,V,FREQ,DELTAO,IL,VL,MOO,K1,
     1MF,MO,OMEGA,DELTAF,ZETA)
      DIMENSION FD(5),F(5,1),FF(5,5)
      REAL*4 MO,MOO,MU,IF,IL,K1,MF
C     SLIGHT ERROR FOR IL.NE.0 BUT.LT.35
      KAT=0
      K=0
      IF(IL.GE.35.0) GO TO 50
      MU=0.0
      BETA=3.1416/2.
      IF=(1./(MF*1.732))*((4.17E-04)*VL-0.75*IL*DELTAO)
      W=0.0
      V=IL
      GO TO 51
50    X=SQRT((18*FREQ*DELTAO*IL)/(4*VL+18*FREQ*DELTAO*IL))
      CALL ARCSIN(X)
      MU=2*X
      ZETA=SIN(MU/2)/(MU/2)
      A=-(((3.1416*DELTAO)/(6*(1-COS(MU))*MOO))+(1-K1)*SIN(MU)
     1+ZETA*K1*SIN(MU/2))/((1-K1)*COS(MU)+ZETA*K1*COS(MU/2))
      B=ATAN(A)
      IF(B.GE.0.) GO TO 2
      BETA=3.1416+B
      GO TO 3
2     BETA = B
3     IF=(1/(1.732*MF*SIN(BETA+MU)))*((VL/(6*FREQ))-(0.75*IL*DELTAO)-(
     14.5*IL*ZETA*K1*DELTAF*SIN(MU/2)/3.1416))
      W = IL*K1*(-COS(BETA+MU)+ZETA*COS(BETA+MU/2))
      V=IL*K1*(SIN(BETA+MU)-ZETA*SIN(BETA+MU/2))
C      WRITE(7,510)
510   FORMAT('0',5X,'*****FRANKLIN SOLUTION********')
C     WRITE(7,300)K,BETA,MU,IF,W,V
51    CONTINUE
      DO 70 K=1,200
      KK=0
      A=1.155*IF*MF*SIN(BETA)+1.91*MO*(W*SIN(BETA)
     1+V*COS(BETA))-1.91*MO*IL*SIN(MU)
      B=1.155*IF*MF+1.91*MO*W+1.91*IL*MO*COS(BETA+MU)
      C=1.91*MO*(V-IL*SIN(BETA+MU))
      CALL RHS(IF,MF,BETA,MO,W,V,IL,MU,DELTAO,F,OMEGA,A,B,C,VL)
C     WRITE(7,486)F(1,1),F(2,1),F(3,1),F(4,1),F(5,1)
486   FORMAT(5E20.7)
      DO 71 L=1,5
      FD(L)=-F(L,1)
      Y=ABS(FD(L))
      IF(Y.GT.0.001) KK=1
71     CONTINUE
      IF(KK.GE.1) GO TO 72
      GO TO 75
72    CONTINUE
      CALL JACOB(MF,BETA,IF,W,V,IL,MO,MU,DELTAO,OMEGA,FF,A,B,C)
      IF(KAT.NE.0) GO TO 100
100   KAT=1
      IEQN=5
      IVEC=1
      EPS=0.01
      K10=0
```

```
      CALL GELG(FD,FF,IEQN,IVEC,EPS,K10)
      BETA=BETA+FD(2)
      MU=MU+FD(3)
      IF=IF+FD(1)
      V=V+FD(4)
      W=W+FD(5)
C     WRITE(7,300)K,BETA,MU,IF,W,V
300   FORMAT(' ',1X,I4,3X,'BETA=',E14.7,3X,'MU=',E14.7,
     13X,'IF=',E14.7,3X,'W=',E14.7,3X,'V=',E14.7)
70    CONTINUE
      WRITE(7,78)
78    FORMAT(' ',1X,'NEWTON-RHAPSON DOES NOT CONVERGE')
75    CONTINUE
      IF(K.EQ.1) WRITE(7,500)
500   FORMAT(' ',1X,'NEWTON DID NOT ITTERATE, K=1')
C     WRITE(7,487)
487   FORMAT('0',2X,'*********FINAL SOLUTION *********')
C     WRITE(7,300)K,BETA,MU,IF,W,V
C     WRITE(7,488)
488   FORMAT('0',2X,'THIS IS THE RHS VECTOR FOR TEST')
C     WRITE(7,489)F(1,1),F(2,1),F(3,1),F(4,1),F(5,1)
489   FORMAT(5E20.7)
      RETURN
      END
```

```
      SUBROUTINE NEW3ON(MU,BETA,IF,W,V,FREQ,DELTAO,IL,VL,MOO,K1,
     1MF,MO,OMEGA,DELTAF,ZETA,K)
      DIMENSION FD(5),F(5,1),FF(5,5)
      REAL*4 MO,MOO,MU,IF,IL,K1,MF
C     SLIGHT ERROR FOR IL.NE.O BUT.LT.35
      KAT=0
      IF(IL.GE.35.0) GO TO 50
      MU=0.0
      BETA=3.1416/2.
      IF=(1./(MF*1.732))*((4.17E-04)*VL-0.75*IL*DELTAO)
      W=0.0
      V=IL
      GO TO 51
50    X=((4*3.1416*VL-9*OMEGA*IL*DELTAO)/(4*3.1416*VL
     1+9*OMEGA*IL*DELTAO))
      CALL ARCCOS(X)
      MU=X
      ZETA=SIN(MU/2)/(MU/2)
      A=-(((3.1416*DELTAO)/(6*(1-COS(MU))*MOO))+(1-K1)*SIN(MU)
     1+ZETA*K1*SIN(MU/2))/((1-K1)*COS(MU)+ZETA*K1*COS(MU/2))
      B=ATAN(A)
      IF(B.GE.O.) GO TO 2
      BETA=3.1416+B
      GO TO 3
2     BETA = B
3     IF=(1/(1.732*MF*SIN(BETA+MU)))*((VL/(6*FREQ))-(0.75*IL*DELTAO)-(
     14.5*IL*ZETA*K1*DELTAF*SIN(MU/2)/3.1416))
      W = IL*K1*(-COS(BETA+MU)+ZETA*COS(BETA+MU/2))
      V=IL*K1*(SIN(BETA+MU)-ZETA*SIN(BETA+MU/2))
51    CONTINUE
      DO 70 K=1,200
      KK=0
      A=1.155*IF*MF*SIN(BETA)+1.91*MO*(W*SIN(BETA)
     1+V*COS(BETA))-1.91*MO*IL*SIN(MU)
      B=1.155*IF*MF+1.91*MO*W+1.91*IL*MO*COS(BETA+MU)
      C=1.91*MO*(V-IL*SIN(BETA+MU))
      CALL RHS(IF,MF,BETA,MO,W,V,IL,MU,DELTAO,F,OMEGA,A,B,C,VL)
C     WRITE(7,486)F(1,1),F(2,1),F(3,1),F(4,1),F(5,1)
486   FORMAT(5E20.7)
      DO 71 L=1,5
      FD(L)=-F(L,1)
      Y=ABS(FD(L))
      IF(Y.GT.0.01) KK=1
71     CONTINUE
      IF(KK.GE.1) GO TO 72
      GO TO 75
72    CONTINUE
      CALL JACOB(MF,BETA,IF,W,V,IL,MO,MU,DELTAO,OMEGA,FF,A,B,C)
      IEQN=5
      IVEC=1
      EPS=0.01
      K10=0
      CALL GELG(FD,FF,IEQN,IVEC,EPS,K10)
      BETA=BETA+FD(2)
      MU=MU+FD(3)
      IF=IF+FD(1)
      V=V+FD(4)
```

```
      W=W+FD(5)
C     WRITE(7,300)K,BETA,MU,IF,W,V
300   FORMAT(' ',1X,I4,3X,'BETA=',E14.7,3X,'MU=',E14.7,
     13X,'IF=',E14.7,3X,'W=',E14.7,3X,'V=',E14.7)
70    CONTINUE
      WRITE(7,78)
78    FORMAT(' ',1X,'NEWTON-RHAPSON DOES NOT CONVERGE')
75    CONTINUE
      IF(K.EQ.1) WRITE(7,500)
500   FORMAT(' ',1X,'NEWTON DID NOT ITTERATE, K=1')
C     WRITE(7,487)
487   FORMAT('0',2X,'*********FINAL SOLUTION *********')
C     WRITE(7,300)K,BETA,MU,IF,W,V
C     WRITE(7,488)
488   FORMAT('0',2X,'THIS IS THE RHS VECTOR FOR TEST')
C     WRITE(7,489)F(1,1),F(2,1),F(3,1),F(4,1),F(5,1)
489   FORMAT(5E20.7)
      RETURN
      END
```

```
      SUBROUTINE PHACON(IF,MF,BETA,MO,W,V,IL,MU,DELTAO,OMEGA,VL,MOO)
      REAL*4 IF,MF,MO,IL,MU,MOO,OMEGA
      DIMENSION FD1(4),F1(4,1),FF1(4,4)
      KAT=0
      BETA=BETA+(5.0*3.1416/180.0)
      DO 100 K=1,70
      KK=0
      A=1.155*IF*MF*SIN(BETA)+1.91*MO*(W*SIN(BETA)
     1+V*COS(BETA))-1.91*MO*IL*SIN(MU)
      B=1.155*IF*MF+1.91*MO*W+1.91*IL*MO*COS(BETA+MU)
      C=1.91*MO*(V-IL*SIN(BETA+MU))
      CALL RHS4B4(IF,MF,BETA,MO,W,V,IL,MU,DELTAO,F1,OMEGA,A,B,C,VL)
      DO 101 L=1,4
      FD1(L)=-F1(L,1)
      Y=ABS(FD1(L))
      IF(Y.GE.0.01) KK=1
101    CONTINUE
      IF(KK.GE.1) GO TO 102
      GO TO 105
102    CONTINUE
      CALL JACOB4(MF,BETA,IF,W,V,IL,MO,MU,DELTAO,OMEGA,FF1,A,B,C)
      IF(KAT.NE.0) GO TO 300
300   KAT=1
      IEQN=4
      IVEC=1
      EPS=0.01
      K10=0
      CALL GELG(FD1,FF1,IEQN,IVEC,EPS,K10)
      BETA=BETA+FD1(1)
      MU=MU+FD1(2)
      V=V+FD1(3)
      W=W+FD1(4)
100    CONTINUE
      WRITE(7,2000)
2000   FORMAT(' ',1X,'NEWT-RAP DOESN T CONV FOR PHASE CONTROL')
105   IF(K.EQ.1) WRITE(7,305)
305   FORMAT(' ',1X,'PHACON DID NOT ITTERATE, K=1')
      RETURN
      END
```

```
SUBROUTINE RHS(IF,MF,BETA,MO,W,V,IL,MU,DELTAO,F,OMEGA,A,B,C,VL)
DIMENSION F(5,1)
REAL*4  MO,MU,MF,IL,IF,OMEGA
F(1,1)=DELTAO*W+A*(COS(BETA+MU)-COS(BETA))+(B/4.)*
1(2.*MU-SIN(2.*(BETA+MU))+SIN(2.*BETA))
1+(C/2.)*((SIN(BETA+MU))**2-(SIN(BETA))**2)
F(2,1)=DELTAO*V+A*(SIN(BETA)-SIN(BETA+MU))
1+(B/2.)*((SIN(BETA+MU))**2-(SIN(BETA))**2)
1+(C/4.)*(2.*MU+SIN(2.*(BETA+MU))-SIN(2.*BETA))
F(3,1)=-VL+0.955*OMEGA*(0.75*IL*DELTAO+1.732*IF*MF*
1SIN(BETA+MU)+2.865*MO*(W*SIN(BETA+MU)
1+V*COS(BETA+MU)))
F(4,1)=(0.5774*IF)*MF*COS(BETA)+(0.955*MO)
1*(W*COS(BETA)-V*SIN(BETA))+0.955*MO*COS(MU)*IL
F(5,1)=-DELTAO*IL-(2.3094*IF)*MF*COS(BETA+MU/2)
1*SIN(MU/2)+(1.91*MO)*(W*(SIN(BETA)
1-SIN(BETA+MU))+V*(COS(BETA)-COS(BETA+MU)))
1-1.91*MO*SIN(MU)*IL
F(1,1)=F(1,1)*1.0E 04
F(2,1)=F(2,1)*1.0E 04
F(4,1)=F(4,1)*1.0E 04
F(5,1)=F(5,1)*1.0E 04
RETURN
END
```

```
      SUBROUTINE RHS4B4(IF,MF,BETA,MO,W,V,IL,MU,DELTAO,F,OMEGA,
     1A,B,C,VL)
      DIMENSION F(4,1)
      REAL*4 MO,MU,MF,IL,IF,OMEGA
      F(1,1)=DELTAO*W+A*(COS(BETA+MU)-COS(BETA))+(B/4.)*
     1(2.*MU-SIN(2.*(BETA+MU))+SIN(2.*BETA))
     1+(C/2.)*((SIN(BETA+MU))**2-(SIN(BETA))**2)
      F(2,1)=DELTAO*V+A*(SIN(BETA)-SIN(BETA+MU))
     1+(B/2.)*((SIN(BETA+MU))**2-(SIN(BETA))**2)
     1+(C/4.)*(2.*MU+SIN(2.*(BETA+MU))-SIN(2.*BETA))
      F(3,1)=-VL+0.955*OMEGA*(0.75*IL*DELTAO+1.732*IF*MF*
     1SIN(BETA+MU)+2.865*MO*(W*SIN(BETA+MU)
     1+V*COS(BETA+MU)))
      F(4,1)=-DELTAO*IL-(2.309*IF)*MF*COS(BETA+MU/2.)
     1*SIN(MU/2.)+(1.91*MO)*(W*(SIN(BETA)
     1-SIN(BETA+MU))+V*(COS(BETA)-COS(BETA+MU)))
     1-1.91*MO*SIN(MU)*IL
      F(1,1)=F(1,1)*1.0E 04
      F(2,1)=F(2,1)*1.0E 04
      F(4,1)=F(4,1)*1.0E 04
      RETURN
      END
```

```
      SUBROUTINE RMS(BETA,LLL,MU,RMSIF,IL,DELTAO,MF,MO,W,V,MOO,IF
     1,KF,DELTAF)
      DIMENSION RMSIF(50)
      REAL*4 IK,IF,IL,MU,MF,MOO,MO,KF
      THETA=BETA+MU-(3.1416/3.)
      DTHETA=3.1416/300.
      SIF=0.0
      DO 1 K=1,50
      THETA=THETA+DTHETA
      IK=(1./DELTAO)*((2./1.732)*IF*MF*(SIN(BETA)-SIN(THETA))
     1+(6./3.1416)*(MO*W*(SIN(BETA)-SIN(THETA))+MOO*V*(COS(BETA)
     1-COS(THETA)))-(3./3.1416)*IL*DELTAF*(SIN(MU)+SIN(THETA-
     1BETA-MU)))
      IF(THETA.LT.BETA) IK=0.0
      SIF=(1.732*KF*((3./3.1416)*(W+IL*COS(BETA+MU))-(IL*COS(
     1THETA+3.1416/6.)+IK*SIN(THETA))))**2+SIF
      THETA=THETA+DTHETA
1     CONTINUE
      RMSIF(LLL)=SQRT(SIF)/SQRT(50.)
      RETURN
      END
```

```
      SUBROUTINE TERMA(N,Y,PHI,X,AN1,BN1)
      AN1=Y*(SIN((N+1)*X)*COS(PHI)+COS((N+1)*X)*SIN(PHI))
     1/(2*(N+1))
      AN1=AN1+Y*(SIN((N-1)*X)*COS(PHI)-COS((N-1)*X)*SIN(PHI))
     1/(2*(N-1))
      BN1=Y*(-COS((N+1)*X)*COS(PHI)+SIN((N+1)*X)*SIN(PHI))
     1/(2*(N+1))
      BN1=BN1-Y*(COS((N-1)*X)*COS(PHI)+SIN((N-1)*X)*SIN(PHI))
     1/(2*(N-1))
      RETURN
      END
```

APPENDIX V: DISTRIBUTION LIST

AFAPL/DOE/STINFO
WRIGHT-PATTERSON AFB OH 45433

AIR UNIVERSITY
MAXWELL AFB AL 36112

AFAPL/POD
WRIGHT-PATTERSON AFB OH 45433

AFWL/SY-1/DR. A. GUENTHER
KIRTLAND AFB NM 87117

USA MEROC/COMMANDING OFFICER
ATTN: SMEFB-ES/MR. LARRY AMSTUTZ
FT. BELVOIR, VIRGINIA 22060

BOEING COMPANY
ATTN: ASSISTANT SECRETARY
PO BOX 3999
SEATTLE, WASHINGTON 98124

GARRETT CORPORATION
AIRESEARCH MANUFACTURING COMPANY
ATTN: MR. LEON SCHIPPER
2525 WEST 190TH STREET
TORRANCE, CALIFORNIA 90509

GENERAL DYNAMICS CORPORATION
ATTN: VICE PRESIDENT
ONE ROCKFELLER PLAZA
NEW YORK, NY 10020

GENERAL ELECTRIC COMPANY
AEROSPACE AND DEFENCE SALES AND SERVICE
3430 SOUTH DIXIE
DAYTON, OHIO 45439

GEORGIA TECH
SCHOOL OF ELECTRICAL ENGINEERING
ATTN: DR. DIMITRIUS PARIS
225 NORTH AVENUE, NW
ATLANTA, GEORGIA 30332

HUGHES RESEARCH LABORATORIES
ATTN: DR. M. A. LUTZ
3011 MALIBU CANYON ROAD
MALIBU, CALIFORNIA 90265

LOS ALAMOS SCIENTIFIC LABORATORIES
ATTN: DR. HENRY L. LAQUER
PO BOX 1663
LOS ALAMOS, NM 87544

MAGNETIC CORPORATION OF AMERICA
67 ROGERS STREET
CALBRIDGE, MASSACHUSETTS 02142

MAXWELL LABORATORIES, INC.
ATTN: DR. ALAN KOLB
9244 BALBOA AVENUE
SAN DIEGO, CALIFORNIA 92122

PURDUE UNIVERSITY
SCHOOL OF ELECTRICAL ENGINEERING
ATTN: PROF. DAVID B. MILLER
LAFAYETTE, INDIANA 47907

RCA
ATTN: MGR. MARKETING ADM.
MARNE HIGHWAY
MOORESTOWN, NEW JERSEY 08057

STANFORD RESEARCH INSTITUTE
ATTN: DR. D. CUBICCIOTTI
STANFORD, CALIFORNIA 94305

TECH-TRAN LIGHT
50 INDEL AVENUE
RANCOCAS, NEW JERSEY 08073

TRW, INC.
SYSTEMS GROUP
ONE SPACE PARK
REDONDO BEACH, CALIFORNIA 90278

UNITED AIRCRAFT CORPORATION
RESEARCH LABORATORIES
ATTN: MR. ARTHUR CHALFANT
400 MAIN STREET
EAST HARTFORD, CONNECTICUT 06108

UNITED AIRCAFT CORPORATION
UNITED TECHNOLOGY CENTER
SUNNYVALE, CALIFORNIA 94088

UNIVERSITY OF BUFFALO
ATTN: DR. A. S. GILMORE
3435 MAIN STREET
BUFFALO, NEW YORK 14214

UNIVERSITY OF MICHIGAN
ATTN: MR. KEN BURNS, RM 218
RESEARCH ADMINISTRATION NORTH CAMPUS
ANN ARBOR, MICHIGAN 48105

UNIVERSITY OF WASHINGTON
DEPT. OF AERONAUTICAL ENGINEERING
ATTN: PROF. A. HERZBERG
SEATTLE, WASHINGTON 98105

UNIVERSITY OF WISCONSIN
INSTRUMENTATION SYSTEMS CENTER
ATTN: DR. R. W. BOOM
1500 JOHNSON DRIVE
MADISON, WISCONSIN 53705

WESTINGHOUSE ADVANCED TECHNOLOGY LABORATORIES
ATTN: DR. D. MERGERIAN, MS 3714
PO BOX 1521
BALTIMORE, MARYLAND 21203

WESTINGHOUSE ELECTRIC CORPORATION
ATTN: MR. L. H. POWERS
1306 FARR DRIVE
DAYTON, OHIO 45404

LOCKHEED MISSLES AND SPACE CO.
ATTN: TECHNICAL INFORMATION CENTER
P.O. BOX 504
SUNNYVALE, CA 94088

DOUGLAS AIRCRAFT COMPANY
W.B. YOPP
3855 LAKEWOOD BOULEVARD
LONG BEACH, CALIFORNIA 90801

HUGHES AIRCRAFT COMPANY
ELECTROMAGNETIC ENGINEERING SECTION
COMPONENTS AND MATERIALS LABORATORIES
ATTN: JACK K. KISCH
CULVER CITY, CA

TELEDYNE MEC
ATTN: MR. BEN SMITH
3165 PORTER DRIVE
PALO ALTO, CA 94304

MASSACHUSETTS INSTITUTE OF TECHNOLOGY
DEPARTMENT OF MECHANICAL ENGINEERING
CRYOGENIC ENGINEERING LABORATORY
ATTN: DR. JOSEPH L. SMITH, JR.
CAMBRIDGE, MA 02139